RADICAL SAM ENZYMES IN THIENAMYCIN BIOSYNTHESIS

by

Daniel Roe Marous

A dissertation submitted to The Johns Hopkins University in conformity with the requirements for the degree of Doctor of Philosophy

Baltimore, Maryland
December, 2015

©Daniel Roe Marous 2015
All rights reserved

Abstract

Despite its broad anti-infective activity, the biosynthesis of the paradigm carbapenem antibiotic, thienamycin, remains largely unknown. Apart from the first two biosynthetic steps shared with a simple carbapenem, the pathway sharply diverges to the more structurally complex members of this class of β-lactam antibiotics like thienamycin. Existing evidence points to three putative cobalamin-dependent, radical *S*-adenosylmethionine (RS) enzymes, ThnK, ThnL and ThnP, potentially being responsible for assembly of the ethyl side chain at C6, bridgehead epimerization at C5, installation of the C2-thioether side chain and C2/3-desaturation. The C2 substituent has been demonstrated to be derived from stepwise truncation of coenzyme A, but the timing of these events with respect to C2—S bond formation is not known. Using *in vitro* reactions with synthetically-accessed substrates, we show that ThnK of the three apparent cobalamin-dependent RS enzymes performs sequential methylations to build out the C6-ethyl side chain in a stereocontrolled manner. This enzymatic reaction produced the expected RS methylase coproducts *S*-adenosylhomocysteine (SAH) and 5'-deoxyadenosine (5'-dA) by LC-MS and was also found to require cobalamin. For double methylation to occur, the carbapenam substrate must bear a coenzyme A-derived C2-thioether side chain, implying the activity of a prior sulfur insertion by an unidentified enzyme. Heterologous expression of thienamycin biosynthetic enzymes in *Streptomyces* combined with a competition bioassay now implicates ThnL in attachment of the thioether. Additional substrate profiling with ThnK suggests that CoA itself is added to the bicyclic carbapenam nucleus. These insights allow refinements of the central steps in complex carbapenem biosynthesis.

Thesis Advisor:

Dr. Craig A. Townsend, Department of Chemistry, The Johns Hopkins University

Reader:

Dr. Caren L. Freel Meyers, Department of Pharmacology and Molecular Sciences, The Johns Hopkins University

Additional Committee Members:

Dr. Philip A. Cole, Department of Pharmacology and Molecular Sciences, The Johns Hopkins University

Dr. James T. Stivers, Department of Pharmacology and Molecular Sciences, The Johns Hopkins University

Acknowledgements

First, I am grateful to my mentor, Dr. Craig Townsend, for inviting me to join his lab and granting me both flexibility and support as I developed as a scientist. I admire his passion and rigor for science as well as his tenacity for pursuing difficult projects while encouraging his students to “never give up”. For his guidance over the years, I am appreciative.

I would also like to thank my thesis committee members Professors Phil Cole, Caren Meyers, and Jim Stivers for their suggestions and helpful critique. I am particularly indebted to Dr. Cole and Dr. Meyers for career advice and guidance and to Dr. Meyers for being an official reader of my dissertation and granting me the opportunity to teach with her. Additionally, I am grateful to Dr. Phil Mortimer for his helpful suggestions and tireless efforts to keep the MS facilities up and running. My thanks also goes to the Pharmacology faculty and support staff, especially Amy Paronto and Mimi Guercio, for all their help over many years. I had a supportive group of classmates in Pharmacology, including Evelyn Gurulé, whom I wish all the best as they launch into their careers. I would like to thank the Booker lab at Penn State including Professor Squire Booker, Dr. Tyler Grove, and Anthony Blaszczyk for their generous training and guidance.

Completion of my graduate work would not have been possible without the wonderful members of the Townsend lab. Dr. Kristos Moshos, Dr. Andrew Buller, and Dr. Rongfeng Li were great mentors and friends who helped me to develop the synthetic, biochemical, and microbial aspects of my research. I am indebted to all of them. Dr. Courtney Hastings has been a fount of wisdom for both research and career advice, and I thank him for many awesome conversations. It has been a pleasure working with my

fellow members of Remsen 249 including Evan Lloyd, Ryan Oliver, and Darcie Long. I thank both Evan and Darcie for their critical readings and helpful edits of my dissertation. Darcie has been a cheerful deskmate and was always willing to allow me to interrupt her to talk about life or science. I appreciate Evan's friendship over many years and his accompaniment and assistance during multiple trips to Penn State as we went through the struggles and then successes with the radical SAM enzymes. I am also indebted to Evan, Christina, and Hercules for graciously inviting me into their home when I was in the final stages of grad school. Additionally, Dr. Nicole Gaudelli, Michel Lau, Phil Storm, Callie Huitt-Roehl, Adam Newman, Doug Cohen, Jacob Kravetz, Dr. Eric Hill, Dr. Victor Outlaw, Jordan Chadwick, and Felipe d'Andrea were great colleagues. I enjoyed working with first-year graduate student Erica Sinner and wish her success as she continues grad school.

I have been blessed with many supportive friends and family and without them, graduate school would not have been possible. Mandy and I had many visitors during our time in Baltimore and have fond memories of our times with the Hahns, Isons, and Oxleys, among others. We're especially grateful to Justin and Kerri Tank for helping us move to and from Maryland and for the plethora of visits in between, including bringing Mandy for weekend trips prior to our marriage. We've enjoyed friendships with fellow Marylanders Ryan and Kelly Hamilton, Andy Bates, and the leaders at Loch Raven High School. Finally, I am the person I am today because of my family. To Uncle Don, Aunt Diane, and my grandparents - thank you for shaping me and for your unconditional support. To my "new" siblings Aaron, Ashley, and Dan - thank you for your love and encouragement. To Sarah - thank you for believing in me, even when I doubt myself. To

Mom and Dad Crosser - thank you for loving me as your son and for your ceaseless prayers and reassurance. To Dad - although we work in different fields, thank you for modeling the dedicated pursuit of truth, while balancing a loyal, loving commitment to your family. To Mom - thank you for your nurturing, unwavering love, that formed me into the man I am today. You raise me up, so I can stand on mountains. To Mandy - thank you for being my best friend and wife. I've cherished walking this journey with you. Thanks for picking me up, every time I fall.

Dedication

For Mandy, my love-
May we continue to dance and when the kids are old enough,
we're gonna teach them to fly.

Veritas vos liberabit
"The truth shall set you free"
John 8:32

Publications Drawing Upon This Thesis

Marous, DR, Lloyd, EP, Buller, AR, Moshos, KA, Grove, TL, Blaszczyk, AJ, Booker, SJ, and Townsend, CA (2015) Consecutive radical S-adenosylmethionine methylations form the ethyl side chain in thienamycin biosynthesis. *Proc. Natl. Acad. Sci. USA* 112(33):10354-10358.

Table of Contents

Chapter 1: Introduction…… 1

β-Lactam Antibiotics: Discovery, Classes, and Mechanism of Action…….. 1

Biosynthesis and Production: Penicillin…….. 4

Bacterial Resistance to β-Lactams……...5

Thienamycin and the Carbapenems…….5

Production and Biosynthesis: Thienamycin…….6

RS Enzymes……...12

Thesis Goals…….. 17

References……..18

Chapter 2: Synthesis of Potential Substrates and Product Standards for Thienamycin RS Enzymes…….22

Introduction……22

Results and Discussion…….. 23

Initial Synthetic Library…… 23

Additional Synthetic Targets……. 31

Conclusions……35

Materials and Methods…….. 35

References……. 59

Chapter 3: Consecutive Radical SAM Methylations by ThnK Form the Ethyl Side Chain in Thienamycin Biosynthesis…… 61

Introduction……... 61

Results and Discussion…….. 61

Detection of SAH and 5'-dA……. 64

Cobalamin Dependence of ThnK…….. 67

Sequential Methylations by ThnK……68

Conclusions……73

Materials and Methods…….. 74

References……. 80

Chapter 4: Attachment of Large, CoA-Derived Thiol Provides Side Chain in Complex Carbapenem Biosynthesis……83

Introduction……83

Results and Discussion…….. 85

ThnK Activity with C2-Substituted Carbapenams……87

Heterologous Expression of RS Enzymes in *Streptomyces*…….. 88

CarC Competition Assay with EML strains…….. 93

Conclusions……94

Materials and Methods…….. 96

References……102

Chapter 5: Thienamycin RS Enzymes: Current State and Future Directions……105

Introduction……. 105

Results and Discussion…… 105

ThnK Mechanism and Structure……..105

ThnK Homologs…….. 107

ThnL and ThnP…… 110

Conclusions……. 116

Materials and Methods…….117

References……120

Curriculum Vitae…… 122

List of Tables

Table 3.1: LC-MS mass fragments for detection of SAH and 5'd-A……...79

List of Figures

Figure 1.1: Core structures of major classes of natural β-lactams……. 2

Figure 1.2: β-lactams form a stable acyl enzyme intermediate that blocks further chemistry by the transpeptidase……...3

Figure 1.3: Outline of the biosynthesis of penicillin…….. 4

Figure 1.4: Thienamycin and related clinical carbapenems……..... 6

Figure 1.5: Structures of cysteine, pantothenic acid, and coenzyme A……..8

Figure 1.6: Outline of carbapenem biosynthesis…… 9

Figure 1.7: Activity of lysine 2,3-aminomutase……... 12

Figure 1.8: Reductive cleavage of SAM by an [4Fe-4S] cluster……. 13

Figure 1.9: Examples of Class B RS methylases……..15

Figure 1.10: Traditional methylases use SAM as a methyl donor, producing SAH…….16

Figure 1.11: Proposed mechanism of many Class B RS methylases……...17

Figure 2.1: Synthetic targets for probing RS activity……... 23

Figure 2.2: Synthetic route to compounds **8** and **9**……... 25

Figure 2.3: DBU isomerization of **23** by ^{1}H-NMR…….. 26

Figure 2.4: Synthetic route to compounds **10** and **11**……..……28

Figure 2.5: Chiral HPLC analysis of compound **38**……..……29

Figure 2.6: Stereoisomers from thiol addition……..…30

Figure 2.7: HPLC separation of **10** and **11**……..……30

Figure 2.8: Additional synthetic targets for probing RS activity……..……31

Figure 2.9: Synthetic route to C2 and C6-substituted carbapenams **41** and **43**……..…..32

Figure 2.10: Synthesis and Purification of **44-49**……33

Figure 2.11: HPLC separation of **44**/**45** and **48**/**49**……...34

Figure 3.1: Carbapenam synthetic library and detection and quantification of SAM products of ThnK……..…….... 62

Figure 3.2: UV-Visible spectrum and SDS-PAGE of ThnK……..……..... 63

Figure 3.3: Detection of SAM-derived products of ThnK with **3**, **8**, and **9**……..……64

Figure 3.4: LC-MS/MS comparison of enzymatic turnover using different iron-sulfur cluster reductants……..……..……... 65

Figure 3.5: Fe/S cluster required for ThnK activity……..……66

Figure 3.6: Cobalamin required for ThnK activity……..…….67

Figure 3.7: ThnK product detection and additional synthetic compounds……..…....68

Figure 3.8: Detection of β-lactam parent and fragment ions……..…….. 69

Figure 3.9: Product detection of ThnK assays with d_3-SAM……..……. 70

Figure 3.10: Detection of SAM-derived products of ThnK with compound **41b**……..... 71

Figure 4.1: Overview of the synthesis of C2-substituted carbapenams to test with ThnK……..……..…….. 85

Figure 4.2: Sequential methylations by ThnK……..……86

Figure 4.3: LC-MS/MS detection of enzymatic SAM-derived coproducts SAH…..…...87

Figure 4.4: Southern blot verifying insertion of *thnE* and *thnM* into *S. lividans* TK24-EM and *S. coelicolor* M1154 EM……..……..……... 89

Figure 4.5: Production of the antibiotic 4 from the CarC assay with synthetic (3*S*,5*S*)-carbapenam **3**……..……..…… 90

Figure 4.6: Production of zones of inhibition are dependent on CarC activity……..... 91

Figure 4.7: Detection of ThnL and ThnK in TK24-EML and EMK strains…… 92

Figure 4.8: Schematic of CarC competition assay with EML or EMK strains…..…..… 93

Figure 4.9: CarC competition assay with TK24-EM, EML, and EMK strains……...… 94

Figure 4.10: Plasmid Maps for pUWL201/*ermEp-EM* (A) and pMS82/*ermEp-EM* (B). 98

Figure 5.1: 5'-dA accumulation with ThnK……..……..... 106

Figure 5.2: Chemical structures of PS-6 and Asparenomycin A-C…… 107

Figure 5.3: Extracted-ion chromatograms (EICS) showing “aerobic” methylation by ThnK……..……..……... 109

Figure 5.4: Extracted-ion chromatograms (EICS) showing “aerobic” methylation by TokK……..……..……... 110

Figure 5.5: SDS-PAGE gel showing soluble ThnK, L, and P……..……..……111

Figure 5.6: LC-MS/MS detection of enzymatic SAM-derived coproducts SAH and 5′-dA with ThnL……..……..…….. 112

Figure 5.7: LC-MS/MS detection of enzymatic SAM-derived coproducts SAH and 5′-dA with ThnP……..……..……...113

Figure 5.8: ThnK substrates tested with ThnP……...……114

Figure 5.9: Extracted-ion chromatograms (EICS) showing low levels of methylation by ThnP……..……..……114

Figure 5.10: Extracted-ion chromatograms (EICS) to detect carbapenam(em) products from ThnK-ThnP coupled assays……115

Figure 5.11: Outline of proposed thienamycin biosynthesis…….. 117

Chapter 1

Introduction

β-Lactam Antibiotics: Discovery, Classes, and Mechanism of Action

The genesis of modern antimicrobial therapy, a turning point for human medicine, began with a fortuitous discovery in 1928 by Alexander Fleming when he observed that contaminating *Penicillium* mold killed nearby staphylococcus colonies growing on the same plate. As he later reported, "It was found that broth in which the mould had been grown at room temperature for one or two weeks had acquired marked inhibitory, bactericidal and bacteriolytic properties to many of the more common pathogenic bacteria" (1). Fleming reasoned that there was a substance from the mold that could function as an antibiotic (1) and many others were involved in the development of this compound to a clinical antimicrobial (2), which became known as penicillin. Several years later, Dorothy Hodgkin's crystal structure revealed that penicillin contained a 4-member cyclic amide called a β-lactam (2, 3), a moiety that would prove to be essential to the efficacy of this antibiotic.

In addition to penicillin, several other natural β-lactams have been subsequently discovered. While all β-lactam antibiotics contain the namesake heterocycle, a possible fused second ring as well as additional side chains can differ, forming different β-lactam classes. The classes of naturally occurring β-lactams include: the penams (penicillins), cephems (cephalosporins, cephamycins), carbapenems (and carbapen*ams*, which lack the characteristic double bond), clavams, and monobactams (2, 4). More variations have been generated synthetically (2). The core structures of these major classes are depicted in Figure 1.1. Derivatives of these natural β-lactams have been very successful clinically,

pairing both efficacy and safety and accounting for billions of dollars in annual sales (2, 4).

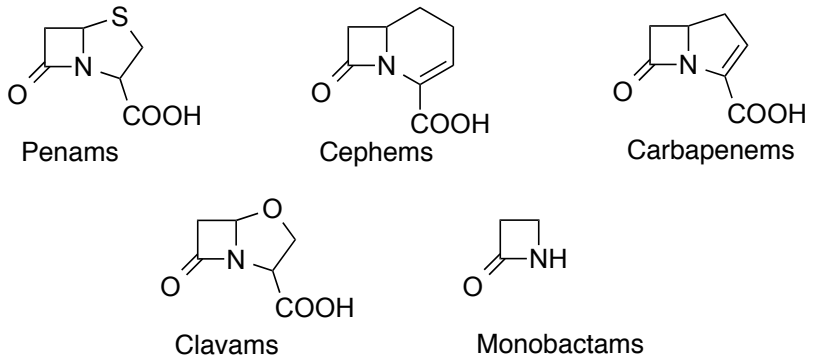

Figure 1.1: Core structures of major classes of natural β-lactams.

As single celled organisms, bacteria are surrounded by a peptidoglycan layer that aids in the structural integrity of the isolated cell. While both Gram-negative and Gram-positive bacteria contain peptidoglycan, the layer is generally smaller in Gram-negative bacteria, which also possess a second membrane on the outside of this structure. Peptidoglycan consists of alternating sugar residues-*N*-acetylglucosamine (NAG) and *N*-acetylmuramic acid (NAM)-that have been polymerized. Attached to the NAM residues are small chains of five or more amino acids ending with a D-Ala-D-Ala motif. There are transpeptidases (also called high molecular weight penicillin binding proteins) that form a peptide bond between an amine on a neighboring chain and the penultimate D-Ala, a process that releases the terminal D-Ala residue. β-lactam antibiotics mimic the D-Ala-D-Ala terminus, a concept termed the Tipper-Strominger Hypothesis, resulting in attack on the β-lactam ring by an active site serine of the transpeptidase to form a covalent acyl-enzyme intermediate. The enzyme is unable to clear the antibiotic from its catalytic

center due to distortion of the protein owing to the steric bulk of the antibiotic structure and exclusion of a nucleophile, thus effectively inhibiting the transpeptidase from performing further catalytic cycles. Figure 1.2 depicts how β-lactams mimic the D-Ala-D-Ala terminus, react with the active site serine, and block further reaction from occurring with the acyl-enzyme intermediate. (2) β-lactams antibiotics eventually kill microbes by blocking their ability to maintain their cell wall. This class of antibiotics is specific for bacteria because human cells, in contrast, lack a cell wall. (2)

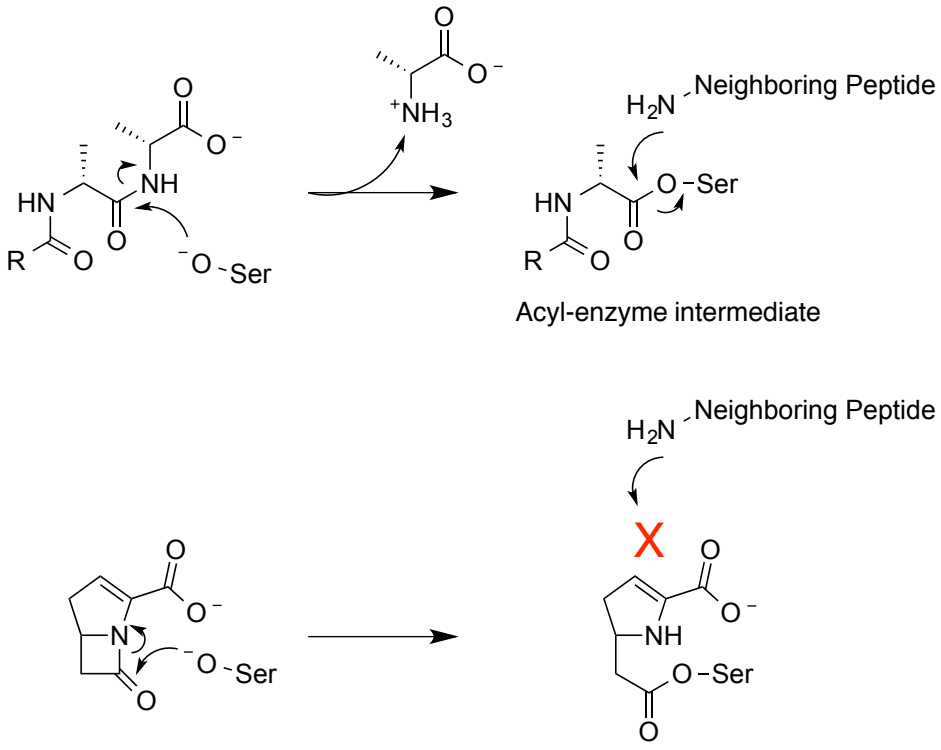

Figure 1.2: β-lactams form a stable acyl enzyme intermediate that blocks further chemistry by the transpeptidase. Figure is modeled from (2).

Biosynthesis and Production: Penicillin

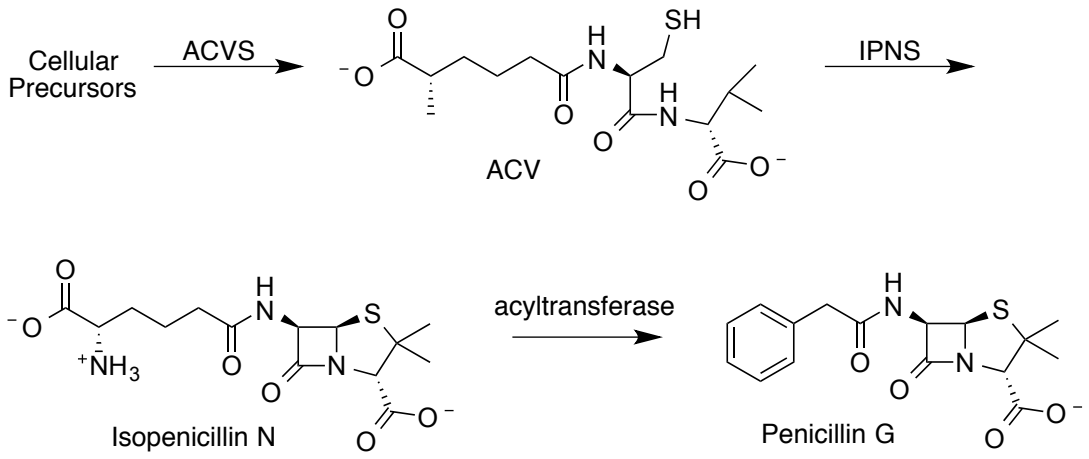

Figure 1.3: Outline of the biosynthesis of penicillin.

In its native producers, penicillin is made by a nonribosomal peptide synthetase (NRPS), δ-(L-α-aminoadipyl)-L-cysteine-D-valine synthetase (ACVS), which forms a tripeptide using the amino acids: L-α-aminoadipic acid, L-cysteine, and L-valine. The NRPS is responsible for catalyzing peptide bond formation in an ordered manner and epimerization of the L-valine residue. The resulting product, ACV, is a substrate for isopenicillin N synthase (IPNS), a remarkable enzyme requiring iron and oxygen, which is able to form the bicycle isopenicillin N. (5) Finally, an acyltransferase is able to exchange the L-α-aminoadipic acid moiety for another group such as phenylacetic acid, forming penicillin G. This process is outlined in Figure 1.3. Additionally, isopenicillin N serves as an intermediate in the biosynthesis of the cephalosporins and cephamycins. (6)

Efficient *in vivo* production of penicillins and cephalosporins is now feasible because of understanding of penicillin biosynthesis along with the development of production strains and fermentation technology. Greater than 90% of penicillin G or V can be recovered from producers and high titers of both penicillin (40–50 g/L) and

cephalosporin (20–25 g/L) is possible. (7) Isolated fermentative products, such as 6-aminopenicillanic acid (6-APA), can also be used as intermediates in semi-synthetic processes to make penicillin and cephalosporin derivatives (7).

Bacterial Resistance to β-Lactams

Although important antibiotics, the β-lactams, along with other antimicrobials, face resistance from bacteria. Bacterial resistance to β-lactams was already becoming problematic within a few years of the introduction of penicillin in the clinic (4). Microbes have evolved several mechanisms to overcome antibiotic treatment. Gram-positive bacteria have developed penicillin-binding proteins that no longer recognize β-lactams, while Gram-negative bacteria can utilize β-lactamases, a class of enzymes similar to transpeptidases, but with the ability to hydrolyze the antibiotic from the active site nucleophile. Additionally, bacteria can become impermeable to the drugs or actively transport them away out of the cell; both strategies effectively lower the concentration of the antibiotic near the desired target. (2) The spread of resistance is increasingly alarming and some infections are becoming virtually untreatable, hastening the need for new and effective therapeutics.

Thienamycin and the Carbapenems

Though not completely able to overcome bacterial resistance, the carbapenems are often immune to clinically-relevant β-lactamases, making them critical antibiotics (4). Indeed, the paradigm naturally-occurring carbapenem thienamycin is “one of the most potent, broad- spectrum, non-toxic antibacterial compounds ever discovered” (7).

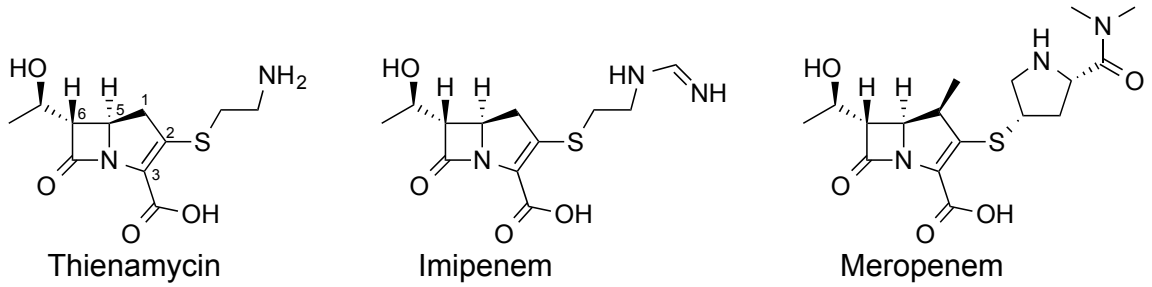

Figure 1.4: Thienamycin and related clinical carbapenems.

Thienamycin was isolated in the late 1970s from *Streptomyces cattleya* (8). While a sulfur atom is not present in the 5-member ring, the numbering convention still places carbon-1 in the same location, as depicted in Figure 1.4. Instead, thienamycin and related carbapenems contain a sulfur side chain at C2. Additionally, they possess *trans* stereochemistry across C5 and C6 and lack an amide bond in the C6 side chain, unlike penicillin (9). Thienamycin itself is chemically unstable, thus the N-formimidoyl analog (Imipenem) is used clinically (4). This drug is co-administered with cilastatin to prevent degradation by a mammalian dehydropeptidase in the kidney. Other carbapenems, such as Meropenem, have been synthesized that are resistant to the peptidase due to the presence of a 1-β-methyl group at C1 (See Figure 1.4). Clinically, carbapenems can be used to treat infections from several Gram-negative and Gram-positive bacteria. (4)

Production and Biosynthesis: Thienamycin

Unlike other β-lactam antibiotics, clinical carbapenems are made by total synthesis because thienamycin is not chemically stable, *S. cattleya* fermentation titers are low, and the host producer is difficult to manipulate genetically (4). A synthetic route of production leads to a higher cost of manufacture, translating to a higher price of the drug

itself. As an example, a 500 mg dose of Meropenem can cost around $39, while a 500 mg dose of Amoxicillin, a penicillin, costs around $0.14 (10). Outside the clinic, one common vendor sells 5 grams of Amoxicillin for $40, while 250 mg of Imipenem costs around $230 (11). Additional biosynthetic understanding could benefit development of a semi-synthetic route of production and a corresponding decrease in cost.

Biosynthetically, early labeling studies supported that glutamate was the source of the pyrroline ring in thienamycin and that C6 and C7 of the β-lactam ring were derived from acetate (9). Furthermore, labeled methionine experiments indicate that the carbons and hydrogens in the C6-ethyl side chain originate from the *S*-methyl of this amino acid. The isolation of a thienamycin co-metabolite northienamycin, which contains a C6-hydroxylmethyl side chain, suggests that the C8 and C9 carbons are added in stepwise fashion to the core structure. (9) It was also observed that Co^{II} and cobalamin increased carbapenem titers in cultures of producing strains (9), though it is not intuitively obvious why these cofactors aid production. Regarding the C2 side chain, ^{14}C or ^{35}S-cystine was fed to *S. cattleya* and incorporation was greater than 70% of the theoretical maximum. Labeled cystamine and ^{35}S-pantethine were found to be incorporated at much lower levels (9). Collectively, these experiments suggested that cysteine is the source of the C2 side chain of thienamycin. Interestingly, however, the OA-6129 series of metabolites, which contain a pantetheinyl moiety at C2, have also been isolated from carbapenem producers, suggesting that side chains longer than cysteine could play roles in carbapenem biosynthesis (12). One possible explanation that is consistent with all of these observations involves the utilization of coenzyme A (CoA, see Figure 1.5).

In CoA biosynthesis, pantothenic acid (Vitamin B5) is phosphorylated by the kinase PanK. Next, an amide bond is formed with cysteine, followed by a decarboxylation of the cysteinyl moiety, giving 4'-phosphopantetheine. Finally, two enzymes PPAT and DPCK attach adenosine monophosphate (AMP) and the 3'-ribose phosphate, respectively, to form CoA. (13) Importantly, cysteine is used to make CoA, so if a CoA metabolite were used in carbapenem biosynthesis, it would rationalize the labeling experiments as well as the presence of OA-6129 products with the extended C2 side chains.

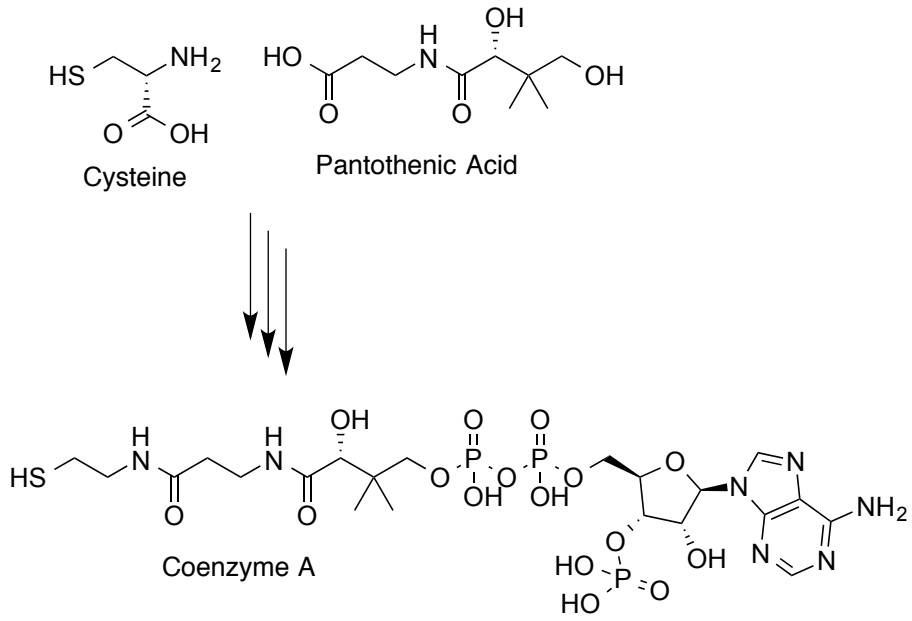

Figure 1.5: Structures of cysteine, pantothenic acid, and coenzyme A.

Through sustained efforts, several steps in carbapenem biosynthesis have been determined, though much still remains to be elucidated. The simplest carbapenem (see Figure 1.6) is produced in *Pectobacterium carotovorum*, rather than in actinomyces (14). Three enzymes are able to build the antibiotic from primary cellular metabolites (15). The first enzyme CarB utilizes L-pyrroline-5-carboxylic acid **1** and malonyl-CoA to give carboxymethylproline **2**. Using ATP, the second enzyme CarA forms the β-lactam ring, giving the (3*S*,5*S*)-carbapenam **3**. (14, 15) Finally, the nonheme iron α-ketoglutarate-dependent oxygenase performs an epimerization and desaturation to form the simple carbapenem **4** (15).

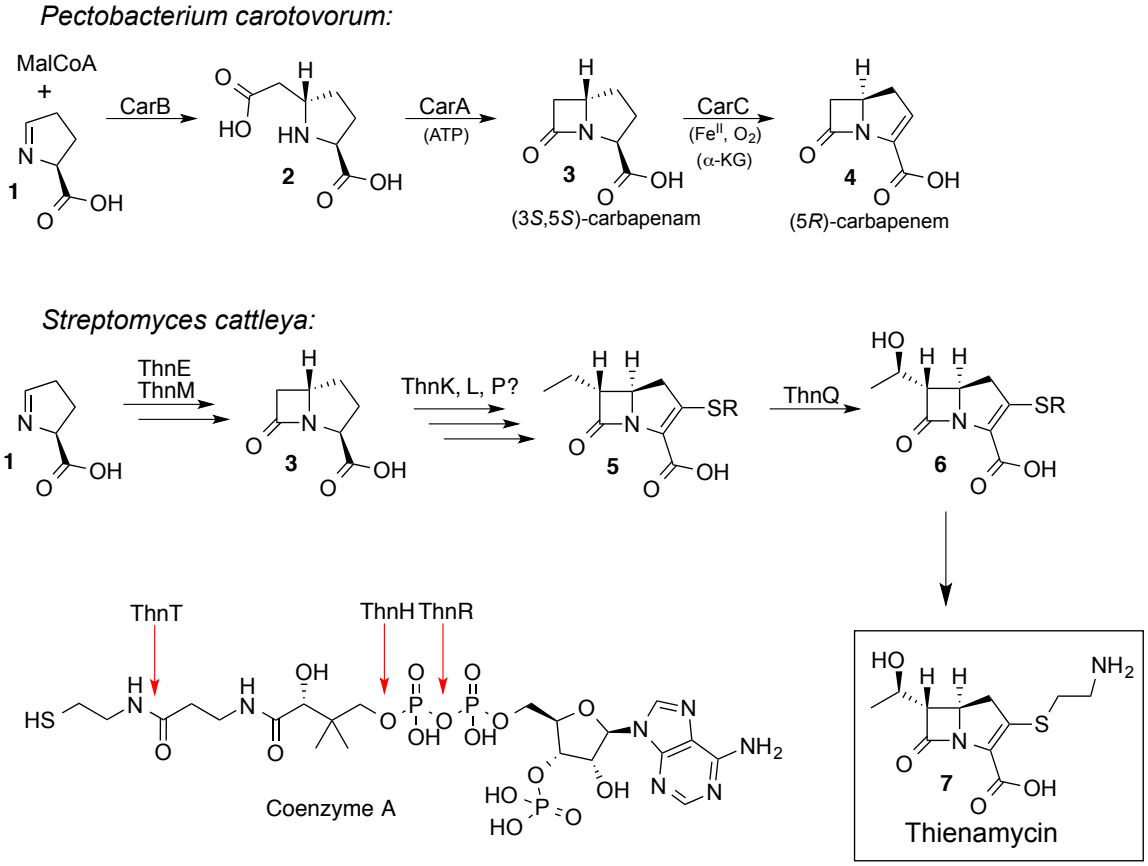

Figure 1.6: Outline of carbapenem biosynthesis.

Technical difficulties manipulating the producing strain *S. cattleya* prevented analysis of the thienamycin gene cluster for over 20 years. However, in 2003 Núñez, Salas, and coworkers obtained the cluster, which was initially thought to contain 22 genes *thnA* through *thnV* (16). It was later determined that ThnU was actually involved in cephamycin C biosynthesis and is no longer thought to be a part of the cluster (17). Additional insight into the thienamycin cluster came more recently when sequence analysis of a related gene cluster in *Streptomyces argenteolus* revealed that homologs of *thn*A-*thn*D, *thn*V, and *cph*U (*thn*U) were not present with the other *S. argenteolus* carbapenem genes (18). Thus, it appears that the thienamycin gene cluster actually begins with *thnE* and ends with *thnT*.

Biochemical experiments support that the early steps of thienamycin biosynthesis parallel those of the simple carbapenem **4**. ThnE performs the same three coupled reactions as CarB and, like CarA, ThnM is able to make the (3*S*,5*S*)-carbapenam **3** (14), as shown in Figure 1.6. From this point, the pathways diverge. The thienamycin cluster contains two putative nonheme iron, α-ketoglutarate-dependent oxygenases, which could potentially perform chemistry similar to CarC. However, ThnQ has been shown to install the hydroxyl group at C8 and ThnG is able to oxidize the C2 side-chain of thienamycin (19). Interestingly, a ThnG knockout strain is still able to produce thienamycin, suggesting that the enzyme does not play a role in the biosynthesis of this antibiotic (20).

Additional biochemical studies have shown that ThnR, ThnH, and ThnT truncate coenzyme A, phosphopantetheine, and pantetheine, respectively, to ultimately afford the cysteamine side chain present in thienamycin (see Figure 1.6), while ThnF is able to acetylate the cysteamine side chain (21). The identity of the thiol that is added to the

carbapenam(em) nucleus is not known, nor is it clear what the timing of the truncations is with respect to other biosynthetic events. Efforts were made to probe stereochemical preferences of the truncation enzymes by making several carbapenams(ems) with various C2 side chains, though most of the enzymes appeared to be nonspecific (22). ThnH, however, was the exception, preferring that the C2-C3 double bond be present before removing the phosphate from phosphopantetheine. The enzyme, however, was seemingly indifferent to the stereochemistry at the bridgehead position (22). Curiously, both ThnT and ThnR knockout strains still produce thienamycin, though this may indicate that some other enzymes are able to complement their function (20). While initial feeding experiments were interpreted to suggest that the sulfur-containing side chain was derived from cysteine, the presence of the truncation enzymes in the cluster supports the addition of a CoA-derived thiol.

Of the remaining genes in the cluster, *thnI*, *thnJ*, and *thnS* are likely involved in regulation, transport, and self-resistance, respectively (16). Thus, there are 5 remaining enzymes encoded in the cluster without assigned functions (ThnN, O, K, L, and P) and several remaining biosynthetic transformations including attachment of the C2 and C6 side chains, bridgehead epimerization, and desaturation (Figure 1.6). Gene knockout analyses indicate that all 5 enzymes are essential for carbapenem production (18, 20). Additional crossing-feeding experiments between secretor-convertor pairs suggest an ordering of N, O, L, P in the pathway (20), though the placement of ThnK is not known. While ThnN and ThnO have not been shown to have clear functions, sequence homology suggests that they could be involved in the formation of L-pyrroline-5-carboxylic acid **1**, placing them early in the biosynthetic pathway (23). ThnK, ThnL, and ThnP by sequence

analysis are thought to be cobalamin-dependent radical *S*-adenosylmethionine (RS) enzymes and are all annotated as class B RS methylases (24). Biosynthetic studies of the C6-hydroxyethyl side chain in thienamycin imply that a functional methylase(s) is present in the pathway and ThnK, L, and P would be likely candidates. If these three enzymes do utilize cobalamin, it would offer a rational explanation as to why feeding this cofactor leads to increased production of carbapenems in *Streptomyces* hosts.

RS Enzymes

RS enzymes, including ThnK, ThnL, and ThnP, were identified by the presence of a Cx_3Cx_2C motif, which is responsible for coordinating a [4Fe-4S] cluster (25). The $[4Fe\text{-}4S]^{1+}$ oxidation state is thought to be required for activity and a reducing agent, such as dithionite, is required for *in vitro* reactions. Unfortunately, exposure to oxygen (for example, during a routine protein purification) can degrade the cluster and render the enzyme inactive. (25) Thus, comprehensive work with these enzymes requires the use of an anaerobic chamber.

Work on this enzyme class began over 45 years ago with lysine 2,3-aminomutase (LAM), which converts the α-amino acid lysine into a corresponding β-amino acid (26) (Figure 1.7).

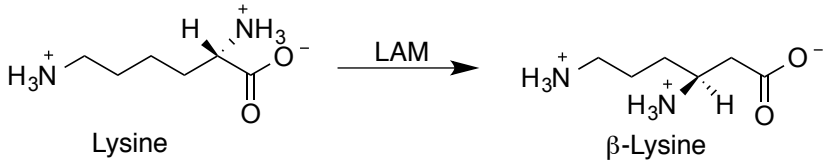

Figure 1.7: Activity of lysine 2,3-aminomutase.

This enzyme requires the cofactor pyridoxal-5'-phosphate and dithionite and activity was increased upon the addition of iron. The protein was sensitive to the presence of oxygen. At the time, it was intriguing that the protein also required a S-adenosylmethionine (SAM) cofactor (26). The enzyme class is now understood to use the [4Fe-4S] cluster to reductively cleave a molecule of SAM to form a 5'-deoxyadenosyl radical (Figure 1.8), the same radical formed in adenosylcobalamin-utilizing (vitamin B_{12}) reactions (25).

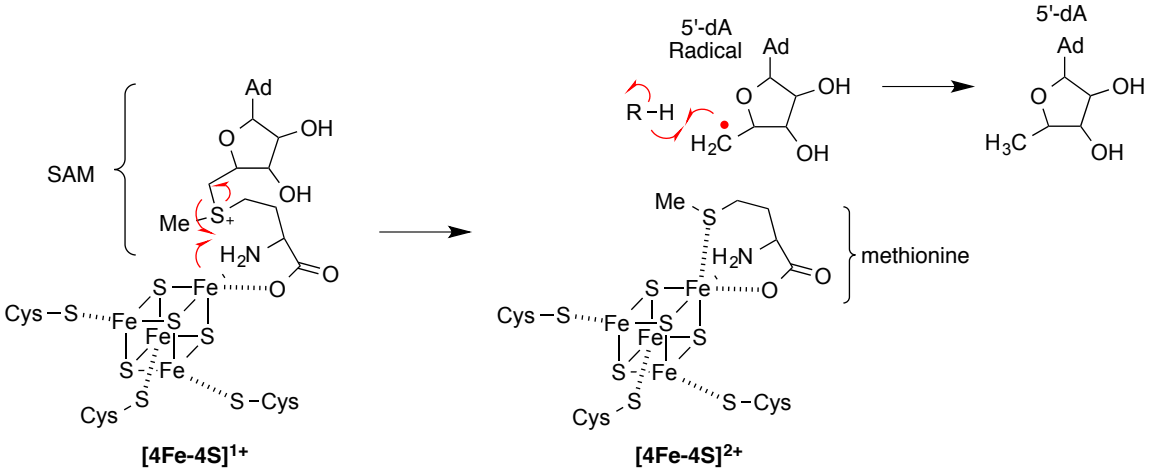

Figure 1.8: Reductive cleavage of SAM by an [4Fe-4S] cluster, modeled from (30).

This high-energy primary radical species can initiate many diverse reactions including rearrangements, cyclizations, sulfur-insertions, and methylations by abstracting a hydrogen atom from a substrate (25). If SAM is used stoichiometrically, then the enzyme produces 5'-deoxyadenosine (5'-dA) and methionine as SAM-derived coproducts.

The presence of the C2-sulfur-containing side chain in thienamycin suggests that one of the RS enzymes could be playing a role. Sulfur-insertion has precedence with RS

enzymes; for example, biotin synthase is known to convert dethiobiotin into biotin (25). Many studies on biotin synthase now support a mechanism whereby a second [2Fe-2S] cluster is cannibalized by the enzyme and provides the source of the sulfur atom (25). A CoA-derived side chain, not elemental sulfur, would provide the source of the C2-thioether in thienamycin, so it is unclear whether a second cluster would be required in this case.

There is likely at least one RS methylase in the thienamycin cluster as well. To date four classes of RS methylases have been described, termed Classes A, B, C, and D (27). The Class A methylases, exemplified by RlmN and Cfr, have two additional conserved cysteines, one of which is methylated as an intermediate. These enzymes methylate sp^2-hybridized carbons, such as C2 or C8 of adenosine. (27) In contrast, the Class B methylases are identified by a putative *N*-terminal cobalamin (Cbl)-binding domain and thought to use methyl-Cbl (Me-Cbl). Descriptions of the characterized members of this class are included below. Class C enzymes have a domain similar to the RS protein HemN and also methylate sp^2-hybridized carbons, but lack the conserved cysteine residues contained in Class A members. Finally, instead of using additional SAM for methyl group addition, Class D enzymes appear to use methylenetetrahydrofolate. (27)

The cobalamin-dependent RS enzymes, including ThnK, ThnL, and ThnP, form the most diverse class of RS methylases as they can methylate both carbon and phosphorus atoms and at multiple hybridization centers. The first *in vitro* characterization of a Class B enzyme was carried out with PhpK from *Kitasatospora phosalacinea* and it was shown to methylate a phosphinate intermediate in bialaphos

biosynthesis (28) (Figure 1.9B). The protein was insoluble and required solubilization and refolding as well as anaerobic reconstitution of the [4Fe-4S] cluster. Upon the addition of SAM, dithionite, substrate, and Me-Cbl, it was possible to follow the reaction by NMR. Using ^{13}C-labeled Me-Cbl, the authors showed that Me-Cbl is used as the source of the methyl group. (28)

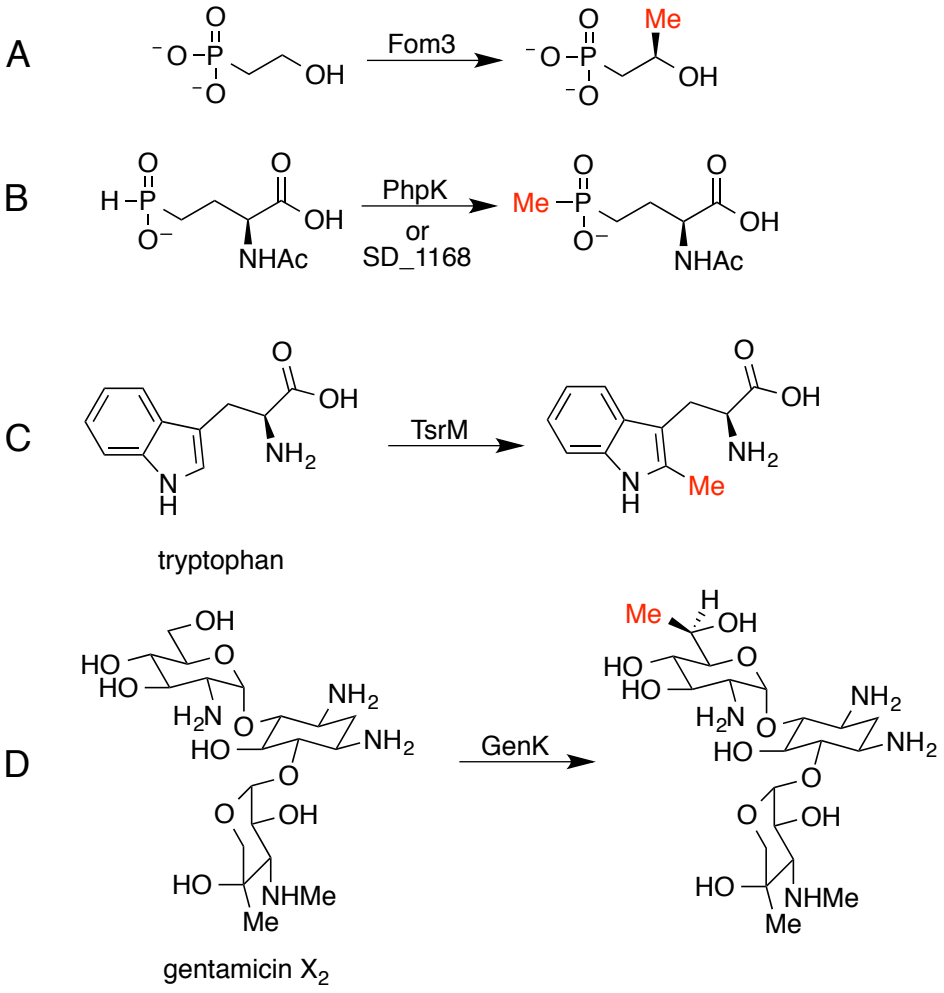

Figure 1.9: Examples of Class B RS methylases.

Following this work, TsrM was demonstrated to be a tryptophan-methylase (29), as shown in Figure 1.9C. TsrM was isolated as soluble protein and, interestingly, worked

better without dithionite present and did not produce 5'dA, but only *S*-adenosylhomocysteine (SAH), demethylated SAM, a by product seen with classical SAM-dependent methylases (Figure 1.10). The production of SAH was not dependent on the presence of the [4Fe-4S] cluster (29).

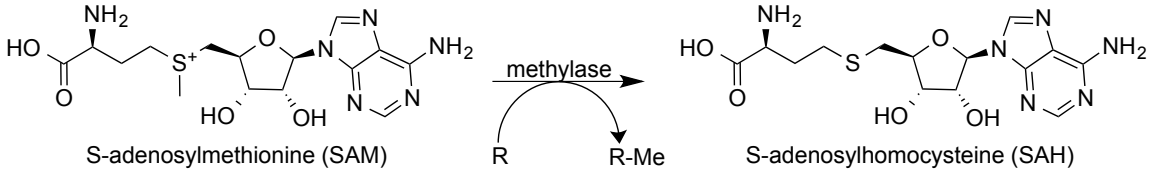

Figure 1.10: Traditional methylases use SAM as a methyl donor, producing SAH.

While this work also supported a Me-Cbl intermediate, TsrM is likely mechanistically distinct from other members of the class since it does not appear to use the canonical 5'-deoxyadenosyl radical intermediate (29). More recently, Liu and coworkers demonstrated that GenK performs a methylation in gentamicin biosynthesis (as shown in Figure 1.9D) (30). Like PhpK, GenK was isolated from inclusion bodies, refolded, and reconstituted anaerobically. Dithionite was found not to be useful with GenK (it was speculated to be due to interference by the SO_2^- ion with the cobalt), but instead the researchers employed a combination of methyl viologen and NADPH. The enzyme produced a 1:1 ratio of SAH and 5'-dA, which implied the utilization of two molecules of SAM per methylation. The work also supported a Me-Cbl intermediate in the enzymatic mechanism.

Overall, it is thought that many Class B methylases, like GenK, utilize one molecule of SAM as the methyl donor, which yields a methyl group to the cobalamin. A second SAM is then consumed in traditional RS fashion to form a 5'-dA radical that

abstracts a hydrogen atom, forming a substrate radical. This new radical then reacts with methyl-cobalamin, resulting in a methylation of the substrate. (24) This reaction sequence is summarized in Figure 1.11. Other examples of Class B members have also been characterized (31-33), albeit in less detail. More work is needed with members of Class B to ascertain the generality of the proposed mechanism within the family.

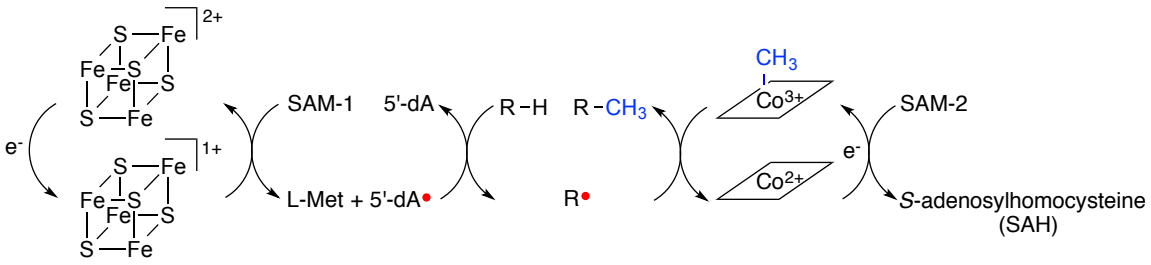

Figure 1.11: Proposed mechanism of many Class B RS methylases, (modeled from (24)).

Thesis Goals:

Once the thienamycin gene cluster became known, the presence of *three* putative cobalamin-dependent RS enzymes was an oddity, considering that only two carbons are present in the C6-hydroxyethyl side chain. Since all three enzymes are required to make carbapenems (18, 20), it is highly probable that at least one of the enzymes has a non-methylase function, which would be unprecedented for the enzyme family. Furthermore, it was possible that these three enzymes perform *all* of the remaining steps in the biosynthesis (C2, C6 side chain attachment, epimerization, desaturation, see Figure 1.6). Thus, the activities of ThnK, ThnL, and ThnP were of paramount interest both for their unknown roles in the biosynthesis of an important antibiotic and for their potentially unique enzymatic activities.

The overall goal of this dissertation is to illuminate the unknown central steps of thienamycin biosynthesis by deciphering the chemical transformations performed by the triad of RS enzymes. This objective faced multiple challenges. First, the ordering of the enzymes and their respective substrates was largely unknown. To address these questions, a library of potential carbapenam substrates was synthesized as will be described. Secondly, the enzymes themselves suffer from low solubility and high sensitivity to oxygen. Efforts were taken to obtain soluble, active RS proteins, both from *in vitro* and *in vivo* systems, and will also be delineated. Collectively, the combination of biochemical and synthetic strategies applied has advanced our understanding of the roles of the RS enzymes in thienamycin biosynthesis.

References:

1. Fleming A (1929) On the antibacterial action of cultures of a penicillium, with special reference to their use in the isolation of *B. influenzae*. *Br. J. Exp. Pathol.* 10(3):226-236.

2. Testero SA, Fisher JF, & Mobashery S (2010) β-Lactam antibiotics. *D.J. Abraham, D.P. Rotella (Eds.), Burger's Medicinal Chemistry, Drug Discovery and Development* 7:257–402.

3. Hodgkin D (1964) The X-ray analysis of complicated molecules. *Nobel Lecture*.

4. Coulthurst SJ, Barnard AML, & Salmond GPC (2005) Regulation and biosynthesis of carbapenem antibiotics in bacteria. *Nat. Rev. Microbiol.* 3(4):295-306.

5. Schofield CJ*, et al.* (1997) Proteins of the penicillin biosynthesis pathway. *Curr. Opin. Struct. Biol.* 7(6):857-864.

6. Brakhage A*, et al.* (2004) Regulation of penicillin biosynthesis in filamentous fungi. *Adv. Biochem. Engin/Biotechnol.* 88:45-90.

7. Elander RP (2003) Industrial production of β-lactam antibiotics. *Appl. Microbiol. Biotechnol.* 61(5-6):385-392.

8. Kahan JS*, et al.* (1979) Thienamycin, a new beta-lactam antibiotic. I. Discovery, taxonomy, isolation and physical properties. *J. Antibiot. (Tokyo)* 32(1):1-12.

9. Williamson J (1986) The biosynthesis of thienamycin and related carbapenems *Crit. Rev. Biotechn.* 4(1):111-131.

10. http://www.hopkinsguides.com/hopkins/index/Johns_Hopkins_ABX_Guide/All_Topics/A. (9-21-2015).

11. https://http://www.goldbio.com/product/3253/imipenem (9-21-15).

12. Okabe M*, et al.* (1982) Studies on the OA-6129 group of antibiotics, new carbapenem compounds. I. Taxonomy, isolation and physical properties. *J. Antibiot. (Tokyo)* 35(10):1255-1263.

13. Spry C, Kirk K, & Saliba KJ (2008) Coenzyme A biosynthesis: an antimicrobial drug target. *FEMS Microbiol. Rev.* 32(1):56-106.

14. Bodner MJ*, et al.* (2011) Definition of the common and divergent steps in carbapenem β-lactam antibiotic biosynthesis. *ChemBioChem* 12(14):2159-2165.

15. Li R, Stapon A, Blanchfield JT, & Townsend CA (2000) Three unusual reactions mediate carbapenem and carbapenam biosynthesis. *J. Am. Chem. Soc.* 122(1483):9296-9297.

16. Núñez LE, Méndez C, Braña AF, Blanco G, & Salas JA (2003) The biosynthetic gene cluster for the beta-lactam carbapenem thienamycin in *Streptomyces cattleya*. *Chem. Biol.* 10(4):301-311.

17. Rodríguez M*, et al.* (2008) Identification of transcriptional activators for thienamycin and cephamycin C biosynthetic genes within the thienamycin gene cluster from *Streptomyces cattleya*. *Mol. Microbiol.* 69(3):633-645.

18. Li R, Lloyd EP, Moshos KA, & Townsend CA (2014) Identification and characterization of the carbapenem MM 4550 and its gene cluster in *Streptomyces argenteolus* ATCC 11009. *ChemBioChem* 15(2):320-331.

19. Bodner MJ, Phelan RM, Freeman MF, Li R, & Townsend CA (2010) Non-heme iron oxygenases generate natural structural diversity in carbapenem antibiotics. *J. Am. Chem. Soc.* 132(1):12-13.

20. Rodríguez M*, et al.* (2011) Mutational analysis of the thienamycin biosynthetic gene cluster from *Streptomyces cattleya*. *Antimicrob. Agents Chemother.* 55(4):1638-1649.

21. Freeman MF, Moshos KA, Bodner MJ, Li R, & Townsend CA (2008) Four enzymes define the incorporation of coenzyme A in thienamycin biosynthesis. *Proc. Natl. Acad. Sci. USA* 105(32):11128-11133.

22. Moshos KA (2011) Design and synthesis of substrates and standards used to elucidate activities of enzymes in carbapenem gene clusters. Ph.D. Thesis (The Johns Hopkins University, Baltimore, MD).

23. Suzuki H, Ohnishi Y, & Horinouchi S (2007) GriC and GriD constitute a carboxylic acid reductase involved in grixazone biosynthesis in *Streptomyces griseus*. *J. Antibiot. (Tokyo)* 60(6):380-387.

24. Zhang Q, van der Donk WA, & Liu W (2012) Radical-mediated enzymatic methylation: a tale of two SAMS. *Acc. Chem. Res.* 45(4):555-564.

25. Broderick JB, Duffus BR, Duschene KS, & Shepard EM (2014) Radical *S*-adenosylmethionine enzymes. *Chem. Rev.* 114(8):4229-4317.

26. Frey PA, Hegeman AD, & Ruzicka FJ (2008) The radical SAM superfamily. *Crit. Rev. Biochem. Mol. Biol.* 43(1):63-88.

27. Bauerle MR, Schwalm EL, & Booker SJ (2015) Mechanistic diversity of radical *S*-adenosylmethionine (SAM)-dependent methylation. *J. Biol. Chem.* 290(7):3995-4002.

28. Werner WJ*, et al.* (2011) In vitro phosphinate methylation by PhpK from *Kitasatospora phosalacinea*. *Biochemistry* 50(42):8986-8988.

29. Pierre S*, et al.* (2012) Thiostrepton tryptophan methyltransferase expands the chemistry of radical SAM enzymes. *Nat. Chem. Biol.* 8(12):957-959.

30. Kim HJ*, et al.* (2013) GenK-catalyzed C-6' methylation in the biosynthesis of gentamicin: isolation and characterization of a cobalamin-dependent radical SAM enzyme. *J. Am. Chem. Soc.* 135(22):8093-8096.

31. Allen KD & Wang SC (2014) Initial characterization of Fom3 from *Streptomyces wedmorensis*: The methyltransferase in fosfomycin biosynthesis. *Arch. Biochem. Biophys.* 543:67-73.

32. Allen KD & Wang SC (2014) Spectroscopic characterization and mechanistic investigation of *P*-methyl transfer by a radical SAM enzyme from the marine bacterium *Shewanella denitrificans* OS217. *Biochimica et Biophysica Acta (BBA) - Proteins and Proteomics* 1844(12):1-10.

33. Huang C*, et al.* (2015) Delineating the biosynthesis of gentamicin X2, the common precursor of the gentamicin C antibiotic complex. *Chem. Biol.* 22:251-261.

Chapter 2

Synthesis of Potential Substrates and Product Standards for Thienamycin RS Enzymes

Introduction

The synthesis of a variety of possible substrates and product standards was undertaken to provide a library to screen against the thienamycin RS enzymes. The first desired compound was the only known intermediate in thienamycin biosynthesis, the (3S,5S)-carbapenam **3**, which is the product of ThnE and ThnM (1). If methylation were the next step after bicycle formation, then C6-methyl and ethyl variations of **3**, compounds **8** and **9**, respectively, could also be intermediates. Alternatively, C2-thioether formation could precede methylation. A few possible thiols could be attached to the core structure by an unknown enzyme. For the library, we selected a pantetheinyl C2 side chain that matches the OA-6129 series of isolated natural carbapenems (2). Earlier work in the Townsend lab also suggested that at least one late-stage enzyme (ThnQ) functions with a C2-pantetheinyl group (3). Furthermore, pantetheine represents an intermediate length of possible thiols ranging from CoA to cysteamine (4). To assess possible enzymatic stereochemical preferences, both pure C2-diastereomers **10** and **11** were desired. In case C5-epimerization occurs early in the pathway, the C5-diastereomer of **10** and **11**, compound **12**, would also be synthesized. Figure 2.1 depicts the synthetic targets.

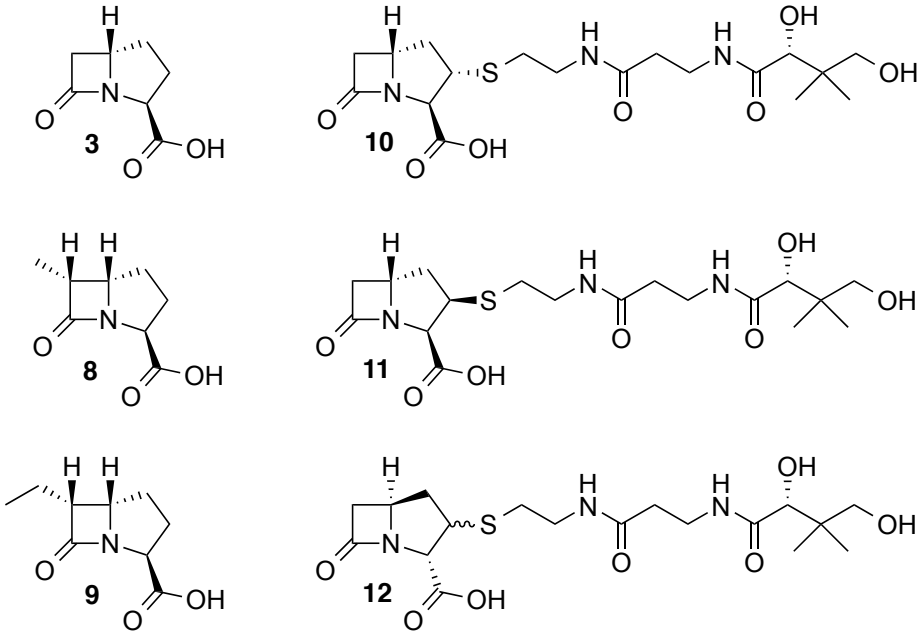

Figure 2.1: Synthetic targets for probing RS activity.

Results and Discussion

*Synthesis of Compounds **3**, **8**, and **9***

The (3*S*,5*S*)-carbapenam **3** had been previously synthesized in the Townsend lab by C.J. Hastings and others following previously described procedures (5) and did not need to be generated for the RS experiments. A route based on the work of Ohta *et al*. (6) was employed (Figure 2.2) to make compounds **8** and **9**. In their paper, the authors began with L-pyroglutamic acid to make a carbapenem with the "antibiotic" bridgehead. We desired the opposite "non-antibiotic" bridgehead and thus began with D-pyroglutamic acid **13**. This compound was protected with benzyl bromide and benzyl chloroformate, sequentially. The desired protected material **14** was purified by recrystallization from hot ethyl acetate/hexanes (~80% yield). Next, either *tert*-butyl propionate **15** was needed to provide a C6-methyl group or *tert*-butyl butyrate **16** for a C6-ethyl group. While **15** is available commercially, **16** was synthesized from butyryl chloride and potassium *tert*-

butoxide. The resulting oil was purified by vacuum distillation to yield a clear oil. The enolate of either **15** or **16** was reacted with compound **14** to provide compounds **17** and **18**, respectively, in approximately 70% yield. A reductive amination using palladium on carbon under a hydrogen atmosphere cyclized the five-member ring, generating **19** (methyl) or **20** (ethyl). Each of these products is a mixture of diastereomers at the site where the methyl or ethyl group is attached. During the reductive amination, the carboxylic acid directs the desired stereochemistry at what will become C5 in the carbapenam. A Boc protection followed by a PNB protection formed **21** and **22.** These compounds were deprotected by removing the Boc and *tert*-butyl groups. A coupling reaction with *N,N′*-dicyclohexylcarbodiimide (DCC) produced the carbapenams **23** and **24** in greater then 80% yield. The ratio of the C5-C6 *trans* isomer to the *cis* isomer is approximately 1:2 (6). These diastereomers are not separable by silica chromatography. Treatment with 1,8-diazabicyclo[5.4.0]undec-7-ene (DBU) and mild heating selectively isomerized at the α-position (C3) to the protected carboxylic acid, forming carbapenams **25**-**28**. This reaction was a departure from the Ohta synthesis and was inspired by the observation by Bateson *et al*. that *endo*-esters at C3 in carbapenams can be isomerized to *exo* using DBU (7). The isomerization can be monitored by ^{1}H-NMR in acetonitrile-d_3 (Figure 2.3). The doublet corresponding to the C8 methyl hydrogens in **23** (~ 1 ppm) has a diagnostic chemical shift depending if the C5-C6 orientation is *cis* or *trans* (Figure 2.3). Both of these doublets shift during the C3-epimerization.

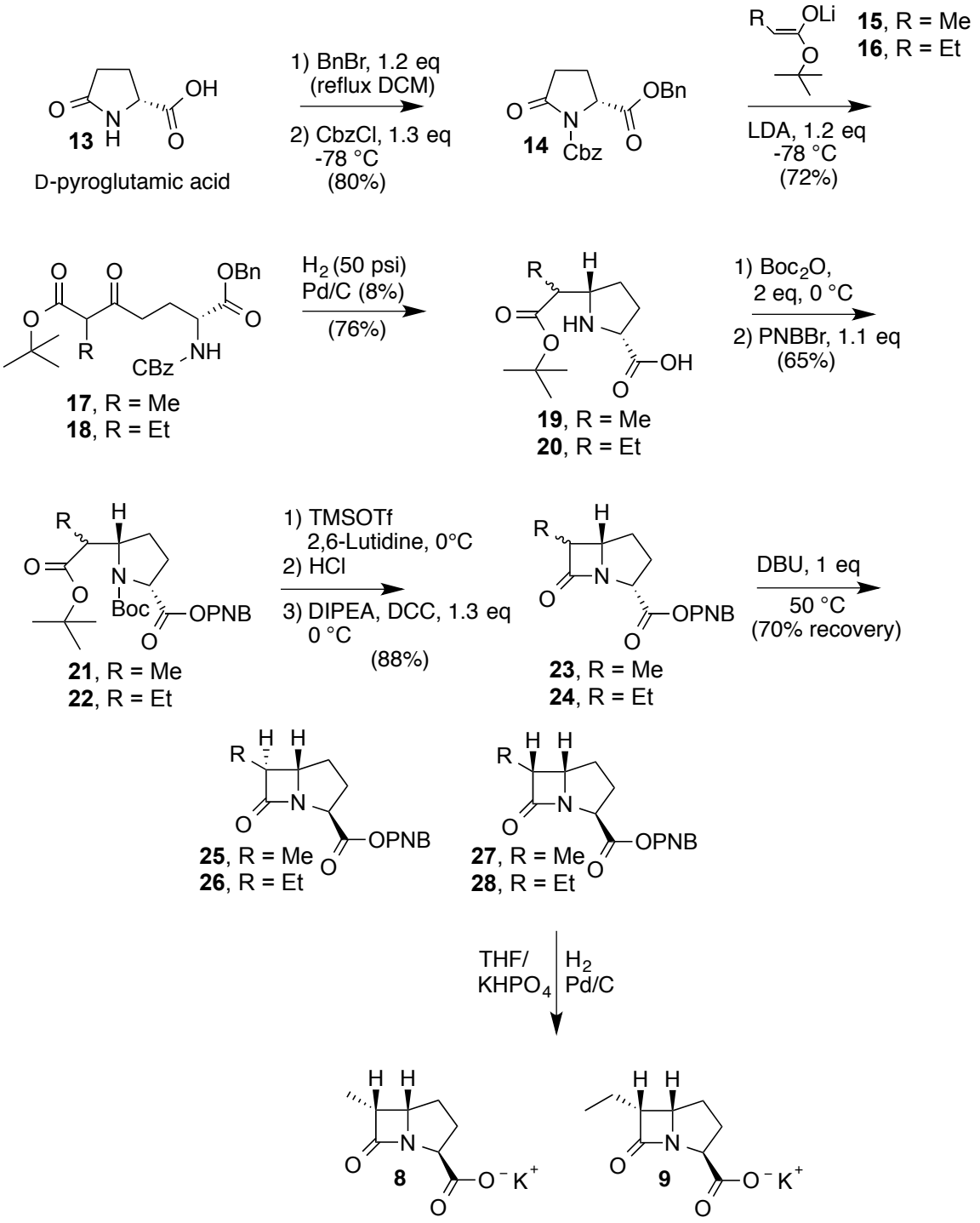

Figure 2.2: Synthetic route to compounds 8 and 9.

Additionally, the resonances corresponding to the C3 hydrogens overlap for the *cis* and *trans* diastereomers in **23**; however, both signals shift downfield (to 4.4 ppm) and

resolve during isomerization, resulting in the *trans* diastereomer **25** triplet being more downfield than the *cis* **27** triplet by ca. 0.06 ppm. The C6-diastereomers (**25** and **27** or **26** and **28**) were then separable by silica gel chromatography, with the C5-C6 *cis* isomer eluting first (6). The two isomers can be distinguished by the coupling constant between H5 and H6 (*cis*: ~5.5 Hz, *trans*: ~2 Hz). To generate the final deprotected carbapenams **8** and **9**, the PNB-protected *cis* compounds **27** and **28** were hydrogenated in THF/0.5 M potassium phosphate buffer. A desalting column with HP-20 was needed to remove excess buffer.

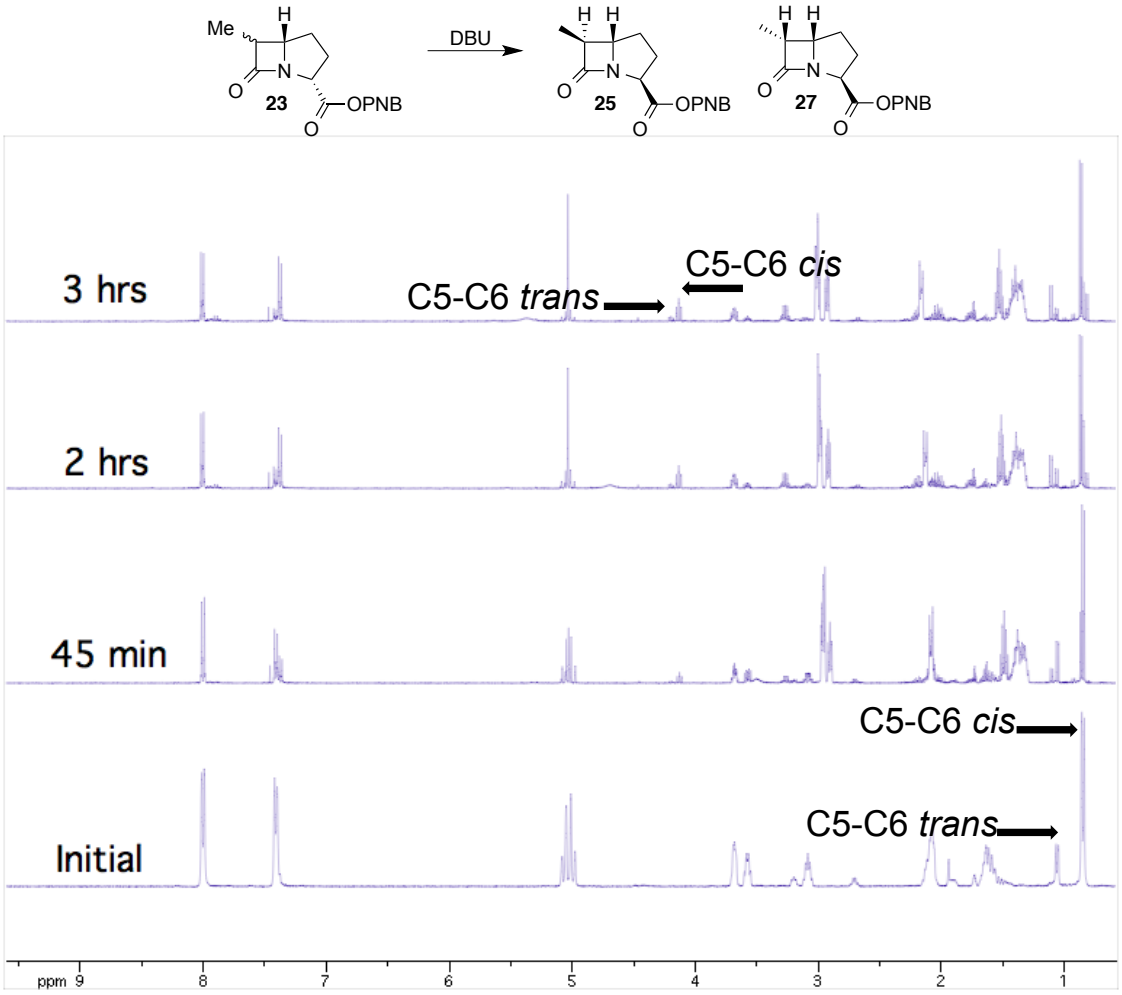

Figure 2.3: DBU isomerization of 23 by ^{1}H-NMR.

*Synthesis of Compounds **10-12***

To synthesize the C-2 substituted carbapenams **10-12**, a route was based on previously described strategies (8, 9) and further developed by K.A. Moshos (3, 10) in the Townsend lab (Figure 2.4). The synthesis began with the relatively inexpensive precursors, sorbic acid **29** and menthol **30**, which were coupled using DCC to give the ester **31**. The diene **31** was isomerized using lithium diisopropylamide (LDA) whereupon the resulting terminal double bond was reacted with an isocyanate, yielding the β-lactam **32** as a mixture of diastereomers. The diastereomers were separated by fractional crystallization from diethylether in which the *S*-isomer **33** was less soluble. **33** can be recrystallized to good optical purity from ether (mp: 129-132 °C, lit: 125-128 °C, (9)). The diastereomer **34** can be removed from the mother liquor by the addition of pentanes, although it typically contains residual **33**. Additional recrystallizations beyond the procedures of Ueda *et al.* and Moshos were employed to help address this contamination. Compound **34** was recrystallized from MeOH/water using approximately 20 mL MeOH per gram of **34** (mp: 78.5-80 °C, lit: 77.5-78.5 °C, (9)). Another isomerization using 1,4-diazabicyclo[2.2.2]octane (DABCO) gives **35**, which was reacted with the hydrated aldehyde **36**. The PNB-glyoxylate **36** was generated from PNB-protected tartaric acid, which was oxidatively cleaved using periodic acid. Reaction with thionyl chloride followed by the addition of triphenyl phosphine resulted in the formation of the ylide **37**. Reductive ozonolysis (dimethylsulfide) gave the corresponding aldehyde. Upon basic work-up, an intramolecular Wittig reaction ensued to give the carbapenem **38**.

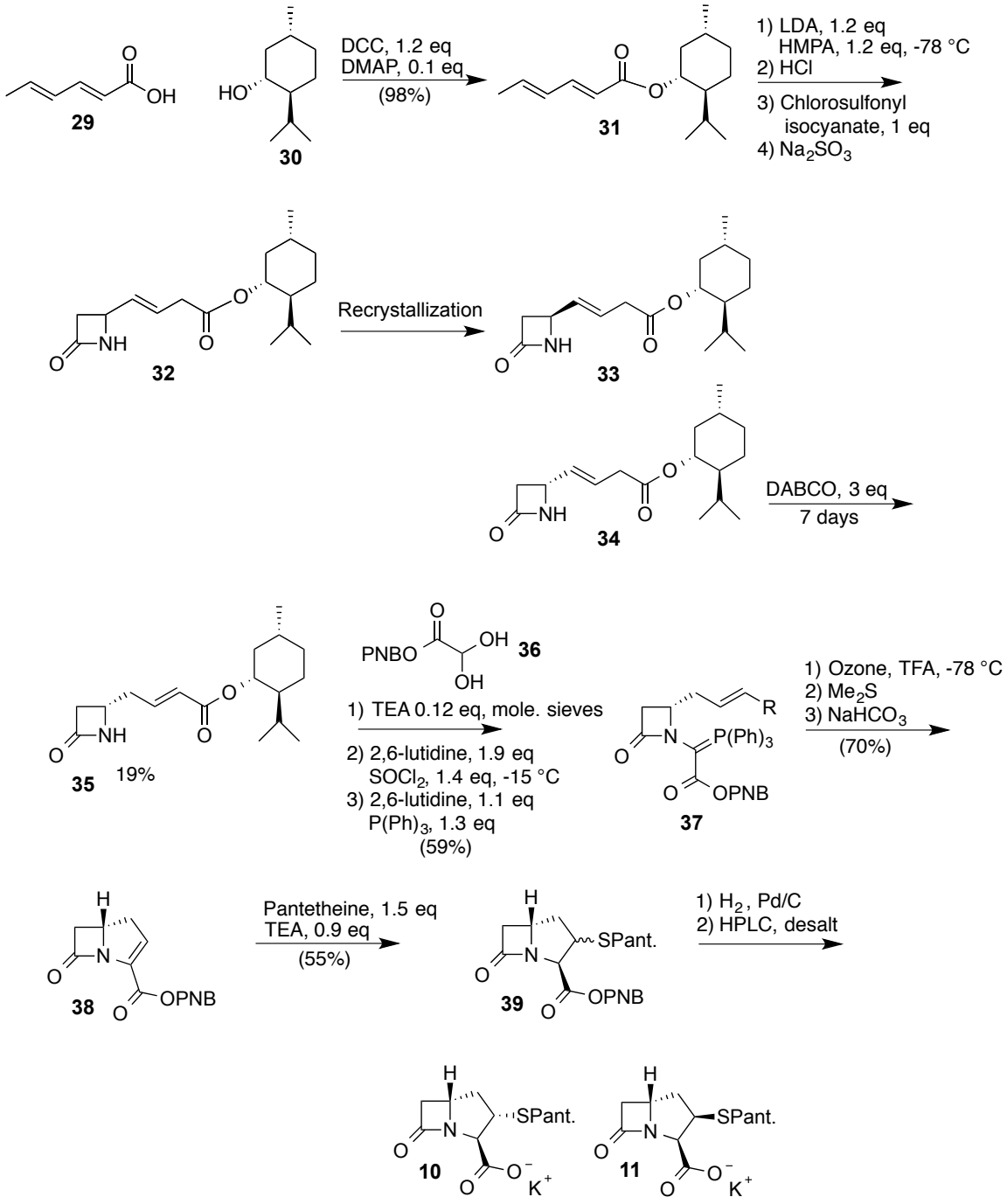

Figure 2.4: Synthetic route to compounds 10 and 11.

The enantiopurity of **38** can be assessed by chiral HPLC (Pirkle covalent (*R*,*R*) Whelk-01 5100, 50% ACN/H_2O, 267 nm); a slight difference (ca. 0.5 min) in retention time between **38** and its enantiomer **40** was observed (Figure 2.5). Unfortunately, a single

MeOH/H_2O recrystallization of **34** did not lead to a significant increase in purity of **38** when compared to a sample that was not recrystallized (Figure 2.5). Further recrystallization(s) in principle should achieve the goal.

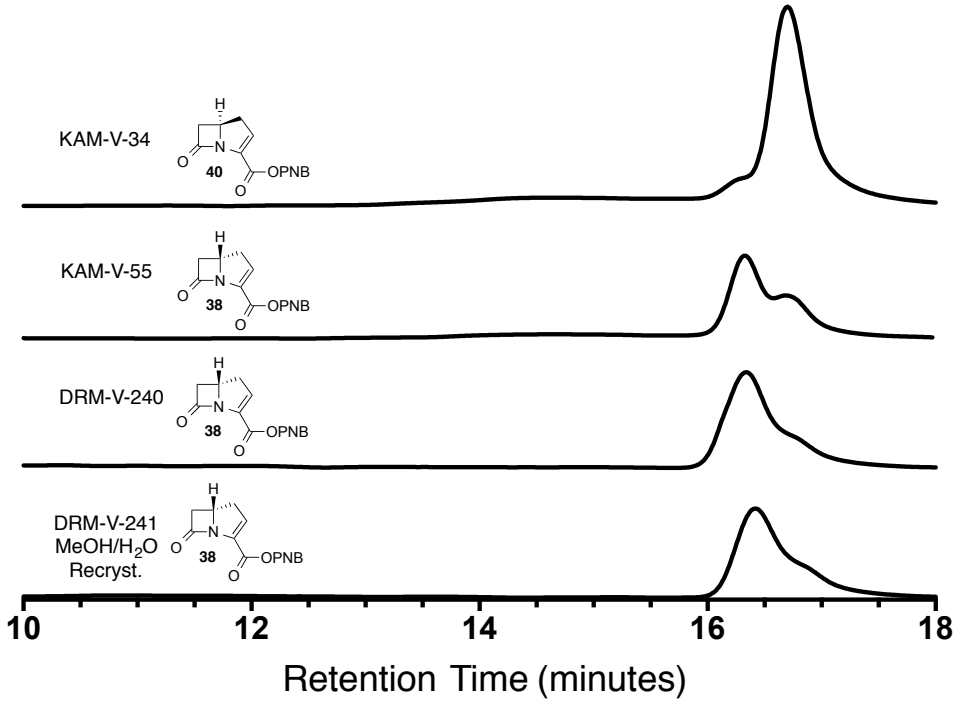

Figure 2.5: Chiral HPLC analysis of compound 38.

With **38** (or its enantiomer **40**) in hand, the desired thiol, pantetheine in this case, was attached in a β-addition to the carbapenem. This reaction resulted in the formation of several of the possible stereoisomers at C2 and C3. On the basis of previous stereochemical analyses (7) and Nuclear Overhauser Effect (n.O.e.) NMR experiments performed by K. A. Moshos (3), the isomer with the H3 doublet farthest downfield as assessed by ^{1}H-NMR (~4.8 ppm) has the *cis*-*exo* stereochemical relationship (Figure 2.6). The other main isomer observed from the pantetheine addition (H3 doublet at ~4.4 ppm) was assigned by Moshos to have the *trans*-*endo* thioether stereochemical relationship. This assignment and corresponding chemical shift is consistent with the report of Bateson

et al. where *N*-acetylcysteamine (SNAC) was added to a carbapenem instead of pantetheine (11). Another isomer corresponding to the *cis-endo* stereochemistry can also be observed depending on the conditions (7).

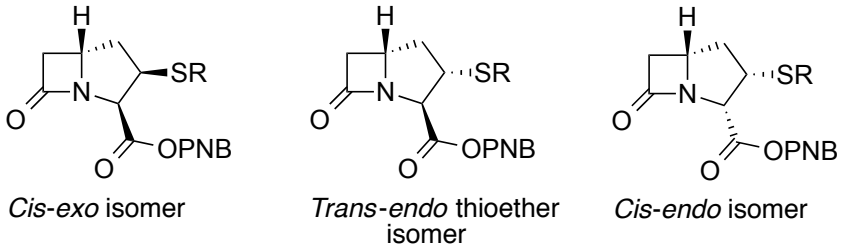

Figure 2.6: Stereoisomers from thiol addition.

Hydrogenation of **39** followed by a desalting column gave **10** and **11** as a mixture. Moshos was able to generate the diastereomer **12** with the inverted bridgehead using the same approach, but using **33** in lieu of **34** at the appropriate step (3, 10). To isolate **10** and **11** individually, the compounds were separated using preparative HPLC (C18, 25% MeOH/75% 10 mM K_2PO_4 pH 6.65, 210 nm). Figure 2.7 shows a typical HPLC trace for the separation.

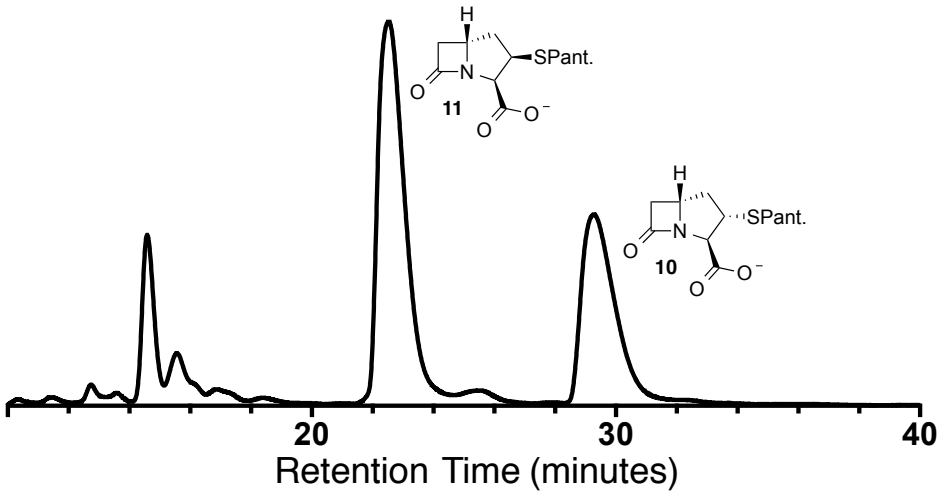

Figure 2.7: HPLC separation of 10 and 11.

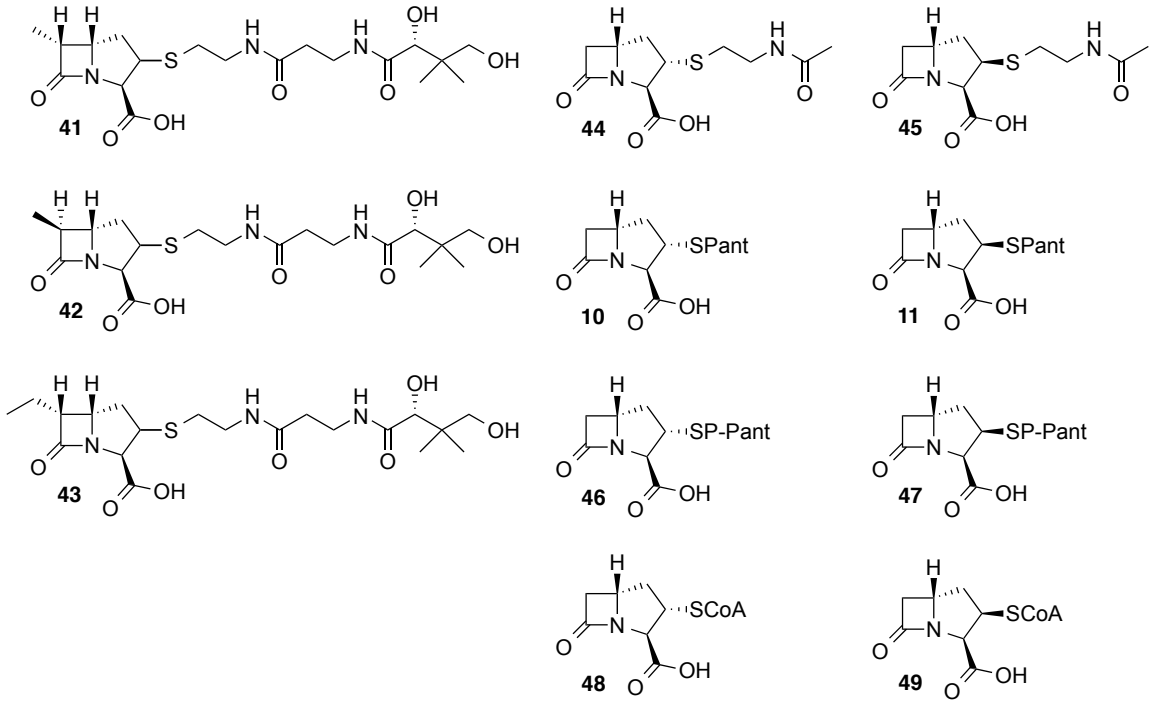

Figure 2.8: Additional synthetic targets for probing RS activity.

Additional Synthetic Targets

After the initial library including **3** and **8**-**12** was completed and tested *in vitro*, it became clear that additional potential substrates/product standards were needed. The first set of compounds to be generated (**41**-**43**) contained both a C2-pantetheinyl moiety, matching **10**-**12**, and an alkyl group at C6 (Figure 2.8). The second set of molecules (**44**-**49**) was designed to probe various C2 side chains. In addition to **10** and **11** with a C2-pantetheine, which had been synthesized previously, we sought to prepare analogs bearing SNAC, phosphopantetheine, or coenzyme A at C2.

*Synthesis of C2- and C6-Substituted Compounds **41-43***

To generate **41** and **43**, a previously used strategy (6) was initially employed (see Figure 2.2). From **19** and **20**, the carboxylic acid protecting group was switched to a

methyl ester giving **50** and **51** (Figure 2.9). From this point, a route similar to the PNB-ester analogs was used to make the C5-C6 *cis*-carbapenams **56** and **57**.

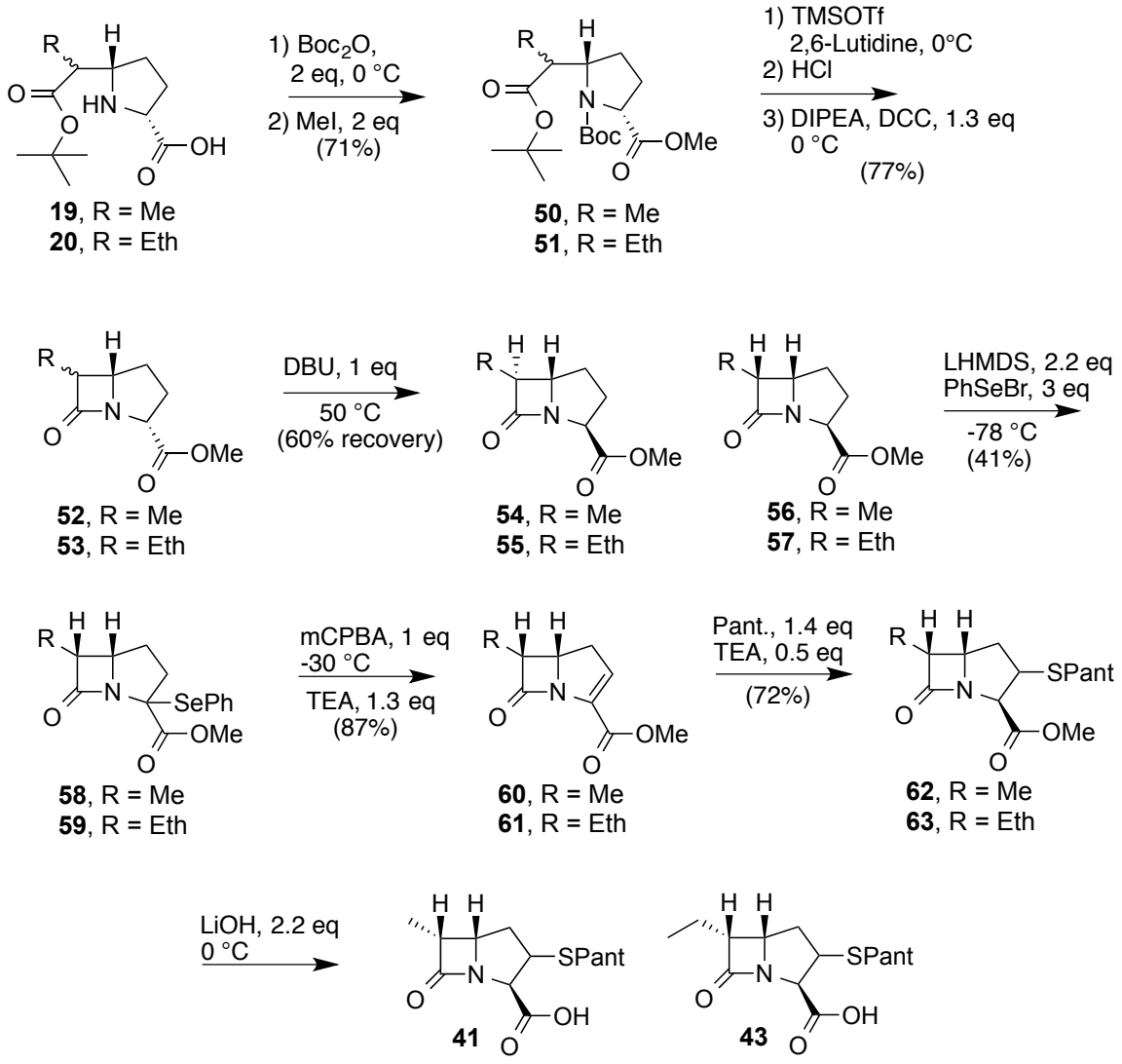

Figure 2.9: Synthetic route to C2 and C6-substituted carbapenams 41 and 43.

Next, phenylselenation followed by an oxidative elimination afforded the carbapenems **60** and **61** in a manner similar to that previously described (6). Pantetheine can be added into the double bond to generate the C2 side chain in **62** and **63**. Two C2/C3-stereoisomers were observed and assigned to be the *cis-exo* and *trans-endo* thioethers based upon the stereochemical analysis carried out with **39**, the analogous

molecule lacking a C6 side chain (see Figure 2.6). Saponification with lithium hydroxide yielded **41** and **43**. Some enrichment of each stereoisomer of **41** (**41a** *trans-endo* thioether, **41b** *cis-exo*) was achieved using HPLC. The analog of **41** having a *trans* C6-methyl (**42**) was prepared as a racemate by Moshos using a route similar to that shown in Figure 2.4 (3, 10).

*Synthesis of C2-Substituted Compounds **44-49***

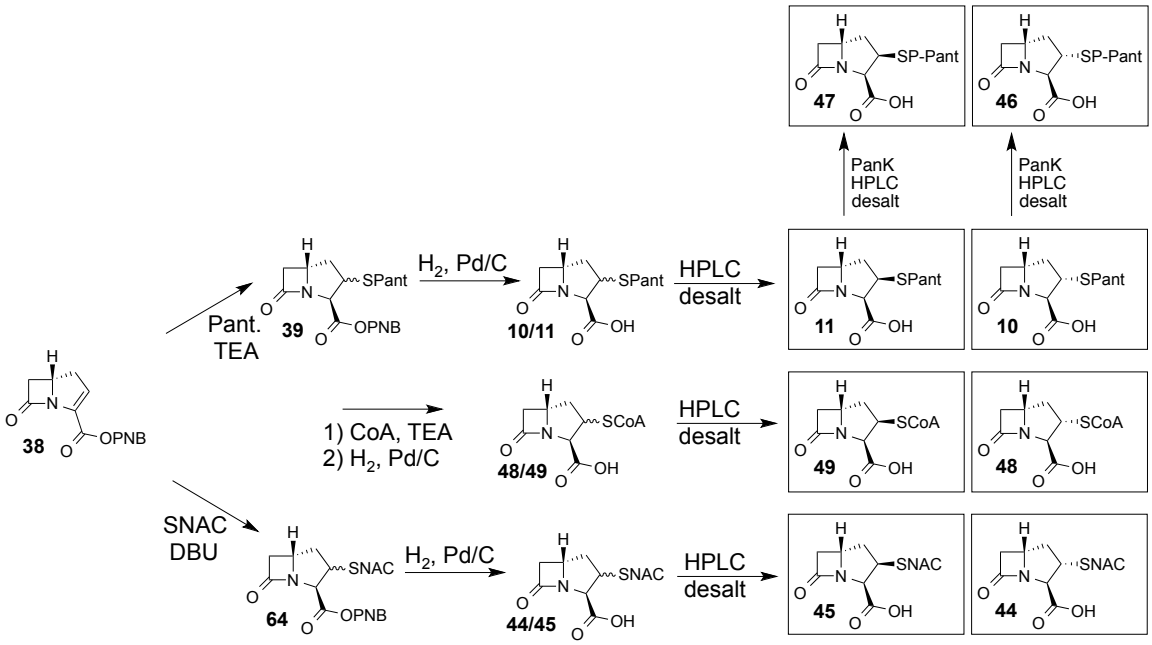

Figure 2.10: Synthesis and Purification of 44-49.

To prepare the additional C2-substituted compounds, the carbapenem **38** was again utilized. SNAC was added into **38** using 0.1 eq of DBU, as described by Moshos (3), to yield **64**. It was discovered that CoA itself could be also be added directly into the carbapenem using similar conditions to those employed for the pantetheine addition. Hydrogenation followed by HPLC purification of the C2-diastereomers resulted in the desired CoA-(**48** and **49**) and SNAC-(**44** and **45**) containing compounds from the corresponding esters (Figure 2.10). Typical HPLC traces for the separation of **44**/**45** and

48/**49** are shown in Figure 2.11. To produce the C2-phosphopantetheine derivatives **46** and **47**, the pantetheinyl compounds **10** and **11** were incubated with PanK (CoaA), a native CoA biosynthetic enzyme (12), and ATP as described previously (13). This enzymatic strategy for forming a phosphopantetheine moiety has been used previously in the Townsend lab (3) and experimental details are provided in the *Materials and Methods* section. HPLC was used to purify **46** and **47** from residual ATP/ADP.

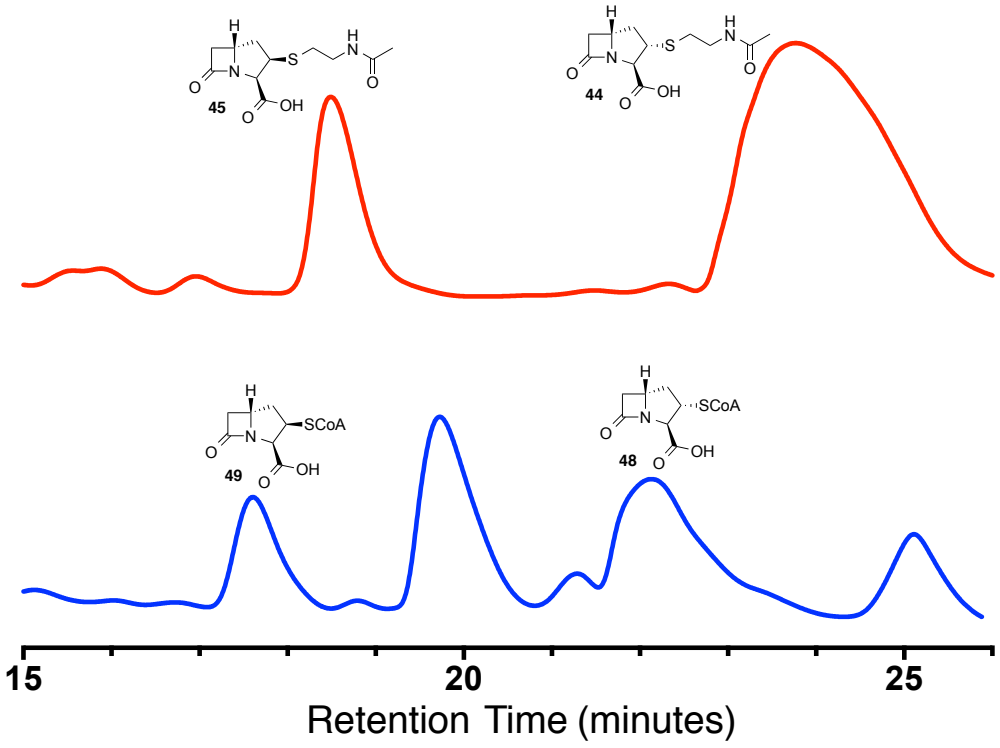

Figure 2.11: HPLC separation of 44/45 and 48/49.

The top trace (red) shows the separation of the C2-SNAC compounds, **44** and **45** (Conditions: C18, 18% MeOH/82% 10 mM K_2PO_4 pH 6.65, 210 nm).
The bottom trace (blue) shows the separation of the C2-CoA compounds, **48** and **49** (Conditions: C18, 13% MeOH/87% 10 mM K_2PO_4 pH 6.65, 254 nm). Since the PNB-protected CoA-carbapenam is not purified prior to hydrogenation due to degradation on silica, the HPLC traces typically contain contaminants. The correct peaks are initially identified by High-Resolution-MS.

Conclusions

To probe the function of the thienamycin RS enzymes, a chemical library of potential substrates was desired. Two general strategies were employed to generate a variety of C2- and C6-substituted carbapenams. For many of the C2-substituted compounds, the route involved reaction of a terminal olefin with an isocyanate to form the β-lactam. An intramolecular Wittig reaction closed the bicycle. For the C6-alkylated compounds, the synthetic pathway began with pyroglutamic acid and used a peptide coupling to install the β-lactam. The combination of approaches afforded all required carbapenams, enabling *in vitro* testing with the RS enzymes (Chapter 3).

Materials and Methods

A Bruker Avance (Billerica, MA) 300 or 400 MHz spectrometer was utilized for all ^{1}H and ^{13}C NMR spectra, which are reported in parts per million (δ) referenced against a TMS standard or residual solvent peak. The JHU Chemistry Department Mass Spectrometry Facility determined exact masses by fast atom bombardment (FAB) or electrospray ionization (ESI).

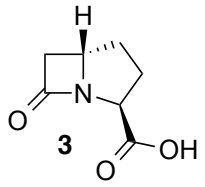

3

Compound 3: The (3*S*,5*S*)-carbapenam (**3**) was synthesized as previously described (5).

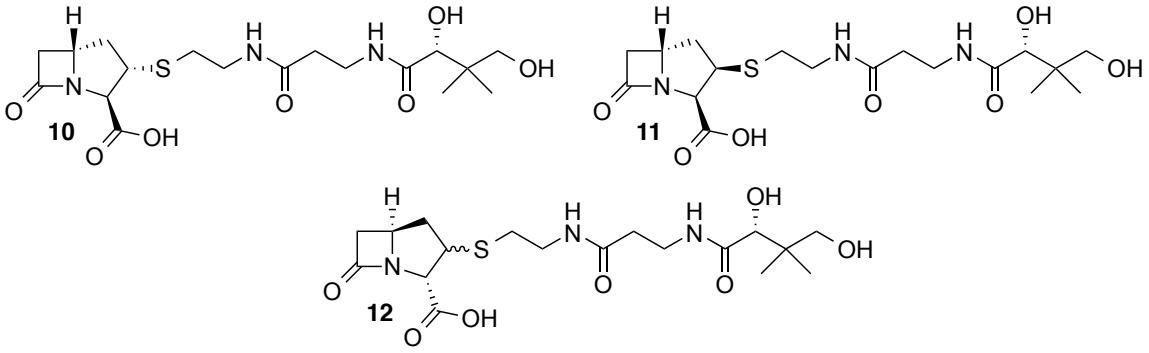

Compounds 10, 11, 12: The C2-pantetheinyl carbapenams were made as previously described (3, 10). The diastereomers **10** and **11** were separated from each other and purified using an Agilent model 1100 HPLC equipped with a multi-wavelength ultraviolet–visible detector in conjunction with a reverse-phase Phenomenex Luna 10µ C18(2) 100 Å preparatory column (250 x 21.20 mm ID). The mobile phase was isocratic 25% methanol and 75% buffer (10 mM potassium phosphate, pH 6.65) at a flow rate of 5 ml per min. Compound **10** eluted at 29 min and compound **11** eluted at 22 min.

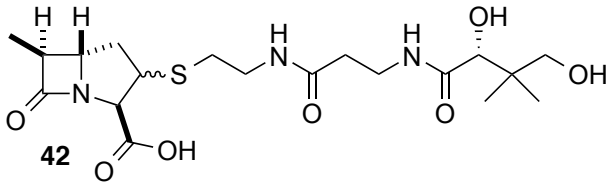

Compound 42: The C6-*trans*-methyl, C2-pantetheinyl carbapenam was prepared as a racemate by K. Moshos (3, 10) using previous strategies (14, 15).

Compounds 8, 9, 41, 43:

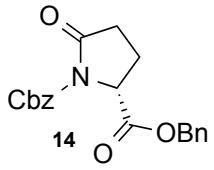

Benzyl (2*R*)-1-carboxybenzyl-5-oxopyrrolidine-2-carboxylate (14).

Diisopropylethylamine (54 mL, 310 mmol) was added to D-pyroglutamic acid (20 g, 160 mmol, TCI America/AK Scientific) in dichloromethane (500 mL). Benzyl bromide (22 ml, 190 mmol) was added and the solution was refluxed for 4h. The reaction mixture was concentrated *in vacuo* and the crude oil was redissolved in ethyl acetate (400 ml). The cloudy mixture was filtered through silica on top of Celite and the silica/Celite plug was washed twice with ethyl acetate (200 mL). The eluate was concentrated *in vacuo* and redissolved in tetrahydrofuran (600 mL) to which was added lithium bis(trimethylsilyl)amide (155 mL, 1.0 M, 155 mmol) at -78 ˚C and stirred for 10 min. Benzyl chloroformate (30.8 mL, 202 mmol) was added and the reaction mixture was allowed to stir for 10 min. The reaction was quenched with aqueous ammonium chloride (400 mL) and the solution was warmed to room temperature and the phases were separated. The aqueous layer was extracted 5× with ethyl acetate (400 mL) and the combined organic fractions were washed with brine, dried with anhydrous magnesium sulfate, filtered, and concentrated *in vacuo*. The solid crude product was recrystallized from hot ethyl acetate/hexanes to give **14** as white crystals (34.4 g, 63% yield). **^{1}H-NMR** (400 MHz; $CDCl_3$): δ 7.36-7.28 (m, 10H), 5.22 (d, J = 1.3 Hz, 2H), 5.13 (s, 2H), 4.72 (dd, J = 9.4, 2.7 Hz, 1H), 2.68-2.58 (m, 1H), 2.50 (ddd, J = 17.6, 9.3, 3.3 Hz, 1H), 2.34 (ddt, J = 13.4, 10.4, 9.4 Hz, 1H), 2.09-2.02 (m, 1H) ppm; **^{13}C NMR** (101 MHz; $CDCl_3$):

δ 172.9, 170.9, 150.9, 135.10, 135.08, 128.80, 128.73, 128.69, 128.56, 128.41, 128.26, 68.5, 67.5, 58.9, 31.1, 21.9 ppm. **HRMS** (FAB) *m/z*: $[M+H]^+$ calcd. for $C_{20}H_{19}NO_5$ 354.13415; found 354.13342.

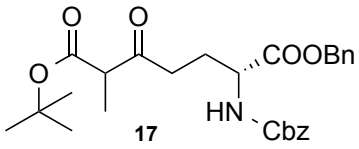

17

7-Benzyl 1-*tert*-butyl (6*R*)-6-(benzyloxycarbonylamino)-2-methyl-3-oxoheptanedioate (17). This synthesis was adapted from the procedures of Ohta *et al.* (6). A solution of lithium diisopropylamide in tetrahydrofuran (17 mL, 2.0 M, 34 mmol) was added to a solution of *tert*-butyl propionate (4.3 ml, 28 mmol) in tetrahydrofuran (300 mL) at -78 ˚C and allowed to stir for 30 min. A solution of **14** in tetrahydrofuran (40 mL) was added slowly to the reaction mixture. After stirring for 30-60 min at -78 ˚C, the reaction was quenched with saturated ammonium chloride and the phases were separated. The aqueous layer was extracted three times with dichloromethane (50 mL). The combined organic layers were washed with brine, dried with anhydrous magnesium sulfate, and concentrated *in vacuo*. The crude oil was purified by silica gel chromatography using 25% ethyl acetate in hexanes to give **17** (9.9 g, 72%) as a colorless oil, which solidified overnight at room temperature. TLC (ethyl acetate:hexanes, 2:3 v/v): R_f = 0.75; **^{1}H-NMR** (400 MHz; $CDCl_3$): δ 7.35 (s, 10H), 5.30-5.46 (m, 1H), 5.17 (s, 2H), 5.09 (s, 2H), 4.31-4.47 (m, 1H), 3.34-3.36 (m, 1H), 2.47-2.73 (m, 2H), 1.94-2.22 (m, 2H), 1.42 (s, 9H), 1.23 (bd, *J* = 6.8 Hz, 3H) ppm; **^{13}C NMR** (101 MHz; $CDCl_3$): δ 205.2, 171.8, 169.6, 156.0, 136.2, 135.3, 128.74, 128.62, 128.44, 128.29, 128.20, 82.0, 67.4,

67.2, 53.9, 53.6, 37.3, 28.0, 26.4, 12.8 ppm; **HRMS** (FAB) *m/z*: $[M\text{-}OH]^+$ calcd. for $C_{27}H_{33}NO_7$ 466.22296; found 466.22072.

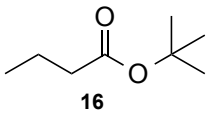

16

***tert*-Butyl butyrate (16).** Conditions were modeled after a similar reaction (http://orgprepdaily.wordpress.com/2007/07/25/2-chloro-5-iodobenzoic-acid-tert-butyl-ester/. [Accessed 09 April 15]). Butyryl chloride (20 mL, 190 mmol) in tetrahydrofuran (40 mL) was added to a slurry of tetrahydrofuran (400 mL) and potassium *tert*-butoxide (23.4 g, 209 mmol) at 0 ˚C. Mixture was stirred for 90 min and then warmed to room temperature. Silica gel (76 g, 1.3 mol) and distilled water (1.14 mL, 62.6 mmol) were added and allowed to stir 20 min. Slurry was filtered through silica gel and concentrated. A yellow oil (18 g, 66%) was isolated. The crude product was purified by vacuum distillation (heating at 35-40 ˚C, and collected over liquid nitrogen) to give a clear oil. **^{1}H-NMR** (400 MHz; $CDCl_3$): δ 2.18 (t, *J* = 7.4 Hz, 2H), 1.61 (sext, *J* = 7.4 Hz, 2H), 1.44 (s, 9H), 0.93 (t, *J* = 7.4 Hz, 3H) ppm; **^{13}C NMR** (101 MHz; $CDCl_3$): δ 173.3, 80.0, 37.6, 28.2, 18.7, 13.7 ppm. The product data matched previous characterization (16).

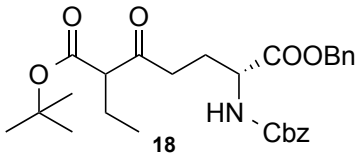

18

7-Benzyl 1-*tert*-butyl (6*R*)-6-(benzyloxycarbonylamino)-2-ethyl-3-oxoheptanedioate (18). Reaction was conducted similarly to that for compound **17**, but utilized **16**. The oil

was purified by silica gel chromatography using ethyl acetate/hexanes (3:20) to give the titled product (56%) as an oil, which solidified to a white solid. TLC (ethyl acetate:hexanes, 2:3 v/v): R_f = 0.69; **^{1}H-NMR** (400 MHz; $CDCl_3$): δ 7.34 (bs, 10H), 5.40-5.34 (m, 1H), 5.16 (s, 2H), 5.09 (s, 2H), 4.42-4.36 (m, 1H), 3.21-3.16 (m, 1H), 2.64-2.48 (m, 2H), 2.20-1.90 (m, 2H), 1.81-1.73 (m, 2H), 1.42 (s, 9H), 0.89-0.85 (m, 3H) ppm; **^{13}C NMR** (101 MHz; $CDCl_3$): δ 204.7, 171.87, 171.85, 168.9, 156.0, 136.2, 135.3, 128.75, 128.62, 128.43, 128.29, 128.19, 82.01, 81.97, 67.4, 67.2, 61.7, 53.57, 53.51, 37.71, 37.61, 28.0, 26.44, 26.31, 21.6, 12.0 ppm; **HRMS** (FAB) *m/z*: $[M+H]^+$ calcd. for $C_{28}H_{35}NO_7$ 498.24918; found 498.24837.

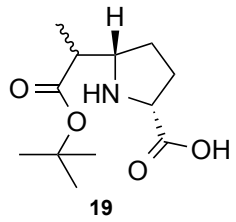

19

(2*R*,5*S*)-5-(1-(*tert*-Butoxy)-1-oxopropan-2-yl)pyrrolidine-2-carboxylic acid (19). This synthesis was adapted from the procedures of Ohta *et al.* (6). Palladium on carbon (0.4 g, 8% w/w) was carefully added to a solution of **17** (5 g, 10 mmol) in acetic acid (1 mL) and ethanol (40 mL) in a bomb flask. The reaction mixture was pressurized to 50 psi with hydrogen gas in a Parr-shaker apparatus and shaken for 16 h. The reaction mixture was then filtered over Celite and concentrated *in vacuo*. The as-isolated product is a thick foam/oil (near quantitative yield). TLC (methanol:acetonitrile, 3:7 v/v): R_f = 0.19; **^{1}H-NMR** (400 MHz; $CDCl_3$): δ 4.05 (t, J = 6.8 Hz, 1H), 3.77-3.59 (m, 1H), 2.85-2.74 (m, 1H), 2.30-2.21 (m, 2H), 2.12-2.00 (m, 1H), 1.66-1.57 (m, 1H), 1.46 (s, 9H), 1.33 (d, J =

7.1 Hz, 2H), 1.27 (d, J = 7.3 Hz, 1H) ppm; **^{13}C NMR** (101 MHz; $CDCl_3$): δ 173.56, 173.52, 172.6, 172.0, 82.33, 82.23, 62.3, 61.4, 60.8, 60.4, 42.5, 42.3, 29.2, 29.0, 28.3, 28.04, 28.01, 27.7, 15.4, 14.4 ppm; **HRMS** (ESI) *m/z*: $[M+H]^+$ calcd. for $C_{12}H_{21}NO_4$ 244.1549; found 244.1551.

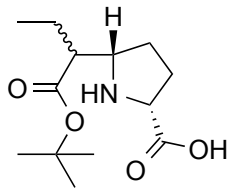

20

(2*R*,5*S*)-5-(1-(*tert*-Butoxy)-1-oxobutan-2-yl)pyrrolidine-2-carboxylic acid (20). Reaction with compound **18** was conducted as described above for **19**. The product is a foam (near quantitative yield), which solidified. TLC (methanol:acetonitrile, 3:7 v/v): R_f = 0.18; **^{1}H-NMR** (400 MHz; $CDCl_3$): δ 4.08 (t, J = 6.1 Hz, 1H), 3.82-3.63 (m, 1H), 2.64-2.53 (m, 1H), 2.31-2.20 (m, 2H), 2.05-2.00 (m, 1H), 1.86-1.69 (m, 2H), 1.69-1.57 (m, 1H), 1.51-1.43 (m, 9H), 0.97 (t, J = 7.2 Hz, 3H) ppm; **^{13}C NMR** (101 MHz; $CDCl_3$): δ 173.50, 173.47, 172.4, 171.5, 82.7, 82.2, 61.3, 60.76, 60.57, 50.7, 49.4, 29.06, 28.88, 28.3, 28.1, 23.7, 23.4, 11.61, 11.47 ppm; **HRMS** (ESI) *m/z*: $[M+H]^+$ calcd. for $C_{13}H_{23}NO_4$ 258.1705; found 258.1699.

*The following protections (**21, 22, 50, 51**) result in mixtures of diastereomers/rotamers, so NMR analyses were done at 50 °C.*

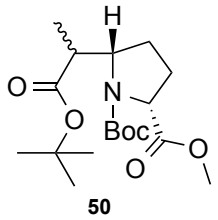

50

Methyl (2*R*,5*S*)-1-(*tert*-butyloxycarbonyl)-5-(1-(*tert*-butoxy)-1-oxopropan-2-yl)pyrrolidine-2-carboxylate (50). This synthesis was adapted from the procedures of Ohta *et al.* (6). Potassium carbonate (3.5 g, 25 mmol) and sodium hydroxide (0.49 g, 13 mmol) were added to a solution of **19** (2.0 g, 8.4 mmol) in water (25 mL) at 0 ˚C. A solution of di-*tert*-butyl dicarbonate (3.7 g, 17 mmol) in tetrahydrofuran (34 mL) was added to the mixture at 0 ˚C over 15 min. The reaction mixture was stirred for 1 h at 0 ˚C and then allowed to warm to room temperature and stirred for 16 h. The reaction mixture was concentrated *in vacuo,* washed with diethyl ether, and acidified to pH = 2 with potassium bisulfate. The solution was then extracted twice with ethyl acetate and the combined organic layers were washed with brine, dried with anhydrous magnesium sulfate, and concentrated *in vacuo*. The crude residue was dissolved in dimethylformamide (84 mL) to which cesium carbonate (3.4 g, 11 mmol) was added and allowed to stir for 10 min. Methyl iodide (1.05 mL, 16.9 mmol) was added to the reaction mixture dropwise and the solution was stirred for 16 h. The reaction was quenched with saturated ammonium chloride, the phases separated, and the aqueous layer was extracted twice with diethyl ether. The combined organic fractions were dried with anhydrous magnesium sulfate and concentrated *in vacuo*. The crude oil was purified by

silica gel chromatography using ethyl acetate:hexanes (1:3) to give **50** (2.39 g, 79%) as an oil, which became a waxy solid overnight. TLC (ethyl acetate:hexanes, 7:13 v/v): R_f = 0.77; (major isomer) **^{1}H-NMR** (400 MHz; $CDCl_3$): δ 4.20 (dd, *J* = 19.9, 8.4 Hz, 1H), 4.03 (app t, *J* = 8.2 Hz, 1H), 3.65 (s, 3H), 2.39-2.10 (m, 2H), 1.92-1.60 (m, 3H), 1.40 (s, 9H), 1.36 (s, 9H), 1.16 (d, *J* = 7.0 Hz, 3H) ppm; (minor isomer) **^{1}H-NMR** (400 MHz; $CDCl_3$): δ 4.24-4.16 (m, 1H), 4.13-4.08 (m, 1H), 3.65 (s, 3H), 2.39-2.10 (m, 2H), 1.92-1.60 (m, 3H), 1.40 (s, 9H), 1.36 (s, 9H), 1.03 (d, *J* = 7.2 Hz, 3H) ppm; (major isomer) **^{13}C NMR** (101 MHz; $CDCl_3$): δ 173.5, 173.0, 153.6, 79.6, 79.1, 59.3, 59.1, 51.5, 44.7, 27.7, 27.4, 25.3, 14.7 ppm; (minor isomer) **^{13}C NMR** (101 MHz; $CDCl_3$): δ 173.1, 172.8, 153.6, 79.4, 79.1, 59.8, 59.3, 51.3, 44.7, 27.7, 27.4, 23.3, 9.5 ppm; **HRMS** (FAB) *m/z*: $[M+H]^+$ calcd. for $C_{18}H_{31}NO_6$ 358.22296; found 358.22304.

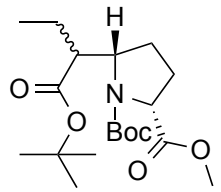

51

Methyl (2*S*,5*S*)-1-(*tert*-butyloxycarbonyl)-5-(1-(*tert*-butoxy)-1-oxobutan-2-yl)pyrrolidine-2-carboxylate (51). Reaction with compound **20** was conducted as described above. The crude oil was purified by silica gel chromatography using 20% ethyl acetate in hexanes to give **51** (73%) as an oil. TLC (ethyl acetate:hexanes, 1:4 v/v): R_f = 0.52; (major isomer) **^{1}H-NMR** (400 MHz; $CDCl_3$): δ 4.20 (dd, *J* = 16.3, 7.9 Hz, 1H), 4.00 (m, 1H), 3.64 (s, 3H), 2.30-2.22 (m, 2H), 1.90-1.52 (m, 5H), 1.41 (s, 9H), 1.36 (s, 9H), 0.84 (t, *J* = 7.4 Hz, 3H) ppm; (minor isomer) **^{1}H-NMR** (400 MHz; $CDCl_3$): δ

4.18 (dd, J = 16.1, 7.6 Hz, 1H), 4.00 (m, 1H), 3.64 (s, 3H), 2.15-2.07 (m, 1H), 1.90-1.52 (m, 6H), 1.40 (s, 9H), 1.36 (s, 9H), 0.83 (t, J = 7.3 Hz, 3H) ppm; (major isomer) **^{13}C NMR** (101 MHz; $CDCl_3$): δ 173.0, 172.7, 153.5, 79.7, 79.1, 59.3, 59.0, 52.4, 51.4, 28.2, 27.6, 27.5, 25.4, 22.5, 11.5 ppm; (minor isomer) **^{13}C NMR** (101 MHz; $CDCl_3$): δ 172.4, 172.3, 153.5, 79.4, 59.8, 59.0, 52.4, 51.3, 28.2, 27.6, 27.5, 25.5, 22.5, 12.3 ppm; **HRMS** (FAB) *m/z*: $[M+H]^+$ calcd. for $C_{19}H_{33}NO_6$ 372.23727; found 372.23770.

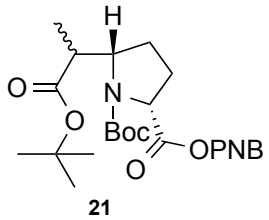

21

***p*-Nitrobenzyl (2*R*,5*S*)-1-(*tert*-butyloxycarbonyl)-5-(1-(*tert*-butoxy)-1-oxopropan-2-yl)pyrrolidine-2-carboxylate (21).** The Boc protection of **19** was conducted as described above for **50**. The residue (0.20 g, 0.58 mmol) was redissolved in dimethylformamide (6 mL) and diisopropylethylamine (0.22 ml, 1.3 mmol) followed by the addition of *p*-nitrobenzyl bromide (0.14 g, 0.64 mmol) in dimethylformamide (3 mL). Solution was stirred 80 min. Saturated ammonium chloride was added to the solution and was extracted twice with ethyl acetate. The combined organic layers were washed with brine, dried, and concentrated. Silica gel chromatography (ethyl acetate/hexanes, 1:4) was used to purify the oil (0.23 g, 65% over both steps). TLC (ethyl acetate:hexanes, 1:4 v/v): R_f = 0.21; (major isomer) **^{1}H-NMR** (400 MHz; $CDCl_3$): δ 8.22 (d, J = 8.7 Hz, 2H), 7.64 (d, J = 8.7 Hz, 2H), 5.34, 5.23 (ABq, J_{AB} = 14 Hz, 2H), 4.31 (q, J = 8.0 Hz, 1H), 4.07-4.02 (m, 1H), 2.39-2.28 (m, 2H), 1.98-1.84 (m, 2H), 1.64 (q, J =

5.7 Hz, 1H), 1.39 (s, (H), 1.33 (s, 9H), 1.11 (d, J = 7.0 Hz, 3H) ppm; (minor isomer) **^{1}H-NMR** (400 MHz; $CDCl_3$): δ 8.22 (d, J = 8.7 Hz, 2H), 7.64 (d, J = 8.7 Hz, 2H), 5.34, 5.23 (ABq, J_{AB} = 14 Hz, 2H), 4.31 (q, J = 8.0 Hz, 1H), 4.12 (dt, J = 8.0, 4.2 Hz, 1H), 2.39-2.28 (m, 1H), 2.21-2.14 (m, 1H), 1.98-1.84 (m, 2H), 1.79-1.73 (m, 1H), 1.39 (s, (H), 1.33 (s, 9H), 0.99 (d, J = 7.2 Hz, 3H) ppm; (major isomer) **^{13}C NMR** (101 MHz; $CDCl_3$): δ 173.3, 172.1, 153.6, 147.0, 143.4, 128.3, 123.1, 79.5, 79.2, 64.5, 59.4, 59.1, 44.7, 28.8, 27.6, 27.4, 25.0, 14.7 ppm; (minor isomer) **^{13}C NMR** (101 MHz; $CDCl_3$): δ 173.3, 172.7, 153.6, 147.0, 143.4, 128.3, 123.1, 79.3, 79.2, 64.5, 59.9, 59.4, 44.7, 28.8, 27.6, 27.4, 25.0, 9.4 ppm; **HRMS** (FAB) *m/z*: $[M+H]^+$ calcd. for $C_{24}H_{34}N_2O_8$ 479.23934; found 479.23938.

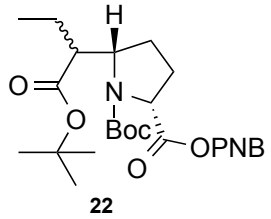

22

***p*-Nitrobenzyl (2*R*,5*S*)-1-(*tert*-butyloxycarbonyl)-5-(1-(*tert*-butoxy)-1-oxobutan-2-yl)pyrrolidine-2-carboxylate (22).** Reaction with **20** was conducted as described above. Multiple rounds of silica gel chromatography (ethyl acetate:hexanes, 1:19 to 3:7) were used to purify the product as an oil (51%). TLC (ethyl acetate:hexanes, 1:4 v/v): R_f = 0.35; (major isomer) **^{1}H-NMR** (400 MHz; $CDCl_3$): δ 8.22 (d, J = 8.4 Hz, 2H), 7.63 (d, J = 8.5 Hz, 2H), 5.34, 5.22 (ABq, J_{AB} = 13.6 Hz, 2H), 4.34-4.27 (m, 1H), 4.05-3.99 (m, 1H), 2.25-2.14 (m, 2H), 1.91-1.83 (m, 2H), 1.67-1.60 (m, 2H), 1.57-1.49 (m, 1H), 1.39 (s, (H), 1.34 (s, 9H), 0.74 (t, J = 8.2 Hz, 3H) ppm; (minor isomer) **^{1}H-NMR** (400 MHz;

$CDCl_3$): δ 8.22 (d, *J* = 8.4 Hz, 2H), 7.63 (d, *J* = 8.5 Hz, 2H), 5.28 (s, 2H), 4.34-4.27 (m, 1H), 4.05-3.99 (m, 1H), 2.35-2.29 (m, 1H), 1.91-1.83 (m, 3H), 1.67-1.60 (m, 2H), 1.57-1.49 (m, 1H), 1.39 (s, (H), 1.34 (s, 9H), 0.77 (t, *J* = 8.1 Hz, 3H) ppm; (major isomer) **^{13}C NMR** (101 MHz; $CDCl_3$): δ 172.6, 172.1, 153.4, 147.1, 143.4, 128.4, 123.2, 79.8, 79.3, 64.5, 59.5, 59.1, 52.4, 28.3, 27.6, 27.5, 25.5, 22.5, 11.4 ppm; (minor isomer) **^{13}C NMR** (101 MHz; $CDCl_3$): δ 172.2, 172.1, 153.7, 147.1, 143.4, 128.4, 123.2, 79.4, 79.3, 64.5, 60.0, 59.1, 52.4, 28.3, 27.6, 27.5, 25.5, 22.5, 12.2 ppm; **HRMS** (FAB) *m/z*: $[M+H]^+$ calcd. for $C_{25}H_{36}N_2O_8$ 493.25499; found 493.25445.

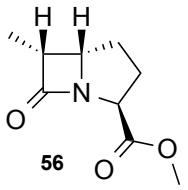

56

Methyl (3*S*,5*S*,6*R*)-6-methylcarbapenam-3-carboxylate (56). This synthesis was adapted from the procedures of Ohta *et al.* (6). 2,6-Lutidine (1.4 mL, 12 mmol) and trimethylsilyl triflate (1.8 mL, 10 mmol) were added slowly to a solution of **50** (1.2 g, 3.3 mmol) in dichloromethane (35 mL) at 0 ˚C and the mixture stirred for 2 h. A solution of hydrochloric acid in dioxane (7.7 mL, 4M, 31 mmol) was added at 0 ˚C and stirred for 10 min. The reaction mixture was concentrated *in vacuo* to yield dark red oil. The crude oil was dissolved in dichloromethane (500 mL) to which diisopropylethylamine (2.6 mL, 15 mmol) followed by a solution of *N,N′*-dicyclohexylcarbodiimide (0.90 g, 4.4 mmol) in dichloromethane (10 mL) were added at 0 ˚C. The mixture was allowed to slowly warm to ambient temperature while stirring over 23 h. The reaction mixture was concentrated *in vacuo* and dissolved in dichloromethane and filtered through Celite. The eluate was

washed 3 × with a cold solution of acetic acid in water (5%), dried with anhydrous sodium sulfate, and concentrated *in vacuo*. The crude oil was purified by silica gel chromatography using ethyl acetate:hexanes (1:2) to give a clear oil (0.45 g, 73%). TLC (ethyl acetate:hexanes, 2:3 v/v): $R_f = 0.36$. 1,8-Diazabicyclo[5.4.0]undec-7-ene (1.13 mL, 7.6 mmol) was added to a solution of the mixture of diastereomers (1.38 g, 7.5 mmol) in acetonitrile (150 mL) and stirred at 50 ˚C for 5 d. The reaction mixture was concentrated *in vacuo* to give a brown oil. The crude product was purified from its diastereomer by silica gel chromatography using ethyl acetate:hexanes (3:17) to give the titled compound (eluted first) as an oil (0.59 g, 43%). TLC (ethyl acetate:hexanes, 2:3 v/v): $R_f = 0.52$; **^{1}H-NMR** (300 MHz; $CDCl_3$): δ 4.35 (t, $J = 7.3$ Hz, 1H), 3.96 (app q, $J = 6.3$ Hz, 1H), 3.73 (s, 3H), 3.50 (qd, $J = 7.7$, 5.5 Hz, 1H), 2.45-2.35 (m, 1H), 2.29-2.17 (m, 1H), 2.06-1.96 (m, 1H), 1.63 (app. ddt, $J = 13.1$, 9.0, 7.8 Hz, 1H), 1.13 (d, $J = 7.7$ Hz, 3H) ppm; **^{13}C NMR** (101 MHz; $CDCl_3$): δ 181.1, 172.0, 58.6, 57.7, 52.5, 45.3, 34.6, 25.2, 9.3 ppm; **HRMS** (ESI) *m/z*: $[M+H]^+$ calcd. for $C_9H_{13}NO_3$ 184.0974; found 184.0966.

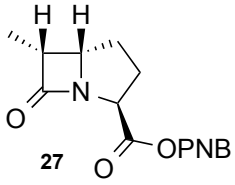

27

***p*-Nitrobenzyl (3*S*,5*S*,6*R*)-6-methylcarbapenam-3-carboxylate (27)**. The coupling reaction was conducted as above using **21**, 63% yield overall. TLC (ethyl acetate:hexanes, 2:3 v/v): $R_f = 0.31$; **^{1}H-NMR** (400 MHz; $CDCl_3$): δ 8.23 (d, $J = 8.8$ Hz, 2H), 7.52 (d, $J = 8.8$ Hz, 2H), 5.25 (s, 2H), 4.43 (t, $J = 7.3$ Hz, 1H), 3.97 (app. dd, $J =$

12.9, 6.5 Hz, 1H), 3.52 (qd, *J* = 7.7, 5.6 Hz, 1H), 2.49-2.41 (m, 1H), 2.29-2.20 (m, 1H), 2.07-1.99 (m, 1H), 1.71-1.63 (m, 1H), 1.15 (d, *J* = 7.7 Hz, 3H) ppm; **HRMS** (FAB) *m/z*: $[M+H]^+$ calcd. for $C_{15}H_{16}N_2O_5$ 305.11375; found 305.11333. The product data matched previous characterization (1).

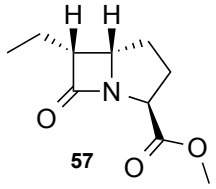

57

Methyl (3*S*,5*S*,6*R*)-6-ethylcarbapenam-3-carboxylate (57). The coupling reaction was conducted as above using **51,** 35% yield overall. TLC (ethyl acetate:hexanes, 2:3 v/v): R_f = 0.61; **^{1}H-NMR** (300 MHz; $CDCl_3$): δ 4.34 (t, *J* = 7.5 Hz, 1H), 3.95 (app dt, *J* = 7.5, 5.9 Hz, 1H), 3.73 (s, 3H), 3.33 (ddd, *J* = 9.6, 7.4, 5.4 Hz, 1H), 2.48-2.37 (m, 1H), 2.29-2.17 (m, 1H), 2.09-1.99 (m, 1H), 1.74-1.40 (m, 3H), 0.98 (t, *J* = 7.4 Hz, 3H) ppm; **^{13}C NMR** (101 MHz; $CDCl_3$): δ 180.3, 172.1, 58.4, 57.2, 52.52, 52.49, 34.6, 25.3, 18.4, 12.0 ppm; **HRMS** (ESI) *m/z*: $[M+H]^+$ calcd. for $C_{10}H_{15}NO_3$ 198.1130; found 198.1126.

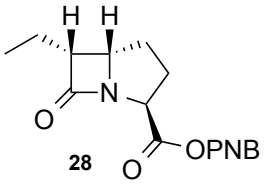

28

***p*-Nitrobenzyl (3*S*,5*S*,6*R*)-6-ethylcarbapenam-3-carboxylate (28).** The coupling reaction was conducted as above using **22,** 29% yield overall. TLC (ethyl

acetate:hexanes, 2:3 v/v): R_f = 0.38; **^{1}H-NMR** (400 MHz; $CDCl_3$): δ 8.23 (d, *J* = 8.7 Hz, 2H), 7.52 (d, *J* = 8.8 Hz, 2H), 5.25 (s, 2H), 4.41 (t, *J* = 7.5 Hz, 1H), 3.97-3.92 (m, 1H), 3.35 (ddd, *J* = 9.6, 7.4, 5.4 Hz, 1H), 2.52-2.39 (m, 1H), 2.31-2.17 (m, 1H), 2.13-1.99 (m, 1H), 1.75-1.57 (m, 2H), 1.55-1.42 (m, 1H), 0.99 (t, *J* = 7.4 Hz, 3H) ppm; **HRMS** (FAB) *m/z*: $[M+H]^+$ calcd. for $C_{16}H_{18}N_2O_5$ 319.12940; found 319.12849. The product data matched previous characterization (1).

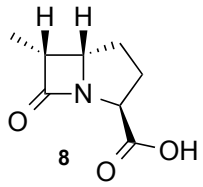

8

Potassium (3*S*,5*S*,6*R*)-6-methylcarbapenam-3-carboxylate (8). **27** (60 mg) was dissolved in tetrahydrofuran (4 mL) and potassium phosphate buffer (2 mL, 0.5M, pH 7.0). 10% palladium on carbon (1:1 w/w with compound **27**) was added and placed under hydrogen (40 psi) for 1 h with shaking. The mixture was filtered through Celite and washed with water and diethyl ether. The aqueous solution was washed with diethyl ether, filtered (0.2 μm, nylon), and lyophilized. The resulting powder was desalted by passage through HP-20 diaion resin. **^{1}H-NMR** (400 MHz; D_2O): δ 4.14 (t, *J* = 7.8 Hz, 1H), 3.95 (dt, *J* = 8.1, 5.6 Hz, 1H), 3.50 (qd, *J* = 7.7, 5.1 Hz, 1H), 2.56-2.48 (m, 1H), 2.14-2.05 (m, 1H), 2.01-1.94 (m, 1H), 1.67-1.57 (m, 1H), 1.11 (d, *J* = 7.8 Hz, 3H) ppm; **HRMS** (ESI) *m/z*: $[M-H]^-$ calcd. for $C_8H_{11}NO_3$ 168.0661; found 168.0648. The product data matched previous characterization (1).

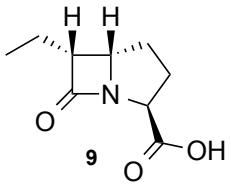

9

Potassium (3*S*,5*S*,6*R*)-6-ethylcarbapenam-3-carboxylate (9). **28** was deprotected in a similar fashion to the C6-methyl analog **27**. **^{1}H-NMR** (400 MHz; D_2O): δ 4.12 (t, *J* = 7.8 Hz, 1H), 3.96-3.91 (m, 1H), 3.38-3.32 (m, 1H), 2.58-2.50 (m, 1H), 2.11-1.96 (m, 2H), 1.65-1.47 (m, 3H), 0.93 (t, *J* = 7.4 Hz, 3H) ppm; **^{13}C NMR** (101 MHz; D2O): δ 184.8, 180.4, 61.6, 57.9, 51.2, 36.1, 25.6, 18.3, 11.6 ppm; **HRMS** (ESI) *m/z*: $[M-H]^-$ calcd. for $C_9H_{13}NO_3$ 182.0817; found 182.0804.

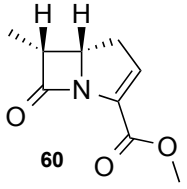

60

Methyl (5*S*,6*R*)-6-methylcarbapenem-3-carboxylate (60). This synthesis was adapted from the procedures of Ohta *et al.* (6). A solution of lithium hexamethyl-disilazane in tetrahydrofuran (3.6 mL, 1M, 3.6 mmol) was added to **56** (301 mg, 1.64 mmol) in tetrahydrofuran (16.4 mL) at -78 ˚C and stirred for 5 min. Phenylselenium bromide (1.16 g, 4.93 mmol) was added at -78 ˚C and allowed to warm to room temperature over 1h. The reaction mixture was diluted with ethyl acetate (20 mL) and washed with water (20 mL), brine (20 mL), dried with anhydrous sodium sulfate, filtered and concentrated *in vacuo*. The crude residue was run through a silica plug with 20% ethyl acetate in hexanes to remove excess phenyl selenium bromide and then concentrated. The resulting oil (257 mg, 0.760 mmol) was dissolved in dichloromethane (41 mL) to which was then

added a solution of *m*-chloroperbenzoic acid (131 mg, 0.760 mmol) in dichloromethane (5 mL) at -30˚C. The reaction was stirred for 15 min at -30˚C before it was quenched with triethylamine (141 µL, 1.01 mmol) and diluted with dichloromethane (150 mL). The reaction mixture was washed twice with saturated ammonium bicarbonate (50 mL), brine (50 mL), dried with anhydrous sodium sulfate, filtered, and concentrated *in vacuo*. The crude residue was purified by silica gel chromatography using ethyl acetate:hexanes (3:7) to give **60** (52 mg, 17%) as a yellow oil. TLC (ethyl acetate:hexanes, 3:7 v/v): R_f= 0.32; **^{1}H-NMR** (300 MHz; $CDCl_3$): δ 6.52 (t, *J* = 2.8 Hz, 1H), 4.37 (ddd, *J* = 10.0, 8.7, 6.2 Hz, 1H), 3.83 (s, 3H), 3.74-3.66 (m, 1H), 2.76 (app. qdd, *J* = 19.4, 9.4, 2.8 Hz, 2H), 1.27 (d, *J* = 7.7 Hz, 3H) ppm; **^{13}C NMR** (101 MHz; $CDCl_3$): δ 180.8, 161.3, 135.9, 132.4, 56.1, 52.5, 47.4, 30.65, 9.9 ppm; **HRMS** (ESI) *m/z*: $[M+H]^+$ calcd. for $C_9H_{11}NO_3$ 182.0817; found 182.0809.

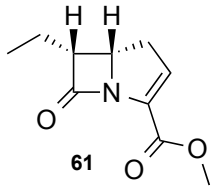

61

Methyl (5*S*,6*R*)-6-ethylcarbapenem-3-carboxylate (61). **57** was desaturated in a similar fashion to the C6-methyl analog (**56**) to give **61** (41 mg, 9.4%). TLC (ethyl acetate:hexanes, 3:7 v/v): R_f= 0.60; **^{1}H-NMR** (400 MHz; $CDCl_3$): δ 6.51 (t, *J* = 2.6 Hz, 1H), 4.35 (ddd, *J* = 9.9, 8.9, 6.1 Hz, 1H), 3.82 (s, 3H), 3.53 (dt, *J* = 9.6, 6.6, 1H), 2.82-2.68 (m, 2H), 1.89-1.78 (m, 1H), 1.65-1.54 (m, 1H), 1.00 (t, *J* = 7.4 Hz, 3H) ppm; **^{13}C**

NMR (101 MHz; $CDCl_3$): δ 180.1, 161.3, 135.7, 132.3, 55.7, 54.3, 52.5, 30.9, 18.9, 11.9 ppm; **HRMS** (ESI) *m/z*: $[M+H]^+$ calcd. for $C_{10}H_{13}NO_3$ 196.0974; found 196.0971.

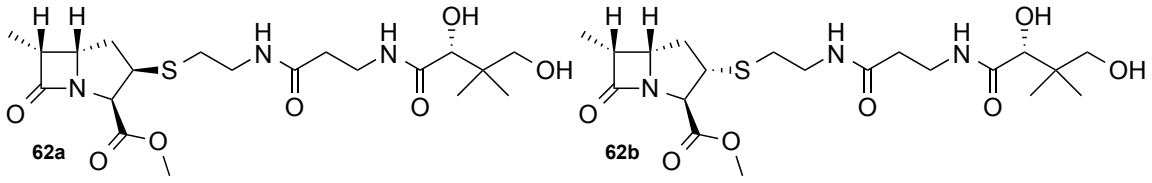

Methyl (3*R*,5*S*,6*R*)-6-methyl-2-pantetheinyl-carbapenam-3-carboxylate (62). Hydrochloric acid (471 µL, 1M) was added to pantetheine acetonide (157 mg, 0.495 mmol, as described elsewhere(4)) in tetrahydrofuran (691 µL) and stirred for 30 min. Sodium hydroxide (471 µL, 1M) was then added to neutralize the reaction mixture. The product pantetheine diol was directly added to **60** (64 mg, 0.35 mmol) in acetonitrile (960 µL) to which was added triethylamine (25 µL, 0.18 mmol) and stirred for 30 min at ambient temperature. The reaction mixture was diluted with ethyl acetate (15 mL), washed with saturated ammonium chloride (4 mL), and brine (10 mL). The combined aqueous layers were extracted with ethyl acetate (15 mL) and the combined organic fractions were dried with anhydrous sodium sulfate, filtered, and concentrated *in vacuo.* The crude oil was purified by silica gel chromatography using ethanol:chloroform (1:9) to give **62** (16 mg) as an inseparable mixture of C2 diastereomers in a ratio of 7:5 (**62a**:**62b**) by ^{1}H-NMR. TLC (ethanol:chloroform, 1:9 v/v): R_f = 0.25; **62a: ^{1}H-NMR** (400 MHz; MeOD): δ 4.67 (d, J = 7.2 Hz, 1H), 4.2-4.14 (m, 2H), 3.89 (s, 1H), 3.74 (s, 3H), 3.58-3.53 (m, 3H), 3.50, 3.36 (ABq, J_{AB} = 14.4 Hz, 2H), 2.84-2.65 (m, 4H), 2.43 (t, J = 6.5 Hz, 2H), 2.28 (ddd, J = 14.0, 8.2, 3.5 Hz, 1H), 1.97 (ddd, J = 13.8, 10.1, 8.3 Hz,

1H), 1.15 (d, J = 7.8, 3H), 0.92 (s, 6H) ppm; **62b: ^{1}H-NMR** (400 MHz; MeOD): δ 4.17 (d, J = 6.1 Hz, 1H), 4.2-4.14 (m, 1H) 3.99 (ddd, J = 8.0, 6.5, 5.4 Hz, 1H), 3.85 (s, 1H), 3.76 (s, 3H), 3.58-3.53 (m, 3H), 3.43, 3.29 (ABq, J_{AB} = 11.2 Hz, 2H), 2.84-2.65 (m, 6H), 2.43 (t, J = 5.7 Hz, 2H), 1.19 (d, J = 7.7, 3H), 0.92 (s, 6H) ppm; **HRMS** (ESI) *m/z*: $[M+H]^+$ calcd. for $C_{20}H_{33}N_3O_7S$ 460.2117; found 460.2112.

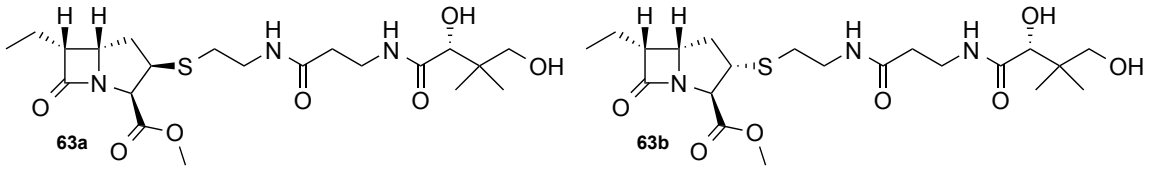

Methyl (3*R*,5*S*,6*R*)-6-ethyl-2-pantetheinyl-carbapenam-3-carboxylate (63).

The carbapenem **61** was reacted with pantetheine in a similar fashion to the C6-methyl analogue (carbapenem **60**) to give **63** (12 mg, 13%) as an inseparable mixture of C2 diastereomers in a nearly equal ratio by ^{1}H-NMR. TLC (ethanol:chloroform, 1:9 v/v): R_f = 0.45; **63a: ^{1}H-NMR** (400 MHz; MeOD): δ 4.60 (d, J = 7.3 Hz, 1H), 4.15-3.98 (m, 1H), 3.83-3.78 (m, 1H), 3.81 (s, 1H), 3.71 (s, 3H), 3.48-3.26 (m, 4H), 3.43, 3.29 (ABq, J_{AB} = 10.8 Hz, 2H), 2.72 (dt, J = 13.0, 6.2, 1H), 2.64 (dt, J = 12.9, 6.5, 1H), 2.36 (t, J = 5.5 Hz, 2H), 2.31-2.13 (m, 2H), 1.61-1.41 (m, 2H), 0.94 (t, J = 7.8 Hz, 3H), 0.85 (s, 6H) ppm; **63b: ^{1}H-NMR** (400 MHz; MeOD): δ 4.08 (d, J = 6.5 Hz, 1H), 4.15-3.98 (m, 1H), 3.94-3.86 (m, 1H), 3.82 (s, 1H), 3.67 (s, 3H), 3.49-3.60 (m, 1H), 3.48-3.26 (m, 4H), 3.43, 3.29 (ABq, J_{AB} = 10.8 Hz, 2H), 3.08-2.79 (m, 2H), 2.55-2.39 (m, 1H), 2.36 (t, J = 5.5 Hz, 2H), 1.61-1.41 (m, 2H), 0.96 (t, J = 7.5 Hz, 3H), 0.85 (s, 6H) ppm; **63a and 63b: ^{13}C NMR** (101 MHz; MeOD): δ 177.0, 175.2, 174.9, 173.1, 172.5, 80.5, 78.3, 71.4, 68.8, 68.4,

67.3, 67.2, 59.2, 55.4, 55.3, 54.6, 54.5, 54.2, 54.1, 53.4, 53.3, 41.4, 37.5, 37.4, 37.3, 34.1, 33.1, 22.4, 22.0, 20.7 20.3, 13.3, 13.0 ppm; **HRMS** (ESI) *m/z*: $[M+H]^+$ calcd. for $C_{21}H_{35}N_3O_7S$ 474.2274; found 474.2267.

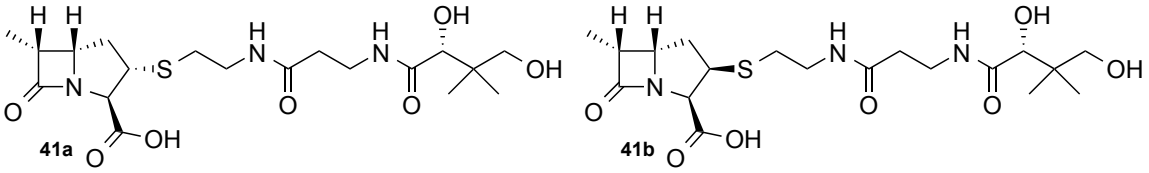

Ammonium (3*R*,5*S*,6*R*)-6-methyl-2-pantetheinyl-carbapenam-3-carboxylate (41a, 41b). A solution of lithium hydroxide in water (1M, 20 μL) was added to **62** (8 mg, 0.018 mmol) in tetrahydrofuran (500 μL) at 0 ˚C and stirred for 20 min, at which time TLC monitoring revealed incomplete reaction. A second batch of lithium hydroxide solution (1M, 20 μL) was then added and after 30 min at 0 ˚C the reaction was quenched with K_2HPO_4 (10 mM, pH = 7.0, 500 μL). The mixture was concentrated *in vacuo* to remove the organic solvent, and immediately injected onto a preparatory reverse-phase HPLC (Phenomonex Luna C18(2) 250 x 21.2 mm 10 micron 100 Å, 10:90 5 mM NH_4HCO_3 in water : acetonitrile, 5 mL/min) for purification. The C2-C3 "*cis*" diastereomer **41b** eluted at 11 min and the C2-C3 "*trans*" diastereomer **41a** eluted at 13 min, allowing for enrichment of each diastereomer. The compounds were collected and lyophilized to give carbapenams **41a** (1.27 mg, 16%) and **41b** (0.63 mg, 8%) as white powders. **41a: ^{1}H-NMR** (400 MHz; D_2O): δ 4.06 (d, J = 5.4 Hz, 1H), 4.08-4.04 (m, 1H), 3.99 (s, 1H), 3.82-3.75 (m, 1H), 3.61 (dd, J = 8.2, 5.3 Hz, 1H), 3.53-3.38 (m, 4H), 3.58, 3.34 (ABq, J_{AB} = 11.0 Hz, 2H), 2.86 (td, J = 13.3, 6.5 Hz, 1H), 2.78 (td, J = 13.0, 6.3 Hz,

1H), 2.51 (t, J = 6.3, 2H), 2.45 (dt, J = 13.9, 6.8 Hz, 1H), 1.7 (dt, J = 14.3, 7.2 Hz, 1H), 1.20 (d, J = 7.9 Hz, 3H), 0.93 (s, 3H), 0.89 (s, 3H) ppm; **HRMS** (ESI) *m/z*: $[M+H]^+$ calcd. for $C_{19}H_{31}N_3O_7S$ 446.1961; found 446.1957; **41b: ^{1}H-NMR** (400 MHz; D_2O): δ 4.34 (d, J = 7.3 Hz, 1H), 4.10 (dd, J = 13.5, 6.2, 1H), 3.90 (s, 1H), 3.71 (s, 1H), 3.67 (dd, J = 12.3, 6.4 Hz, 1H), 3.56 (dd, J = 11.9, 4.7 Hz, 1H), 3.56-3.34 (m, 3H), 3.48, 3.24 (ABq, J_{AB} = 11.6 Hz, 2H), 2.41 (t, J = 6.6, 2H), 2.09 (dt, J = 13.5, 6.8 Hz, 1H), 2.00 (dt, J = 13.4, 6.7 Hz, 1H), 1.04 (d, J = 7.7 Hz, 3H), 0.83 (s, 3H), 0.80 (s, 3H) ppm; **HRMS** (ESI) *m/z*: $[M+H]^+$ calcd. for $C_{19}H_{31}N_3O_7S$ 446.1961; found 446.1952.

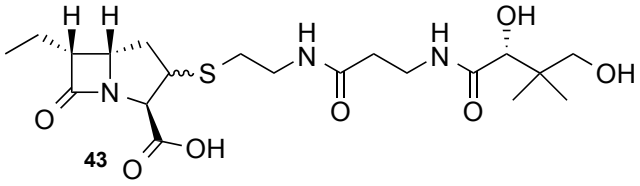

43

Analytical Standard:

Sodium (3*R*,5*S*,6*R*)-6-ethyl-2-pantetheinyl-carbapenam-3-carboxylate (43). An analytical amount of the protected methyl ester **63** was dissolved in 1:1 acetonitrile:H_2O. The solution was adjusted to pH ≥ 10 with NaOH (~1 M) and allowed to react at room temperature for 10 min. The solution was then neutralized to pH = 7 with HCl (~1 M) and analyzed by UPLC-MS. **HRMS** (ESI) *m/z*: $[M+H]^+$ calcd. for $C_{20}H_{33}N_3O_7S$ 460.2117; found 460.2112.

Compounds 44-49:

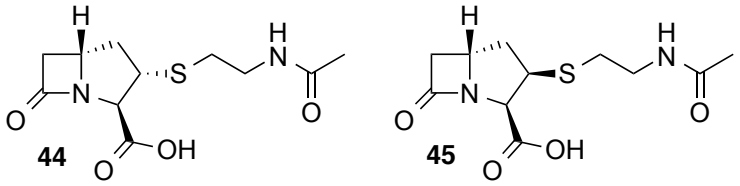

Potassium (2*S*,3*R*,5*R*)-2-(2-acetamidoethylthiol)-carbapenam-3-carboxylate (44) and **potassium (2*R*,3*R*,5*R*)-2-(2-acetamidoethylthiol)-carbapenam-3-carboxylate (45).** The C2-SNAC carbapenams were generated from **38** as previously described and characterized (3). The diastereomers **44** and **45** were separated from each other and purified using an Agilent model 1100 HPLC equipped with a multi-wavelength ultraviolet–visible detector (210 nm) in conjunction with a reverse-phase Phenomenex Luna 10μ C18(2) 100 Å preparatory column (250 x 21.20 mm ID). The mobile phase was 18% methanol and 82% buffer (10 mM potassium phosphate, pH 6.65) at a flow rate of 5 ml per min. Compound **44** eluted at 23 min and compound **45** eluted at 18 min. Excess phosphate buffer was removed using Diaion® HP-20 resin.

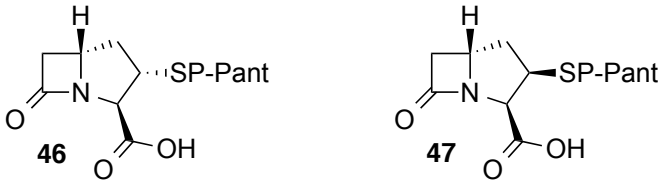

Potassium (2*S*,3*R*,5*R*)-2-(4-phosphopantetheinyl)-carbapenam-3-carboxylate (46) and **potassium (2*R*,3*R*,5*R*)-2-(4-phosphopantetheinyl)-carbapenam-3-carboxylate (47).** The C2-phosphopantetheine carbapenams were generated from the C2-pantetheine analogs **10** and **11** using PanK (provided by D.H. Long, Townsend Lab). Reactions

included: ~ 0.40 mg/mL enzyme, 15 mM substrate (~18 mg), 15 mM ATP, 20 mM KCl, 10 mM $MgCl_2$, and 50 mM Tris, pH 7.5 and were run for at least 2 hours at RT. The protein was removed by centrifugal filtration (Amicon, 10 kDa MWCO). The titled compounds were purified using the 1100 HPLC as described for **44** and **45** (detection: 210 nm). The mobile phase was 15% methanol and 85% buffer (10 mM potassium phosphate, pH 6.65) for **47** and it eluted at approximately 17 min. The mobile phase was 20% methanol and 80% buffer for **46** and it eluted at approximately 17 min. Excess phosphate buffer was removed using Diaion® HP-20 resin. **46** and **47** have been characterized previously by Moshos (3).

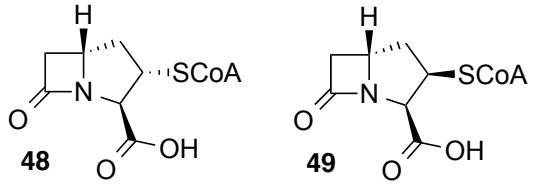

Potassium (2*S*,3*R*,5*R*)-2-CoA-carbapenam-3-carboxylate (48) and **potassium (2*R*,3*R*,5*R*)-2-CoA-carbapenam-3-carboxylate (49).** The C2-CoA carbapenams were generated from the carbapenem **38** (31 mg, 0.11 mmol), which was dissolved in tetrahydrofuran (0.40 mL). Coenzyme A (49 mg, 0.064 mmol) was dissolved in water and added to **38** along with triethylamine (6.3 µL, 0.045 mmol). The solution was stirred for 75 min. The reaction mixture was then transferred to a pressure tube along with 10% Pd on carbon, 0.5 mL 0.5 M potassium phosphate (pH 7), 1 mL water, and 1 mL tetrahydrofuran and shaken on a Parr apparatus for 1 h under hydrogen (20 psi). The catalyst was removed by filtration on Celite. The filtrate was washed with diethyl ether

(15 mL). The aqueous layer was filtered through a 0.2 μm nylon filter and lyophilized. Prior to HPLC injection, the sample was dissolved in water and filtered through a centrifugal device (Amicon, 10 kDa MWCO). The diastereomers **48** and **49** were separated from each other and purified using an Agilent 1100 HPLC (detection: 254 nm). The mobile phase was 13% methanol and 87% buffer (10 mM potassium phosphate, pH 6.65) at a flow rate of 5 ml per min. Compound **48** eluted at 22 min and compound **49** eluted at 17.5 min. Excess phosphate buffer was removed using Diaion® HP-20 resin. **48:** ^{1}H-NMR (300 MHz. D_2O) δ: 8.51 (s, 1H), 8.24 (s, 1H), 6.14 (d, *J* = 6.8 Hz, 1H), 4.52-4.55 (m, 1H), 4.19 (dd, *J* = 4.5, 3.4 Hz, 2H), 4.10 (d, *J* = 5.4 Hz, 1H), 3.95 (s, 1H), 3.90 (dd, *J* = 4.7. 2.2 Hz, 1H), 3.74 (ddd, *J* = 18.0, 11.5, 6.4 Hz, 2H), 3.50 (dd, *J* = 9.9, 5.0 Hz, 1H), 3.42 (td, *J* = 6.5, 2.4 Hz, 2H), 3.36-3.40 (m, 2H), 3.27 (d, *J* = 5.1 Hz, 1H), 2.84 (dd, *J* = 16.3, 2.0 Hz, 1H), 2.73 (q, *J* = 8.0 Hz, 2H), 2.53 (dt, *J* = 14.1, 6.6 Hz, 1H), 2.42 (t, *J* = 6.8 Hz, 2H), 1.62 (dt, *J* = 14.0, 7.0 Hz, 1H), 0.82 (s, 3H), 0.69 (s, 3H); **HRMS** (ESI) *m/z*: $[M+H]^+$ calcd. for $C_{28}H_{43}N_8O_{19}P_3S$ 921.1656; found 921.1636; **49:** ^{1}H-NMR (400 MHz. D_2O) δ: 8.51 (s, 1H), 8.25 (s, 1H), 6.14 (d, *J* = 6.8 Hz, 1H), 4.53-4.55 (m, 1H), 4.47 (d, *J* = 6.7 Hz, 1H), 4.19 (dd, *J* = 4.6, 3.4 Hz, 2H), 3.97-4.06 (m, 1H), 3.95 (s, 1H), 3.88 (td, *J* = 6.5. 3.6 Hz, 1H), 3.73-3.78 (m, 2H), 3.24-3.49 (m, 6H), 2.75 (dd, *J* = 16.6, 2.1 Hz, 1H), 2.70 (dd, *J* = 10.1, 6.8 Hz, 2H), 2.62-2.65 (m, 1H), 2.42 (t, *J* = 6.5 Hz, 2H), 2.20-2.29 (m, 2H), 1.95-2.02 (m, 1H), 0.81 (s, 3H), 0.68 (s, 3H); **HRMS** (ESI) *m/z*: $[M+H]^+$ calcd. for $C_{28}H_{43}N_8O_{19}P_3S$ 921.1656; found 921.1628. **48** and **49** have been characterized previously by Moshos (3) using an enzymatic synthesis of the CoA moiety.

References

1. Bodner MJ*, et al.* (2011) Definition of the common and divergent steps in carbapenem β-lactam antibiotic biosynthesis. *ChemBioChem* 12(14):2159-2165.

2. Okabe M*, et al.* (1982) Studies on the OA-6129 group of antibiotics, new carbapenem compounds. I. Taxonomy, isolation and physical properties. *J. Antibiot. (Tokyo)* 35(10):1255-1263.

3. Moshos KA (2011) Design and synthesis of substrates and standards used to elucidate activities of enzymes in carbapenem gene clusters. Ph.D. Thesis (The Johns Hopkins University, Baltimore, MD).

4. Freeman MF, Moshos KA, Bodner MJ, Li R, & Townsend CA (2008) Four enzymes define the incorporation of coenzyme A in thienamycin biosynthesis. *Proc. Natl. Acad. Sci. USA* 105(32):11128-11133.

5. Stapon A, Li R, & Townsend CA (2003) Synthesis of (3*S*,5*R*)-carbapenam-3-carboxylic acid and its role in carbapenem biosynthesis and the stereoinversion problem. *J. Am. Chem. Soc.* 125(51):15746-15747.

6. Ohta T, Sato N, Kimura T, Nozoe S, & Izawa K (1988) Chirospecific synthesis of (+)-PS-5 from L-glutamic acid. *Tetrahedron Lett.* 29(34):4305-4308.

7. Bateson JH, Roberts PM, Smale TC, & Southgate R (1990) Olivanic acid analogues. Part 5. Synthesis of 3-alkylthio and 3-alkylsulphinyl analogues via Michael addition of thiols to 3-unsubstituted 1-azabicyclo[3.2.0]hept-2-ene-2-carboxylates. X-Ray molecular structure of (2*RS*,3*RS*,5*SR*)-benzyl 3-ethylthio-7-oxo-1-azabicyclo[3.2.0]heptane-2-carboxylate and (2*RS*,3*SR*,5*SR*,6*RS*,1'*RS*)- and (2*RS*,3*SR*,5*RS*,6*SR*,1'*SR*)-benzyl 3-chloro-6-(1-hydroxyethyl)-7-oxo-3-[(*SR*)-phenylsulphinyl]-1-azabicyclo[3.2.0]heptane-2-carboxylate. *J. Chem. Soc. Perk. T. 1* (6):1541.

8. Ueda Y, Damas CE, & Belleau B (1983) Nuclear analogs of β-lactam antibiotics. XVIII. A short synthesis of 2-alkylthiocarbapen-2-em-3-carboxylate. *Can. J. Chem.* 61(9):1996-2000.

9. Ueda Y, Damas CE, & Vinet V (1983) Nuclear analogs of β-lactam antibiotics. XIX. Syntheses of racemic and enantiomeric *p*-nitrobenzyl carbapen-2-em-3-carboxylate. *Can. J. Chem.* 61:2257-2263.

10. Marous DR*, et al.* (2015) Consecutive radical *S*-adenosylmethionine methylations form the ethyl side chain in thienamycin biosynthesis. *Proc. Natl. Acad. Sci. USA* 112(33):10354-10358.

11. Bateson JH, Hickling RI, Roberts PM, Smale TC, & Southgate R (1980) Olivanic acids and related compounds: total synthesis of (±)-PS-5 and (±)-6-epi PS-5. *J. Chem. Soc., Chem. Commun.*:1084-1085.

12. Spry C, Kirk K, & Saliba KJ (2008) Coenzyme A biosynthesis: an antimicrobial drug target. *FEMS Microbiol. Rev.* 32(1):56-106.

13. Worthington AS & Burkart MD (2006) One-pot chemo-enzymatic synthesis of reporter-modified proteins. *Org. Biomol. Chem.* 4(1):44-46.

14. Baxter AJG, Dickenson KH, Roberts PM, Smale TC, & Southgate R (1979) Synthesis of 7-oxo-1-axabicyclo[3.2.0]hept-2-ene-2-carboxylates: the olivanic acid ring system. *J. Chem. Soc. Chem. Commun.*:236-237.

15. Bateson JH, Quinn AM, Smale TC, & Southgate R (1985) Olivanic acid analogues. Part 2. total synthesis of some C(6)-substituted 7-oxo-1-azabicyclo[3.2.0]hept-2-ene-2-carboxylates. *J. Chem. Soc. Perk. T. 1* (11):2219-2234.

16. DeMartino MP, Chen K, & Baran PS (2008) Intermolecular enolate heterocoupling: scope, mechanism, and application. *J. Am. Chem. Soc.* 130(34):11546-11560.

Chapter 3

Consecutive Radical SAM Methylations by ThnK Form the Ethyl Side Chain in Thienamycin Biosynthesis

Introduction

Apart from the identification of ThnE and ThnM in forming the (3*S*,5*S*)-carbapenam **3** (1) and ThnR, ThnH, and ThnT in the stepwise truncation of coenzyme A (CoA) (2), the timing of the carbapenam(em) tailoring events including introduction of the C2-substituent, alkylation at C6, ring inversion, and desaturation remain shrouded in mystery. Unique to the complex carbapenem gene clusters are three apparent cobalamin-dependent radical *S*-adenosylmethionine (RS) enzymes ThnK, ThnL, and ThnP (all annotated as Class B RS methylases) (3), which we now demonstrate likely play critical roles in the central undefined steps of thienamycin biosynthesis. The challenge of deciphering their activities is exacerbated by their intrinsic instability, unknown substrates, and multiple possible enzymatic reactions. We have taken the first step in illuminating the obscure center of the thienamycin biosynthetic pathway by identifying substrates for ThnK and establishing that this enzyme performs two consecutive methylations to generate the C6-ethyl side chain stereospecifically. While other RS cobalamin-dependent enzymes that act on carbon have been investigated (4-7), this is the first *in vitro* characterization of a RS methylase acting sequentially to form a side chain.

Results and Discussion

A library of candidate substrates and product standards was prepared (Chapter 2), including the simple (3*S*,5*S*)-carbapenam **3** and related C2 and C6-substituted derivatives

8-**12**. The library was biased toward structures with the (3*S*,5*S*)-stereochemistry, matching that of the ThnM product **3**, and those bearing the 6*R*-configuration (**8**, **9**) matching that of thienamycin (Figure 3.1A). A pantetheinyl moiety was selected for the side chain at C2 (**10**-**12**) in keeping with the OA-6129 series of metabolites that has been isolated from carbapenem producers (8).

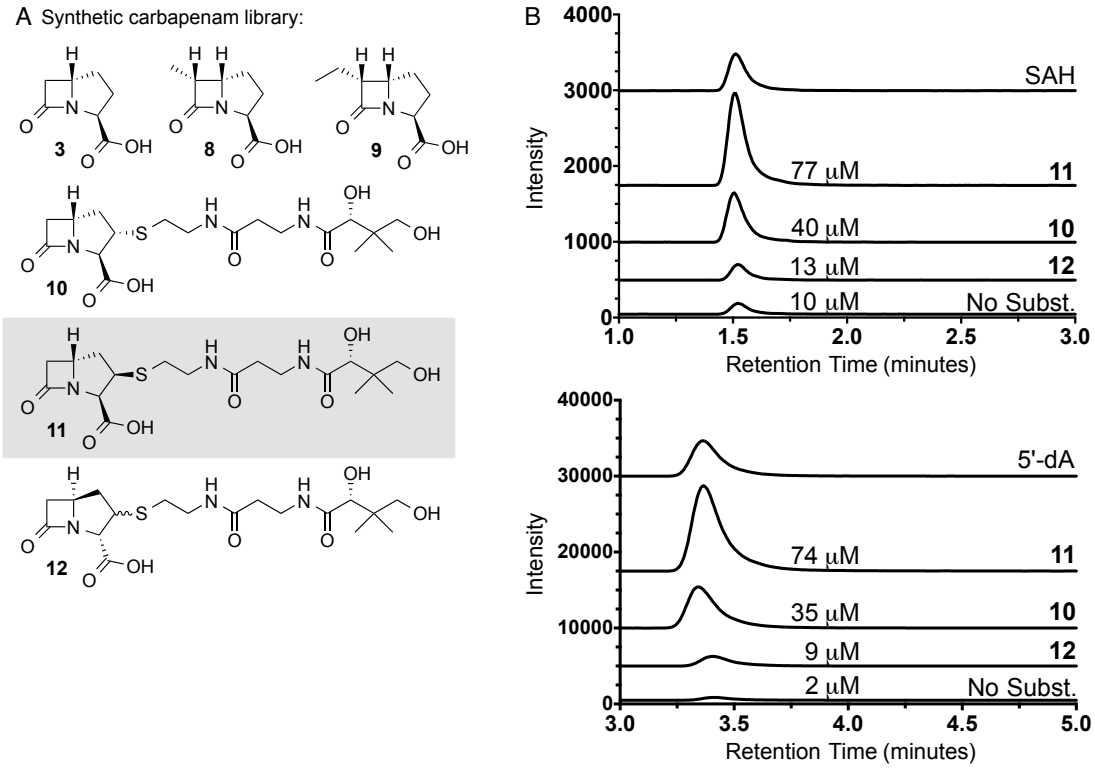

Figure 3.1: Carbapenam synthetic library and detection and quantification of SAM products of ThnK.

(*A*) Compounds synthesized to probe ThnK activity. (B) LC-MS/MS detection of enzymatic SAM co-products, SAH (385.4 → 136 *m/z*) and 5'-dA (252.1 → 136 *m/z*). The extracted-ion chromatograms (EICs) for the transitions of SAH and 5'-dA are shown for each reaction. The reaction with compound **11** gave the highest levels of these SAM co-products. Quantified levels of SAH and 5'dA are shown for each reaction.

Work began with the best behaved of these three RS enzymes. ThnK was cloned from *Streptomyces cattleya,* where experimental conditions were found that gave

moderate levels of soluble protein when expressed with a *C*-terminal His_6-tag in *E. coli* Rosetta 2(DE3). ThnK was expected to utilize both an iron-sulfur (Fe/S) cluster and cobalamin, so protein production was conducted in ethanolamine-M9 medium, which facilitates uptake of externally supplied hydroxocobalamin into *E. coli*, and with concurrent expression of the *Azotobacter vinelandii isc* operon, encoded on plasmid pDB1282. ThnK was purified under strictly anaerobic conditions. Its UV-visible spectrum revealed a 420 nm shoulder (Figure 3.2) typical of a bound iron-sulfur cluster. The relative stoichiometry of iron and sulfide bound by the as-isolated protein was determined to be 7.4 ± 1.4 and 3.7 ± 0.8 per polypeptide, respectively, consistent with the presence of a [4Fe-4S] cluster. Apparent excess iron has been observed with other RS enzymes (6, 9), and was similarly seen in an alanine variant control below.

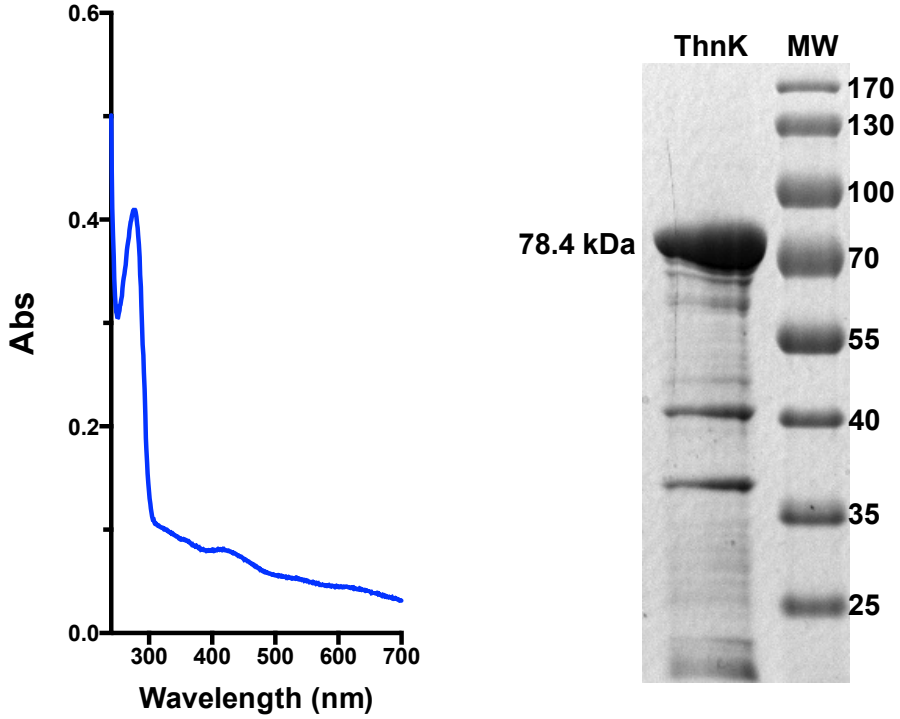

Figure 3.2: UV-Visible spectrum and SDS-PAGE of ThnK.

The UV-visible spectrum of ThnK shows a 420 nm shoulder, indicative of a bound iron sulfur cluster.

To determine whether any of our library compounds was a substrate for ThnK, a LC-MS analytical screen was developed whereby enzymatic reactions were monitored for appearance of the expected RS methylase co-products, *S*-adenosylhomocysteine (SAH) and 5'-deoxyadenosine (5'-dA) (10, 11). Initial screens were conducted with ThnK, SAM, and potential substrates in the presence of methyl viologen and NADPH as the Fe/S cluster reductants (5). The (3*S*,5*S*)-carbapenam and related C6-methyl and ethyl derivatives (**3**, **8**, and **9**) gave nearly background (no-substrate control) levels of SAH and 5'-dA (**Figure 3.3**).

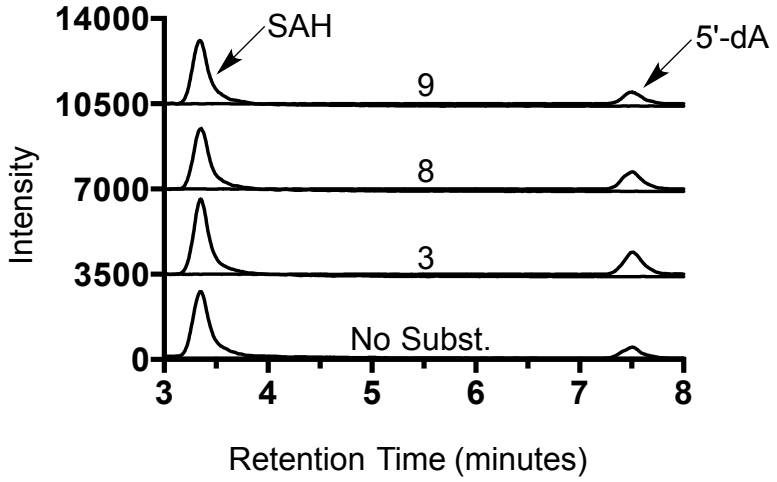

Figure 3.3: Detection of SAM-derived products of ThnK with compounds 3, 8, and 9.

LC-MS/MS was used to detect SAM-derived coproducts, SAH (385.4 → 136 *m/z*) and 5'-dA (252.1 → 136 *m/z*). The extracted-ion chromatograms (EICs) for the transitions of SAH and 5'-dA are overlaid for each reaction. The reactions with compounds **3**, **8**, and **9** show about the same level of turnover as the reaction without substrate. Reactions were run for approximately 2 hours at room temperature.

In contrast, however, these SAM co-products accumulated when ThnK was incubated with C2-substituted carbapenams, suggesting that the full methyl transfer reaction(s) had occurred with these substrates (Figure 3.1B). Alternate Fe/S cluster

reductants, including dithionite and the flavodoxin/flavodoxin reductase/NADPH reducing system were also examined, but did not give improved activity (Figure 3.4).

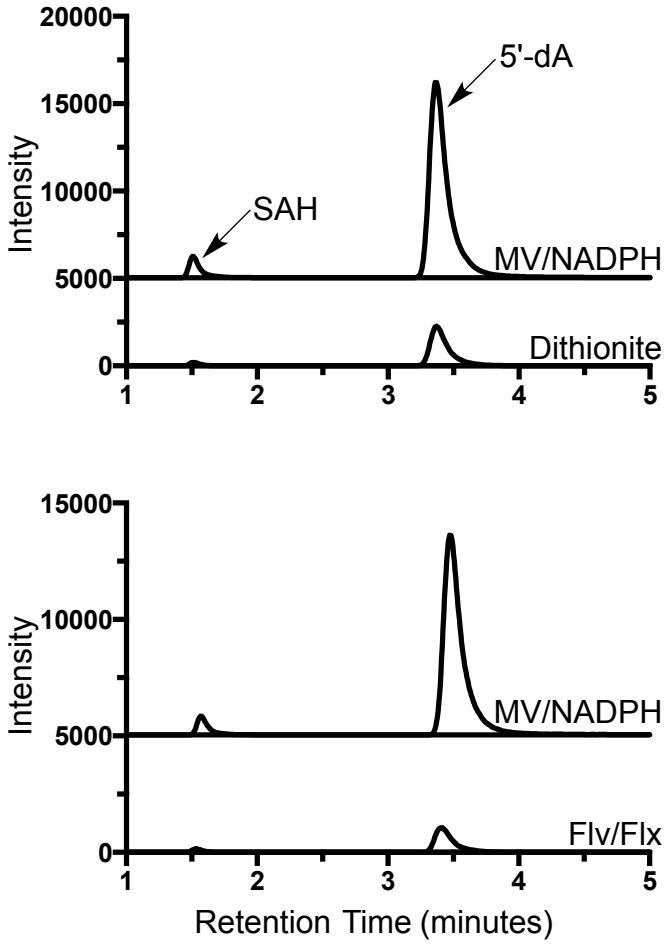

Figure 3.4: LC-MS/MS comparison of enzymatic turnover using different iron-sulfur cluster reductants.

The extracted-ion chromatograms (EICs) for the transitions of SAH (385.4 → 136 *m/z*) and 5'-dA (252.1 → 136 *m/z*) are overlaid for each reaction. Methyl viologen with NADPH gave higher turnover than dithionite or flavodoxin with flavodoxin reductase and NADPH. Reactions were run for approximately 2 hours at room temperature with substrate **11**.

To assess enzymatic turnover, the amounts of SAH and 5'-dA were quantified by LC-MS/MS (Figure 3.1B). Compounds bearing the now (3*R*,5*R*)-stereochemistry with a

pantetheine side chain at C2 gave the greatest levels of turnover. Therefore, each C2 diastereomer (compound **10** or **11**) was tested individually. The (2*R*,3*R*,5*R*)-carbapenam **11** yielded ~2-fold higher amounts of SAM co-products. These stereochemical preferences were found to be reproducible (12) and SAH and 5'dA were present in approximately equimolar amounts in each reaction.

To test the role of the [4Fe-4S] cluster in catalysis, a variant of ThnK was generated where the conserved cluster binding motif Cx_3Cx_2C was changed from three cysteine to three alanine residues. The variant protein was prepared as described above for wild-type ThnK and incubated with substrate **11**. The inactivated enzyme did produce low levels of SAH, but no detectable 5'-dA (**Figure 3.5**) consistent with reliance of the wild-type enzyme on a functional Fe/S cluster.

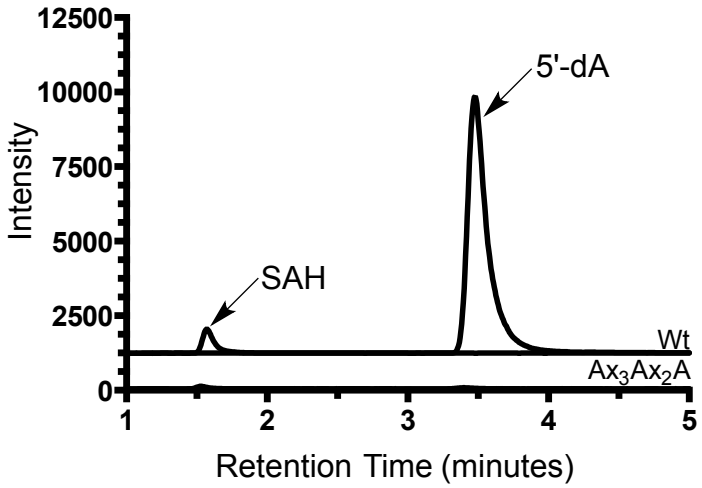

Figure 3.5: Fe/S cluster required for ThnK activity.

LC-MS/MS was used to detect SAM-derived coproducts, SAH (385.4 → 136 *m/z*) and 5'-dA (252.1 → 136 *m/z*). The extracted-ion chromatograms (EICs) for the transitions of SAH and 5'-dA are overlaid for each reaction. Alteration of the Cx_3Cx_2C motif to Ax_3Ax_2A resulted in little SAH production and no 5'-dA production. Reactions were run for approximately 2 hours at room temperature with substrate **11**.

ThnK was also expressed in M9 medium lacking hydroxocobalamin. The purified protein with substrate **11** did not produce SAH or 5'dA; however, enzymatic activity could be rescued if cobalamin was added to the reaction mixture (Figure 3.6).

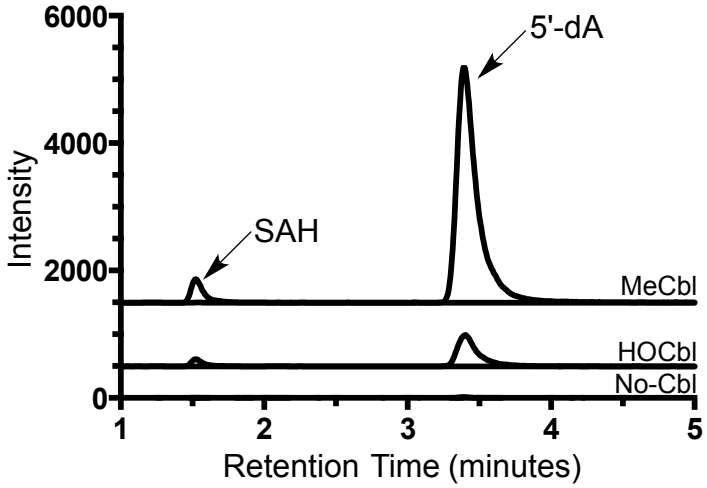

Figure 3.6: Cobalamin required for ThnK activity.

LC-MS/MS was used to detect SAM-derived coproducts, SAH (385.4 → 136 *m/z*) and 5'-dA (252.1 → 136 *m/z*). The extracted-ion chromatograms (EICs) for the transitions of SAH and 5'-dA are overlaid for each reaction. ThnK, expressed in and isolated from *E. coli* cultured in the absence of cobalamin, was either given no cobalamin, HOCbl, or MeCbl. Added cobalamin was able to rescue ThnK activity with MeCbl yielding higher levels of SAH and 5'-dA than HOCbl. Reactions were run for 1 hour and 10 minutes at room temperature with substrate **11**.

The amount of cobalamin that co-purifies with ThnK was quantified for further evidence that cobalamin is a true enzymatic cofactor. A sample of ThnK was purified by Fast Protein Liquid Chromatography (FPLC) and verified to be active. The protein was then reacted with potassium cyanide to generate dicyanocobalamin. The level of cobalamin incorporation was estimated to be 40% by UV/Visible spectroscopy (absorption at 367 nm for dicyanocobalamin).

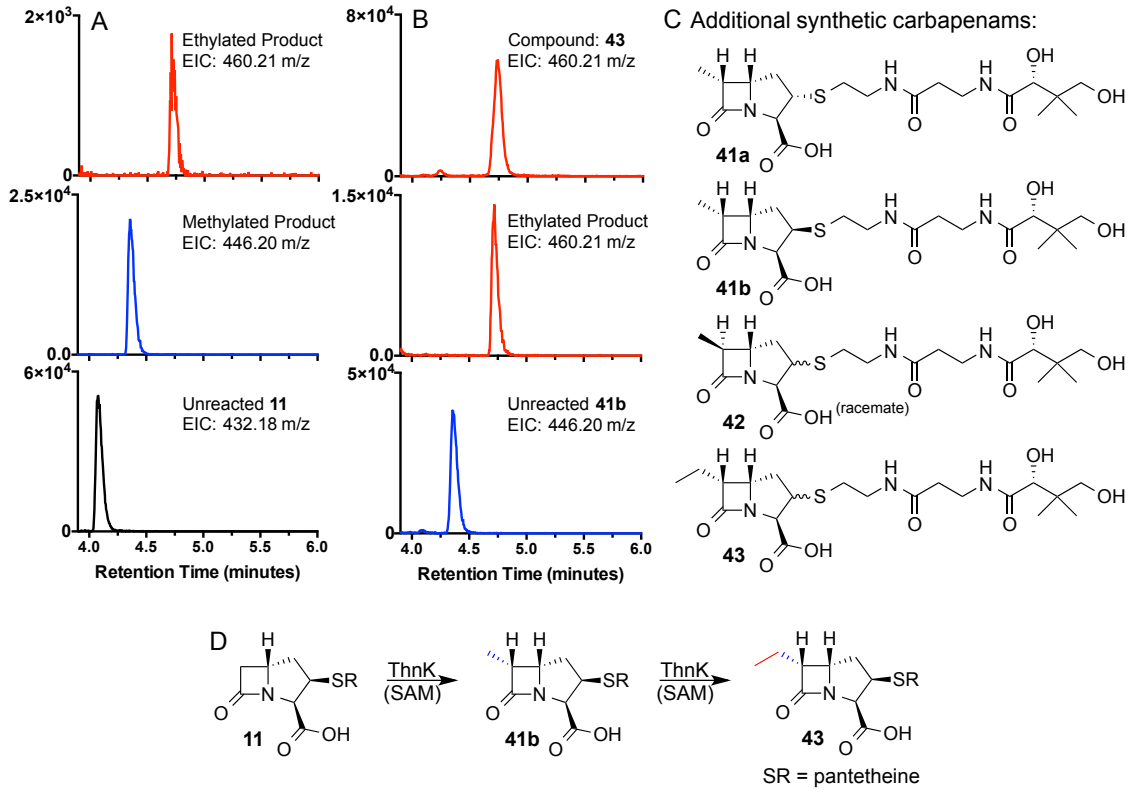

Figure 3.7: ThnK product detection and additional synthetic compounds.

(A) UPLC-HRMS detection of carbapenams from ThnK reaction with compound **11**. The bottom, middle, and top traces show the extracted-ion chromatograms (EICs, *m/z* ± 0.05) for unreacted substrate (432.18 *m/z*), methylated product (446.20 *m/z*), and ethylated product (460.21 *m/z*), respectively. (B) UPLC-HRMS detection of carbapenams from ThnK reaction with compound **41b** as compared to synthetic standard **43**. The bottom, middle, and top traces show the extracted-ion chromatograms (EICs, *m/z* ± 0.05) for unreacted substrate **41b** (446.20 *m/z*), ethylated product (460.21 *m/z*), and C6-ethyl synthetic standard (460.21 *m/z*), respectively. The ethylated product of **11** (A) and the ethlyated product of **41b** match the synthetic standard **43** (B). (C) Additional compounds synthesized to analyze ThnK reaction. Note: Compound **42** is a racemate and diastereomeric at C2; Compounds **41a** and **41b** are diastereomeric at C2, but enriched for the diastereomer shown (approx. 3:1 and 3:2, respectively); Compound **43** is diastereomeric at C2. (D) Summary of ThnK activity.

We next sought to determine how the substrate was transformed during the reaction with ThnK. Assays with **11** were analyzed by UPLC-HRMS. Exact masses were obtained matching methylated (calc: *m/z* 446.1961, found: 446.1954) and twice-

methylated (calc: *m/z* 460.2117, found: 460.2104) modifications of the substrate. The extracted-ion chromatograms for these masses showed retention times that were consistent with increasing hydrophobicity relative to the substrate (Figure 3.7A). The highly diagnostic β-lactam mass fragment (calc: *m/z* 390.1699) corresponding to the loss of a ketene from cleavage of the β-lactam ring (13) was observed (found: *m/z* 390.1701) (Figure 3.8), which was further consistent with methylation at C6.

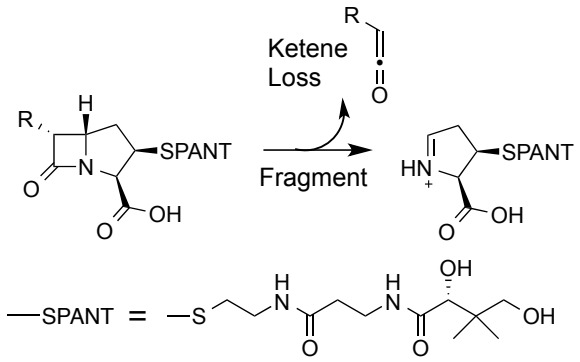

Subst.	Prod. R =	*m/z*		*m/z*
11	$-CH_3$	446.1954		390.1701
41b	$-CH_2CH_3$	460.2111		390.1681
11	$-CD_3$	449.2142		390.1700
41b	$-CH_2CD_3$	463.2299		390.1695

Figure 3.8: Detection of β-lactam parent and fragment ions.

UPLC-HRMS was used to detect carbapenam parent and fragment ions from ThnK reactions with **11** or **41b**. Characteristic MS fragmentation of β-lactam-containing compounds results in loss of a substituted (R) ketene as depicted. Using d_3-SAM or natural abundance SAM in the enzymatic reaction affects the observed *m/z* of the parent ion, but not the observed *m/z* of the fragmentation ion consistent with methylation occurring at C6.

To establish SAM as the methyl donor, additional ThnK reactions were performed with *S*-adenosyl-L-[*methyl*-d_3]methionine (d_3-SAM). The corresponding M+3 *m/z* shift (Figure 3.8 and **Figure 3.9**) was observed for the methylated product and an M+5 *m/z* shift was seen for the twice-methylated product (**Figure 3.9**), fully in accord with formation of the ethyl side chain at C6 in thienamycin by successive methyl transfers.

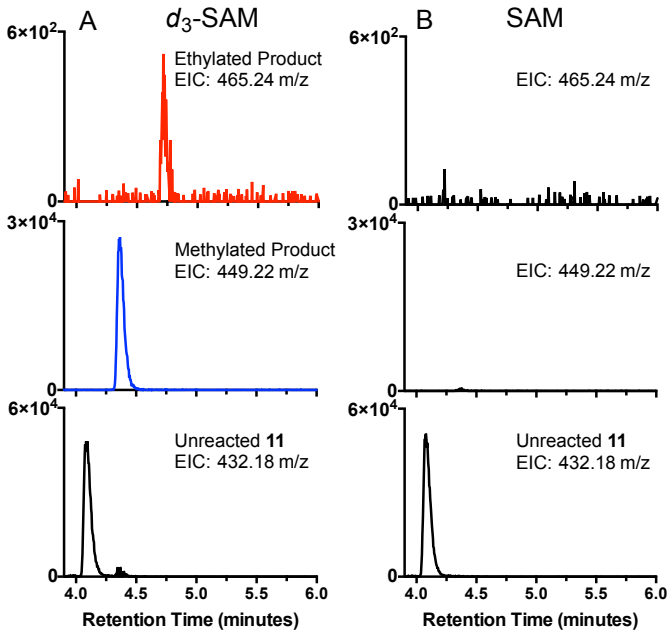

Figure 3.9: Product detection of ThnK assays with d_3-SAM.

(A) UPLC-HRMS detection of carbapenams from ThnK reaction with compound **11** and d_3-SAM. The bottom, middle, and top traces show the extracted-ion chromatograms (EICs, $m/z \pm 0.05$) for unreacted substrate (432.18 *m/z*), methylated product (449.22 *m/z*), and ethylated product (465.24 *m/z*), respectively. The middle and top traces show a +3 m/z and a +5 *m/z* shift, respectively, from Figure 3.7A. (B) UPLC-HRMS detection of carbapenams from ThnK reaction with compound **11** and natural abundance SAM. The shifted masses observed in A are not present in B.

To secure the stereochemistry of the first methylation, synthesis of a set of C6-methylcarbapenams (**41a**, **41b**, **42**, Figure 3.7) was carried out and assayed with ThnK. While compounds **41a** and **42** displayed trace or no measurable activity, respectively, **41b** afforded unequivocal production of SAH and 5'-dA (Figure 3.10). This result underscored the importance of the stereochemical relationship between the C3-carboxylate and the pantetheinyl side chain and confirmed that the C6-methyl is attached in the *R*-configuration, as occurs in thienamycin. By UPLC-ESI/MS analysis, the ethylated product of **41b** (resulting from a single methyl transfer) matched the exact mass

and retention time of the ethylated product of compound **11** (Figure 3.7A and B). In further support, the (6*R*)-ethyl standard **43** was synthesized and determined to match the aforementioned products by retention time, exact mass, and fragmentation pattern, as expected (Figure 3.7A and B). The observed activity of ThnK is summarized in Figure 3.7D.

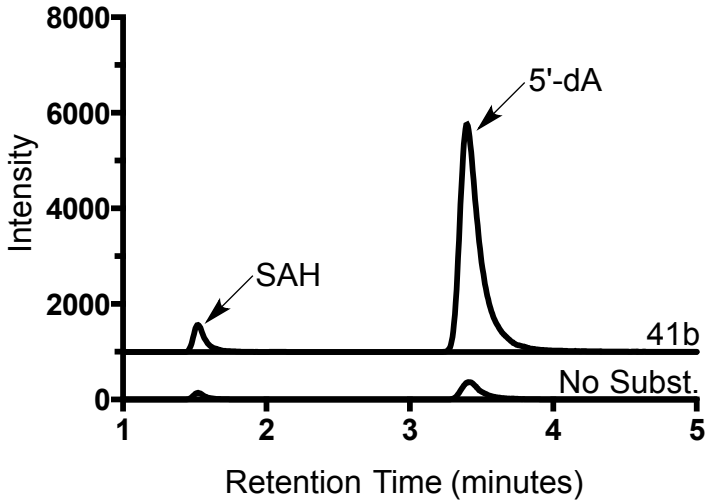

Figure 3.10: Detection of SAM-derived products of ThnK with compound 41b.

LC-MS/MS was used to detect SAM-derived coproducts, SAH (385.4 → 136 *m/z*) and 5'-dA (252.1→136 *m/z*). The extracted-ion chromatograms (EICs) for the transitions of SAH and 5'-dA are overlaid for each reaction. The reaction with compound **41b** shows increased turnover compared to the no substrate control. Reactions were run for 2 hours and ten minutes at room temperature.

Mechanistically, ThnK resembles GenK, a cobalamin-dependent RS C-methylase in gentamicin biosynthesis (5), as both produce near equimolar amounts of SAH and 5'-dA during catalysis. Early labeling experiments established that the C6-ethyl side chain of thienamycin was derived from methionine (14). A labeled carbon was also found in the C6-hydroxymethyl side chain of northienamycin, a minor co-metabolite of thienamycin, suggesting a singly-methylated intermediate in the formation of the ethyl

side chain (14). The present *in vitro* analysis of ThnK agrees with these early experiments. An experiment incorporating chiral [^{1}H, ^{2}H, ^{3}H-*methyl*]-L-methionine demonstrated that the absolute configuration of the terminal methyl in the C6-side chain was largely retained, consistent with an overall methyl transfer process involving two inversions and a methyl-cobalamin intermediate (15). The B_{12}-dependence of ThnK reactions established above supports the role of a methylcobalamin intermediate, as has been implicated in other methyltransferases including TsrM (4, 5) and GenK (5). While the tryptophan methylase TsrM may utilize a similar intermediate, the enzyme is likely mechanistically distinct from ThnK and GenK because it does not produce detectable levels of 5'-dA (4, 5).

The catalysis of consecutive methylations observed for ThnK likely occurs elsewhere in nature. Within the carbapenem family, the carpetimycins have three carbons in their C6 side chain (16) suggesting that a ThnK ortholog may be responsible for three methyl transfers. The natural product pactamycin has traditionally been compared to thienamycin because both possess a hydroxyethyl side chain (14). A recent genetic knockout study suggests, however, that more than one enzyme takes part in attaching the ethyl group (17). While sequential methylations appear not to occur by a single enzyme in pactamycin biosynthesis, other RS enzymes including Swb9 (18) and PoyB or PoyC (19) in quinomycin and polytheonamide biosynthesis, respectively, have been implicated in multiple methylations of a single substrate chain.

Conclusions

These seemingly related biochemical examples notwithstanding, the data reported here establish notable catalytic roles for ThnK. It methylates in two distinct chemical environments (alpha to the β-lactam ring and on a methyl group). The second methyl transfer presumably involves a primary radical intermediate, a particularly high-energy species. By identifying favorable substrates for ThnK and elucidating its activity, we have gained additional clues about the unknown central steps in thienamycin biosynthesis as well. With formation of the ethyl side chain accounted for, ThnL and ThnP can provisionally be assigned non-methyltransferase functions, potentially distinct chemistry for the RS-cobalamin family, as both proteins are essential for carbapenem production (20, 21). Since ThnK activity was only observed when a C2-side chain was present (compounds **10-12** vs. **3**, **8**, and **9**), we deduce that C2-thioether formation likely mediated by ThnL or ThnP precedes C6-methylation in the pathway. The stereochemical preference for (*2R*)-pantetheinyl carbapenams **11** and **41b** indicates that the thiol is possibly introduced in the 2-*exo*-configuration. Furthermore, the observation of activity with substrates matching the (3*S,*5*S*)-carbapenam **3** at C5 (compounds **10**, **11**, and **41b**) suggests that bridgehead epimerization occurs after C6-methylation (ethylation). Consequently, C2-thiol attachment, C6-alkylation, and C5-epimerization likely occur in that order. The orchestration of these biosynthetic events with C2/3-desaturation and maturation of the C2-cysteamine will be addressed in due course.

Materials and Methods

General methods and abbreviations:

hydroxocobalamin (HOCbl)
4-(2-hydroxyethyl)-1-piperazineethane- sulfonic acid (HEPES)
isopropyl β-D-1-thiogalactopyranoside (IPTG)
2-mercaptoethanol (BME)
methylcobalamin (MeCbl)
methyl viologen (MV)
nicotinamide adenine dinucleotide phosphate hydrate (NADPH)
phenylmethysulfonyl fluoride (PMSF)
other reagents were purchased from commercial sources unless otherwise noted

Restriction enzymes, DNA modifying enzymes, and PCR reagents were obtained from New England Biolabs (Ipswich, MA). Plasmid kits were from Thermo Scientific (Waltham, MA). *E. coli* DH5α (Invitrogen) was usually used for DNA cloning and ThnK expression was done in *E. coli Rosetta 2*(DE3) (Novagen). The plasmid pDB1282 was utilized for Fe/S cluster expression (22). SAM and *S*-adenosyl-L-[*methyl*-d_3]methionine (d_3-SAM) were synthesized as described previously (23). Recombinant flavodoxin (Flv) and flavodoxin reductase (Flx) were over-produced in *E. coli* as previously described (24). Plasmid DNA was sequenced by the Synthesis and Sequencing Facility of the Johns Hopkins University.

Cloning and Expression of *Streptomyces cattleya* ThnK.

The *thnK* gene was PCR amplified from genomic DNA of *Streptomyces cattleya* (NRRL8057) using the following primers:

5'– CAAGACATATGACCGTCCCCGCCGCGC – 3',

5'–TATCTCGAGCCGCTGCTCGGTCAGGACGGG – 3'. The *thnK* PCR product was digested using NdeI and XhoI and ligated into the vector pET29b (Novagen) to obtain the *C*-terminal 6-His construct of *thnK*. The plasmid was sequence-verified. The pET29b:t*hnK* was transformed into *E. coli* Rosetta DE3 for expression of ThnK as a C-terminal His_6 construct. The *thnK* Rosetta strain was also transformed with the vector pDB1282, containing the ISC operon with arabinose induction (22). The resulting strain was grown in 4 x 3.5 L of Ethanolamine-M9 medium (25), which included

hydroxocobalamin (HOCbl), and was supplemented with $FeCl_3$ (~0.14 mM) at 37 °C and shaken at 180 rpm. When the optical density of the cultures reached 0.3 at 600 nm, 25 μM $FeCl_3$, 150 μM cysteine, and 0.1% arabinose were added. The cultures were chilled on ice (~45 min) and an additional 25 μM $FeCl_3$, 150 μM cysteine, and 0.1% arabinose were added at optical density 0.4-0.6 (8-10 h). ThnK expression was induced with 1 mM IPTG and the cultures were shaken at 180 rpm overnight at 19 °C. Cells were collected by centrifugation (4,000 × *g*, 12 min), which were then frozen on liquid nitrogen and stored for later use.

Anaerobic Purification of ThnK.

Enzyme purification was performed in an anaerobic chamber (Coy). Frozen cells were resuspended in lysis buffer (10% glycerol, 300 mM KCl, 50 mM HEPES pH 8.0, 10 mM BME, 2-5 mM imidazole) along with lysozyme (1 mg/mL final volume), PMSF (1 mM), DNAse (~ 0.1 mg/mL final volume), and optional HOCbl (~0.4 mg/g cell paste). Cells were lysed by sonication and insoluble material was removed by centrifugation (50,000 × *g* for 1 h at 4 °C). Soluble ThnK was allowed to bind to pre-equilibrated TALON Co^{II} resin (Clontech) and purified by immobilized metal affinity chromatography. The resin was washed with 5 mM and 10 mM imidazole in lysis buffer. The protein was eluted using 250 mM imidazole in the lysis buffer. The enzyme was concentrated using Amicon centrifugal filter devices (Millipore) with a 10 kDA molecular weight limit. Using a PD-10 column (GE Biosciences), the protein was transferred into assay buffer (10% glycerol, 300 mM KCl, 50 mM HEPES pH 7.5, 10 mM BME).

ThnK Protein Analysis.

The concentration of ThnK was determined by the Bradford assay (26) (Varian Cary 50 Bio UV/ Visible Spectrophotometer) using Coomassie Protein Assay Reagent (Thermo Scientific). A concentration correction factor was obtained using amino acid analysis (Molecular Structure Facility, UC Davis). The amount of iron bound by ThnK was determined by established methods (27, 28), and the amount of sulfide was determined as reported (29).

ThnK Activity Assays.

ThnK was mixed with 50-100 mM HEPES pH 7.5, 200 mM KCl, 1 mM SAM or d_3-SAM, 1 mM methyl viologen, 4 mM NADPH, and 1 mM substrate. Initial activity screens also included 0.5 mM HOCbl and 0.5 mM MeCbl, though it was later determined to be unnecessary for activity. Assays of potential substrates lacking a C2-substituent also included 1 mM cysteine and 1 mM coenzyme A. When utilized, dithionite (3 mM) or flavodoxin (90 μM), flavodoxin reductase (9 μM), and NADPH (1 mM) were supplemented at the indicated concentrations in place of methyl viologen and NADPH (default reductant unless otherwise noted). Assays were conducted anaerobically at room temperature and were typically run for 1-2 h.

ThnK SAH and 5'-dA Quantification Assays.

ThnK (50 μM, final concentration) was mixed with 100 mM HEPES pH 7.5, 200 mM KCl, 1 mM SAM or d_3-SAM, 1 mM methyl viologen, 4 mM NADPH, and 1 mM substrate. Assays were run anaerobically for 2 h and 10 min at room temperature.

No-cobalamin ThnK Expression, Purification, and Activity.

The ThnK wild type Rosetta strain was grown in standard M9 medium lacking cobalamin, but supplemented with $FeCl_3$ (~0.14 mM) and thiamine (0.074 mM). Expression and purification of the no-cobalamin ThnK was conducted as described for the wild type protein, but no HOCbl was added during purification. Assays were conducted with 50 μM ThnK and 1 mM HOCbl or 1mM MeCbl when utilized and were otherwise as described for ThnK from ethanolamine medium.

ThnK Cobalamin Quantification.

FPLC-purified ThnK (41 μM by Bradford) was diluted (11.2 μM, 1 mL total reaction volume) and reacted with potassium cyanide (100 mM final). The solution was boiled for 5 min then centrifuged (5 min, max speed). The absorption was measured at 367 nm (dicyanocobalamin, extinction coefficient 30,800 $M^{-1}cm^{-1}$), giving an estimate of 4.7 μM cobalamin or approximately 40% incorporation.

Knockout of Cx_3Cx_2C Motif in ThnK and Mutant Protein Expression, Purification, and Activity.

The pET29b:*thnK* plasmid was used as a template for a two-step PCR method that utilized the following primers: 5'-CGC GGC GCC CCC TAC TCG GCT GCC TTC GCC GAC TGG-3' and 5'-CCA GTC GGC GAA GGC AGC CGA GTA GGG GGC GCC GCG-3'. The C206A-C210A-C213A PCR product was digested with NdeI and XhoI and ligated into the pET29b vector. The resulting plasmid was sequenced and found to be without error. The mutant *thnK* vector was transformed into an *E. coli* Rosetta DE3 strain containing the pDB1282 plasmid. Expression, purification, and

assays of the mutant ThnK (85 μM final concentration) were conducted as described for the wild type protein.

LC-MS Analysis of Carbapenams.

UPLC-MS detection of carbapenams was conducted on a Waters Acquity H-Class UPLC system equipped with a Waters Acquity BEH UPLC column packed with an ethylene bridged hybrid C18 stationary phase (2.1 mm x 50 mm, 1.7 um) followed by a multi-wavelength UV-Vis diode array detector coupled with accurate mass analysis by a Waters Xevo-G2 Q-ToF ESI mass spectrometer. Mobile phase: 0-1 min 100% water + 0.1% formic acid, 1-7.5 min up to 80% acetonitrile + 0.1% formic acid, 7.5 – 8.5 min isocratic 80% acetonitrile + 0.1% formic acid, 8.5-10 min 100% water + formic acid. The flow rate was 0.3 mL/min. The first min of eluant was discarded prior to MS analysis.

LC-MS Analysis of SAH and 5'-dA.

LC-MS detection of *S*-adenosyl-homocysteine (SAH) and 5'-deoxyadenosine (5'-dA) was carried out on an Agilent Technologies (Santa Clara, CA) 1200 system equipped with an autosampler and an Agilent Technologies Zorbax Rapid Resolution Extended-C18 column (4.6 mm × 50 mm, 1.8 μm particle size) and coupled to an Agilent Technologies 6410 QQQ mass spectrometer. Assay mixtures were quenched with H_2SO_4 and insoluble material was pelleted prior to analysis. Method 1 (Compounds **3, 8, 9**): method is similar to that reported previously (30). Mobile phase: The initial conditions included 95% solvent A (40 mM aqueous ammonium acetate, pH 6.0 with glacial acetic acid, and 5% methanol) and 5% solvent B (methanol), 0.5-5 min up to 13% B, 5-6.5 min

up to 27% B, 6.5-7.0 min up to 53% B, 7.0-7.5 min isocratic 53% B, 7.5-8 min down to 5% B, 8.0-10.0 min re-equilibrate at 5% B. Method 2 (Compounds **10-12, 41-43**): Mobile phase: The initial conditions included 90.5% solvent A (0.1% formic acid, pH 2.6) and 9.5% solvent B (methanol), 0-0.2 min 9.5% B, 0.2-3.3 min up to 9.8% B, 3.3-4.1 min up to 30% B, 4.1-4.7 min up to 60% B, 4.7-5.1 min isocratic 60% B, 5.1-5.5 min down to 9.5% B, 5.5-8.7 min isocratic 9.5% B. Data collection and analysis were conducted with the associated MassHunter software package. Detection of SAH and 5'-dA was performed using electrospray ionization in the positive mode (ESI+) with multiple reaction monitoring (MRM). The masses used for the detection of SAH and 5'-dA are shown in Table 3.1. Quantification of SAH and 5'd-A levels was conducted using the MassHunter software with appropriate standard curves and utilized a tyrosine internal standard. The mass transition from the parent ion to product ion 1 (Table 3.1) was used for quantification.

Table 3.1: LC-MS mass fragments for detection of SAH and 5'd-A

	Parent Ion	Product Ion 1	Product Ion 2
SAH	385.4	136	134
5'-dA	252.1	136	119
Tyrosine	182.0	165	123

Table 3.1. Detection of SAH and 5'-dA was performed using electrospray ionization in the positive mode (ESI+) with multiple reaction monitoring (MRM). The masses used for the detection of SAH and 5'-dA are shown. The mass transition from the parent ion to product ion 1 was used for quantification.

FPLC Purification of ThnK.

Fast protein liquid chromatography (FPLC) was conducted on a HiPrep 16/60 S-200 column using an ÅKTA liquid chromatography system (GE Biosciences) in a Coy anaerobic chamber (Grass Lake, MI) using assay buffer as described above.

References:

1. Bodner MJ*, et al.* (2011) Definition of the common and divergent steps in carbapenem β-lactam antibiotic biosynthesis. *ChemBioChem* 12(14):2159-2165.

2. Freeman MF, Moshos KA, Bodner MJ, Li R, & Townsend CA (2008) Four enzymes define the incorporation of coenzyme A in thienamycin biosynthesis. *Proc. Natl. Acad. Sci. USA* 105(32):11128-11133.

3. Zhang Q, van der Donk WA, & Liu W (2012) Radical-mediated enzymatic methylation: a tale of two SAMS. *Acc. Chem. Res.* 45(4):555-564.

4. Pierre S*, et al.* (2012) Thiostrepton tryptophan methyltransferase expands the chemistry of radical SAM enzymes. *Nat. Chem. Biol.* 8(12):957-959.

5. Kim HJ*, et al.* (2013) GenK-catalyzed C-6' methylation in the biosynthesis of gentamicin: isolation and characterization of a cobalamin-dependent radical SAM enzyme. *J. Am. Chem. Soc.* 135(22):8093-8096.

6. Allen KD & Wang SC (2014) Initial characterization of Fom3 from *Streptomyces wedmorensis*: The methyltransferase in fosfomycin biosynthesis. *Arch. Biochem. Biophys.* 543:67-73.

7. Huang C*, et al.* (2015) Delineating the biosynthesis of gentamicin X2, the common precursor of the gentamicin C antibiotic complex. *Chem. Biol.* 22:251-261.

8. Okabe M*, et al.* (1982) Studies on the OA-6129 group of antibiotics, new carbapenem compounds. I. Taxonomy, isolation and physical properties. *J. Antibiot. (Tokyo)* 35(10):1255-1263.

9. Allen KD & Wang SC (2014) Spectroscopic characterization and mechanistic investigation of P-methyl transfer by a radical SAM enzyme from the marine bacterium *Shewanella denitrificans* OS217. *Biochimica et Biophysica Acta (BBA) - Proteins and Proteomics* 1844(12):1-10.

10. Yan F*, et al.* (2010) RlmN and Cfr are radical SAM enzymes involved in methylation of ribosomal RNA. *J. Am. Chem. Soc.* 132(11):3953-3964.

11. Bauerle MR, Schwalm EL, & Booker SJ (2015) Mechanistic diversity of radical *S*-adenosylmethionine (SAM)-dependent methylation. *J. Biol. Chem.* 290(7):3995-4002.

12. Marous DR*, et al.* (2015) Consecutive radical *S*-adenosylmethionine methylations form the ethyl side chain in thienamycin biosynthesis. *Proc. Natl. Acad. Sci. USA* 112(33):10354-10358.

13. Mitscher LA, Showalter HD, Shirahata K, & Foltz RL (1975) Chemical-ionization mass spectrometry of beta-lactam antibiotics. *J. Antibiot. (Tokyo)* 28(9):668-675.

14. Williamson JM*, et al.* (1985) Biosynthesis of the beta-lactam antibiotic, thienamycin, by *Streptomyces cattleya*. *J. Biol. Chem.* 260(8):4637-4647.

15. Houck DR, Kobayashi K, Williamson JM, & Floss HG (1986) Stereochemistry of methylation in thienamycin biosynthesis: example of a methyl transfer from methionine with retention of configuration. *J. Am. Chem. Soc.* 108:5365-5366.

16. Williamson J (1986) The biosynthesis of thienamycin and related carbapenems *Crit. Rev. Biotechn.* 4(1):111-131.

17. Lu W, Roongsawang N, & Mahmud T (2011) Biosynthetic studies and genetic engineering of pactamycin analogs with improved selectivity toward malarial parasites. *Chem. Biol.* 18(4):425-431.

18. Watanabe K*, et al.* (2009) *Escherichia coli* allows efficient modular incorporation of newly isolated quinomycin biosynthetic enzyme into echinomycin biosynthetic pathway for rational design and synthesis of potent antibiotic unnatural natural product. *J. Am. Chem. Soc.* 131(26):9347-9353.

19. Freeman MF*, et al.* (2012) Metagenome mining reveals polytheonamides as posttranslationally modified ribosomal peptides. *Science* 338(6105):387-390.

20. Rodríguez M*, et al.* (2011) Mutational analysis of the thienamycin biosynthetic gene cluster from *Streptomyces cattleya*. *Antimicrob. Agents Chemother.* 55(4):1638-1649.

21. Li R, Lloyd EP, Moshos KA, & Townsend CA (2014) Identification and characterization of the carbapenem MM 4550 and its gene cluster in *Streptomyces argenteolus* ATCC 11009. *ChemBioChem* 15(2):320-331.

22. Lanz ND*, et al.* (2012) RlmN and AtsB as models for the overproduction and characterization of radical SAM proteins. *Method. Enzymol.* 516:125-152.

23. Iwig DF & Booker SJ (2004) Insight into the polar reactivity of the onium chalcogen analogues of *S*-adenosyl-L-methionine. *Biochemistry* 43(42):13496-13509.

24. Grove TL*, et al.* (2011) A radically different mechanism for *S*-adenosylmethionine-dependent methyltransferases. *Science* 332(6029):604-607.

25. Bandarian V & Matthews RG (2004) Measurement of energetics of conformational change in cobalamin-dependent methionine synthase. *Methods Enzymol.* 380:152-169.

26. Bradford MM (1976) A rapid and sensitive method for the quantitation of microgram quantities of protein utilizing the principle of protein-dye binding. *Anal. Biochem.* 72(1):248-254.

27. Beinert H (1978) Micro methods for the quantitative determination of iron and copper in biological material. *Methods Enzymol.* 54:435-445.

28. Kennedy MC*, et al.* (1984) Evidence for the formation of a linear [3Fe-4S] cluster in partially unfolded aconitase. *J. Biol. Chem.* 259(23):14463-14471.

29. Beinert H (1983) Semi-micro methods for analysis of labile sulfide and of labile sulfide plus sulfane sulfur in unusually stable iron-sulfur proteins. *Anal. Biochem.* 131(2):373-378.

30. Grove TL, Radle MI, Krebs C, & Booker SJ (2011) Cfr and RlmN contain a single [4Fe-4S] cluster, which directs two distinct reactivities for *S*-adenosylmethionine: methyl transfer by SN2 displacement and radical generation. *J. Am. Chem. Soc.* 133(49):19586-19589.

Chapter 4

Attachment of Large, CoA-Derived Thiol Provides Side Chain in Complex Carbapenem Biosynthesis

Introduction

The carbapenems are therapeutics of last resort within the β-lactam family of antibiotics due to their relative insusceptibility to common bacterial resistance mechanisms (1). Despite their medical importance, the carbapenems are produced commercially by total synthesis rather than by lower-cost fermentation methods, unlike other clinically-used members of the class (1). Increased understanding of the biological assembly of natural carbapenems, such as the paradigmatic thienamycin **7**, would pave the way for semi-synthetic routes of production.

The early biosynthesis of thienamycin in *Streptomyces cattleya* involves two enzymes, ThnE and ThnM, which make the bicyclic (3*S*,5*S*)-carbapenam **3** (2) from simple metabolic building blocks. These two steps are paralleled in *Pectobacterium carotovorum* during the formation of the "simple" carbapenem **4** (3) where one additional enzyme, CarC, is able to complete the pathway by converting **3** to the antibiotic **4** (3). "Complex" carbapenems, including thienamycin and at least 50 structural variants from actinomyces, do not have a CarC homolog in their gene clusters (4), suggesting evolution of an alternate route to antibiotic formation. After **3** is biosynthesized in *S. cattleya*, however, only fragmentary information about the subsequent steps is known. Recent results, however, have demonstrated that the C6-ethyl side chain is formed by consecutive radical *S*-adenosylmethionine (RS) catalyzed methylations by ThnK (5). These experiments also suggested that the C2-thioether side chain was installed prior to

C6-alkylation. ThnK methyl transfer activity was exhibited with substrates bearing the C2-pantetheinyl moiety. It remains uncertain if this side chain represents a true biosynthetic intermediate. For more than two decades, cysteine was thought to be the source of the thioether, since labeled cystine was shown to be efficiently incorporated into thienamycin (6). However, isolated carbapenems bearing a C2-pantetheine (7) indicate that a larger thiol is attached. More recent experiments associate the sequential truncation of coenzyme A (CoA) with the creation of the cysteamine side of thienamycin (8), yet the identity of the thiol and the enzyme that attaches it to the carbapenam nucleus are unknown.

In addition to ThnK, there are two other RS enzymes encoded by the gene cluster (9), ThnL and ThnP, which are also classified as cobalamin-dependent RS methylases (10). It is likely that these two RS enzymes in fact have non-methylase functions, where one is possibly responsible for mediating the C2-thioether formation, as the two methylations have now been attributed to ThnK. Unfortunately, technical barriers of low enzyme solubility and stability coupled with unknown substrates have thus far impeded efforts to elucidate the functions of these two enzymes. In this work, we describe the synthesis of various C2-substituted carbapenams, including compounds that contain a full CoA moiety at C2, as well as an assessment of the *in vitro* activity of ThnK with these molecules. The high levels of turnover observed with the CoA-functionalized carbapenams strongly suggest that CoA or a closely related thiol is attached to the bicycle in the course of complex carbapenem biosynthesis. In a separate experimental approach, a heterologous expression system combined with a CarC competition assay now places

ThnL likely directly after ThnE/ThnM, implicating this RS protein as the probable candidate for the attachment of the C2-thiol.

Results and Discussion

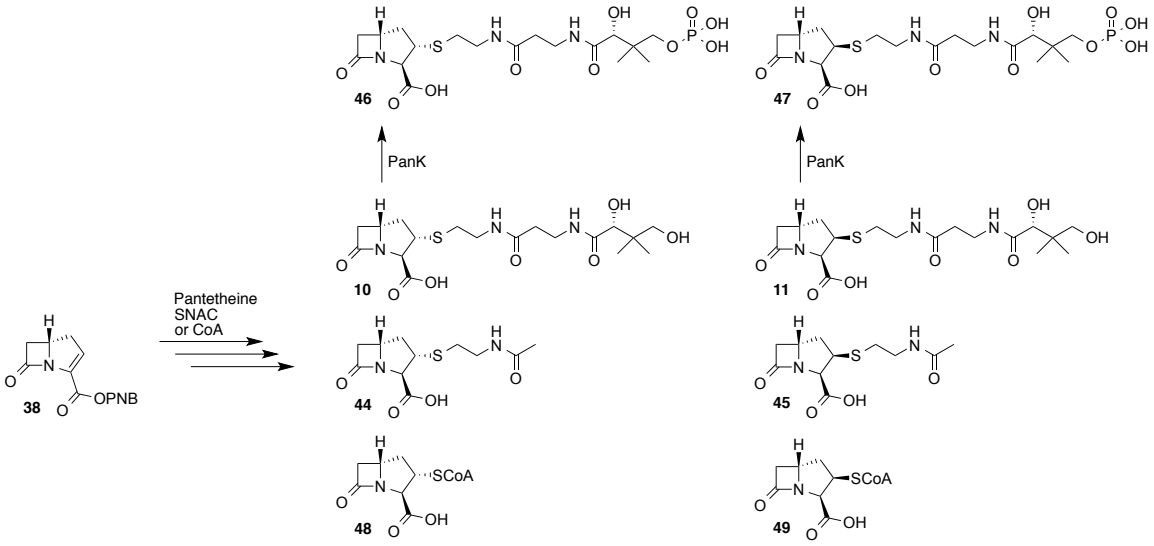

Figure 4.1: Overview of the synthesis of C2-substituted carbapenams to test with ThnK.

To probe the identity of the thiol that is attached to the bicyclic carbapenam nucleus, we chose to evaluate the tolerance of ThnK towards variation in C2 side chain length. Previously, a pantetheinyl group on a carbapenam was shown to be sufficient to observe activity from ThnK (5), but other CoA-derived thioethers are biologically relevant and possible as well. Within the thienamycin cluster, ThnR, ThnH, and ThnT are able to successively cleave CoA to 4-phosphopantetheine, pantetheine, and cysteamine, respectively (8). Thus, additional carbapenams representing the other possible truncation states (Figure 4.1) were desired, but substituting the more chemically inert *N*-acetylcysteamine (SNAC) for cysteamine. We began by synthesizing the carbapenem **38** using previously established methods (11) and from this common

intermediate, pantetheine or SNAC can be inserted in a β-addition, as has been shown (5, 12). Additionally, we found that CoA itself could also be added into the carbapenem directly. High-performance liquid chromatography (HPLC) enabled separation of the C2-diastereomers giving compounds **10**-**11**, **44**-**45**, and **48**-**49** (Figure 4.1). We utilized PanK (CoaA) (13) to convert the pantetheinyl compounds **10** and **11** into their corresponding phosphopantetheinyl analogs **46**-**47**.

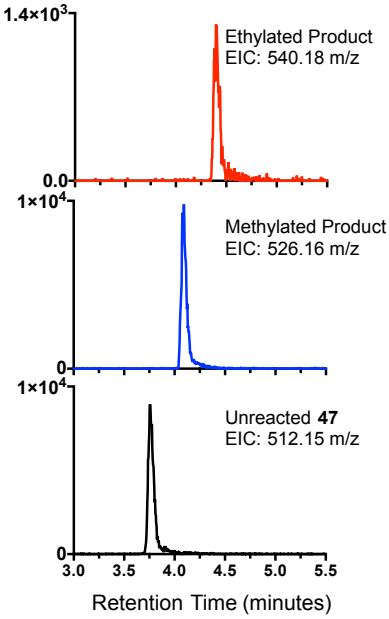

Figure 4.2: Sequential methylations by ThnK.

UPLC-HRMS detection of carbapenams from the ThnK reaction with compound **47**. The bottom, middle, and top traces show the extracted-ion chromatograms (EICs) (m/z ± 0.05) for unreacted substrate (512.15 m/z), methylated product (526.16 m/z), and ethylated product (540.18 m/z), respectively.

ThnK was expressed and anaerobically purified as previously described (5). As a RS enzyme, ThnK requires a [4Fe-4S] cluster to reductively cleave *S*-adenosylmethionine (SAM) to form a 5'-deoxyadenosyl radical, which can initiate chemistry (14). Both the iron-sulfur cluster and the required cofactor cobalamin were

provided in our expression system. The enzyme also uses SAM as the source of the methyl groups that are transferred to the substrate. To evaluate the synthetic substrates, each compound (1 mM) was incubated with ThnK, [4Fe-4S] cluster reductants (methyl viologen, 1 mM and NADPH, 2 mM), and SAM (1 mM). ThnK was confirmed to perform consecutive methylations at C6, as expected (Figure 4.2).

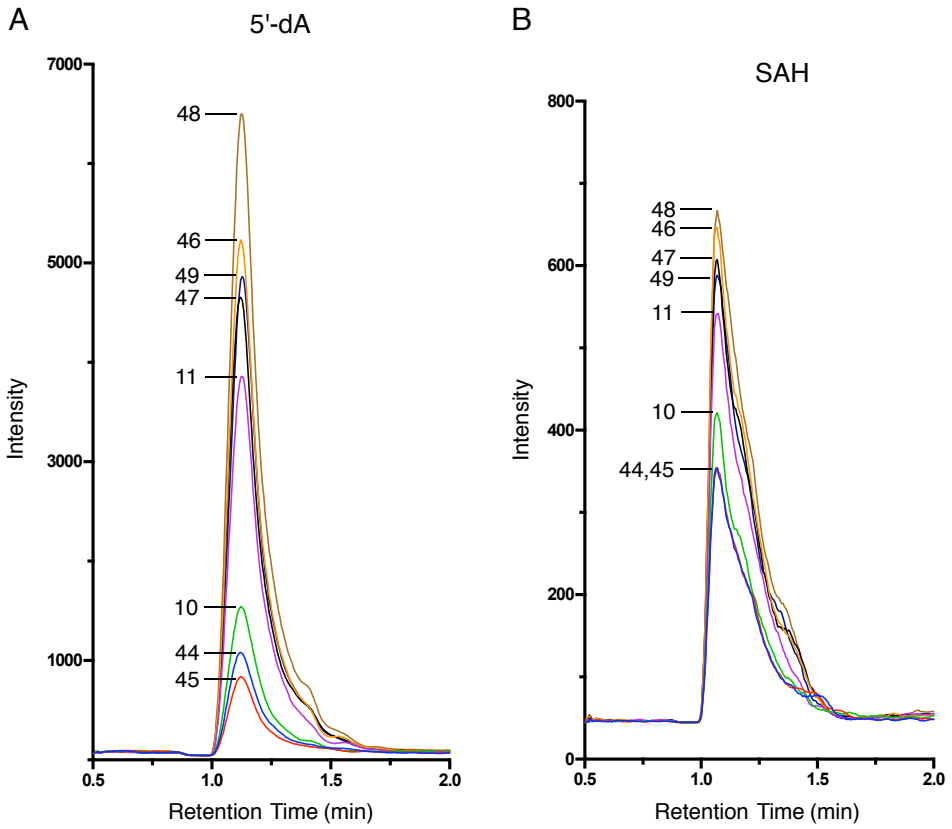

Figure 4.3: LC-MS/MS detection of enzymatic SAM-derived coproducts SAH (385.4 → 136 m/z) and 5′-dA (252.1 → 136 m/z).

The extracted-ion chromatograms (EICs) for the transitions of 5′-dA (A) and SAH (B) are shown for each reaction.

For assessment of the relative turnover with the various substrates, the RS methylase SAM-derived coproducts *S*-adenosylhomocysteine (SAH) and 5′-deoxyadenosine (5′-dA) (15) were monitored by LC-MS/MS. Several trends were

apparent from sampling the levels of accumulated 5′-dA (Figure 4.3A). Three compounds consistently gave the lowest turnover including both C2-SNAC molecules (**44** and **45**) and the pantetheine-substituted **10**. The (2*R*)-carbapenam **11** gave higher levels of 5'-dA than its diastereomer **10**, as had been observed previously (5). With the (2*R*)-series (**45**, **11**, **47**, **49**), only modest gains were made by derivatizing the side chain to phosphopantetheine (**47**) or CoA (**49**). In contrast, with the (2*S*)-series (**44**, **10**, **46**, **48**), the phosphopantetheine (**46**) and CoA (**48**) analogs gave much better activity than the pantetheine compound **10**. The (2*S*)-CoA carbapenam **48** produced the greatest amounts of 5'-dA. Correspondingly, these trends with 5'-dA levels mirrored those of SAH accumulation (Figure 4.3B).

The activity of ThnK with large CoA-derived side chains begs the question of which enzyme is responsible for attaching the C2-appendage. Interestingly, the only difference between substrates for ThnK and the (3*S*,5*S*)-carbapenam **3** is the C2-thioether. We hypothesize that ThnL is directly after ThnE and ThnM in the pathway, providing the missing link between these enzymes and ThnK. Prior work on the thienamycin cluster is consistent with this role for ThnL. In a secretor-convertor pair experiment between knockout strains, it was noted that ThnL acted before ThnP in the pathway (16). Additionally, it has been reported that the ThnL knockout strain in *S. cattleya* accumulated a compound with a mass matching **3** (16).

To indirectly probe the possible biosynthetic activity of ThnL, we turned to *Streptomyces* as a heterologous host since carbapenem biosynthetic pathways occur in actinomyces and the RS protein has very limited solubility in *E. coli*. Specifically, *S. lividans* TK24 (17) and the genome-minimized *S. coelicolor* M1154 (18) strains were

selected. The early biosynthetic genes *thnE* and *thnM* were placed in succession under the *ermEp* promoter using the plasmid pUWL201PW (19). The *ermEp-thnE-thnM* construct was then moved to the integrative plasmid pMS82 (20), which contains a phage integrase for site-specific insertion into the *Streptomyces* genome. By placing the genes into the genome itself, they can be stably maintained, even in the absence of antibiotic selection. The pMS82/*ermEp-EM* plasmid was electroporated into *E. coli* ET12567 (pUZ8002), a methylation deficient strain, for conjugation to germinated spores from the two *Streptomyces* host strains. With the TK24-EM and M1154-EM strains in hand, a Southern blot was performed on digested gDNA isolated from each strain, which verified that both *thnE* and *thnM* were integrated into the hosts (Figure 4.4).

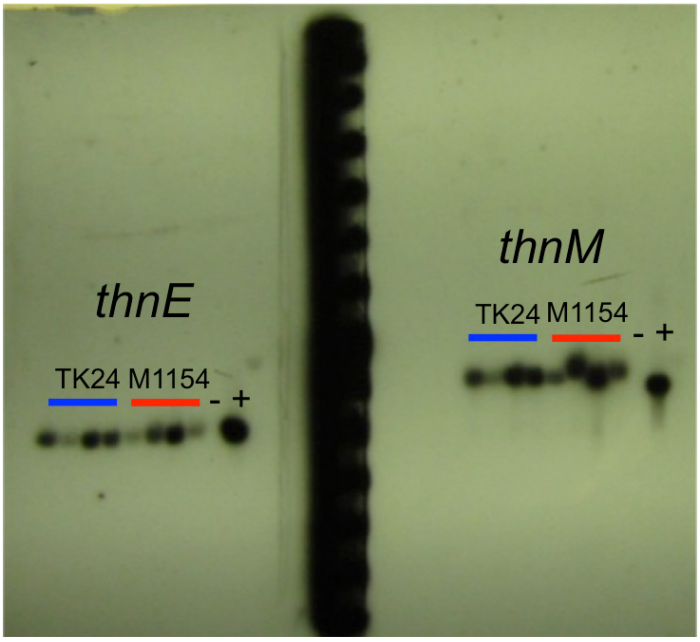

Figure 4.4: Southern blot verifying insertion of *thnE* and *thnM* into *S. lividans* TK24-EM and *S. coelicolor* M1154-EM.

The first four lanes for each gene are *S. lividans* transformants and are followed by four lanes of *S. coelicolor* transformants and a negative and positive control.

To confirm that ThnE and ThnM were expressed and showed activity, an assay was developed to sensitively detect production of the (3*S*,5*S*)-carbapenam **3**. We envisioned using the enzyme CarC to transform **3** into the carbapenem **4**. As an active antibiotic, **4** can be facilely detected using a supersensitive *E. coli* (ESS) strain (21). The assay conditions were tested using synthetically-prepared **3** that was added to α-ketoglutarate (8 mM), ferrous ammonium sulfate (80 μM), and ascorbic acid (2 mM) since CarC is an α-ketoglutarate-dependent, non-heme iron oxygenase (22). This mixture was combined with a cell-free extract (CFE) from *E. coli* cells expressing CarC, analogous to early work establishing the activity of the enzyme (22). The CarC CFE reaction produced a zone of inhibition on an ESS-seeded agar plate (Figure 4.5) as expected, confirming that the carbapenem **4** was produced.

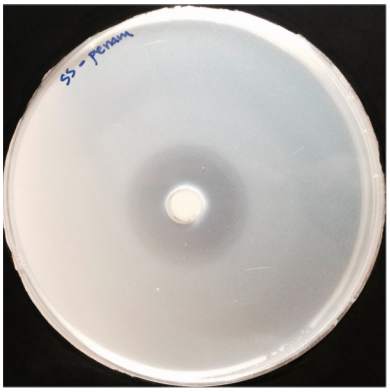

Figure 4.5: Production of the antibiotic 4 from the CarC assay with synthetic (3*S*,5*S*)-carbapenam 3.

The CarC assay included α-ketoglutarate, ammonium iron(II) sulfate, ascorbic acid, and 1.4 mM substrate **3**. The reaction was run at 28 °C for 1 h and 10 min before plating on ESS.

We initially examined the CFE from the *Streptomyces* strains containing ThnE/M, but did not observe production of **3** using the CarC assay. Reasoning that perhaps **3** was

exported from the cell, we assayed the *Streptomyces* growth supernatant after removing the cells; zones of inhibition were evident. Importantly, the *Streptomyces* supernatant without the addition of CarC did not produce this effect. The zones of inhibition are specific for CarC activity since withholding ascorbic acid or α-ketoglutarate abolished the ability to kill ESS (Figure 4.6). The CarC assay confirmed ThnE and ThnM expression and activity in both TK24-EM and M1154-EM.

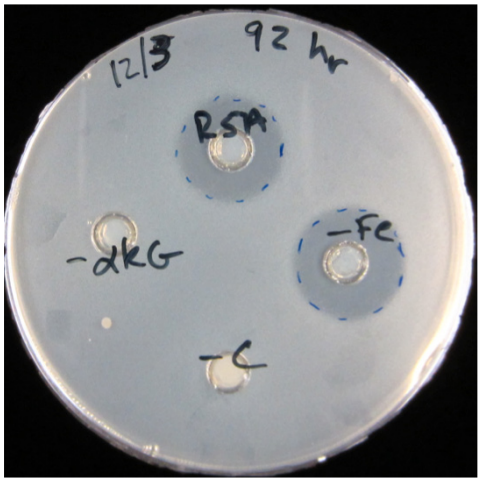

Figure 4.6: Production of zones of inhibition are dependent on CarC activity.

Withholding ascorbic acid (-C) or α-ketoglutarate (-αKG) from the CarC assay prevented formation of a zone of inhibition, which is present when all the cofactors are available (R5A). Additional iron(II) was not necessary for the CarC assay as seen in the –Fe control, presumably because sufficient quantities are already present from the CarC expression. All reactions were conducted with R5A+ medium samples from the same M1154-EM culture.

In an effort to boost carbapenam production levels, we examined multiple growth media and supplements. For both the TK24-EM and M1154-EM strains, R5A+ medium (see *Materials and Methods*) was found to give the best production. Next, this growth medium was supplemented with the substrate for ThnE, L-pyrroline-5-carboxylic acid **1** (P5C), or glutamate, the amino acid building-block for P5C. The P5C or glutamate

additions, however, did not increase (3*S*,5*S*)-carbapenam **3** titers, suggesting that availability of these precursors was not limiting. Production of **3** was monitored for 5-6 days and peak levels were typically observed between 3 and 4 days.

Having integrated ThnE and ThnM into heterologous hosts, we generated EML strains by adding ThnL to the system. In parallel, we elected to make EMK strains for comparison. The *C*-terminal-His_6 constructs of *thnL* and *thnK* were each placed under control of the *ermEp* promoter. Each gene was then moved to the pSET152 vector (23), which is similar to pMS82, but integrates at a different site in the *Streptomyces* genome. Transferring the pSET152 construct to *E. coli* ET12567 (pUZ8002) allowed for conjugation to the EM strains. Verification of protein expression for ThnL and ThnK was readily observed by SDS-PAGE for the TK24-EML and TK24-EMK strains (Figure 4.7), though was less evident in the corresponding strains in *S. coelicolor*.

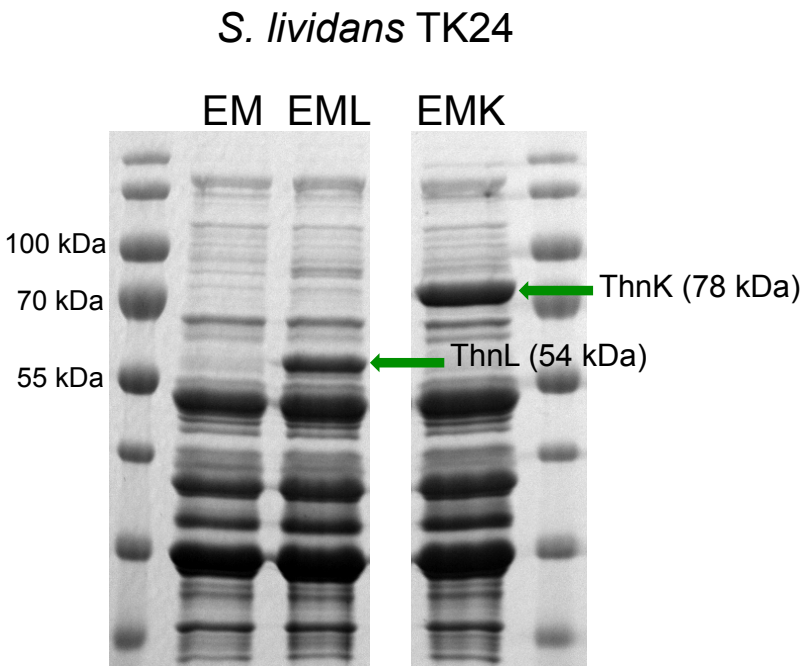

Figure 4.7: Detection of ThnL and ThnK in TK24-EML and EMK strains.

Approximately 12 grams of cells from each strain were lysed and the proteins were concentrated by immobilized metal-affinity chromatography using TALON Co^{II} resin. Samples were then analyzed by SDS-PAGE.

The CarC assay was again utilized to assess the effect of ThnL (Figure 4.8). If ThnL is unable to use the product of ThnE and ThnM, **3** will continue to diffuse into the medium. Upon reaction with CarC, the carbapenam will be converted to the active antibiotic, resulting in a zone on ESS. However, if ThnL is modifying **3**, less is available to react with CarC, which should correspond to a smaller zone size.

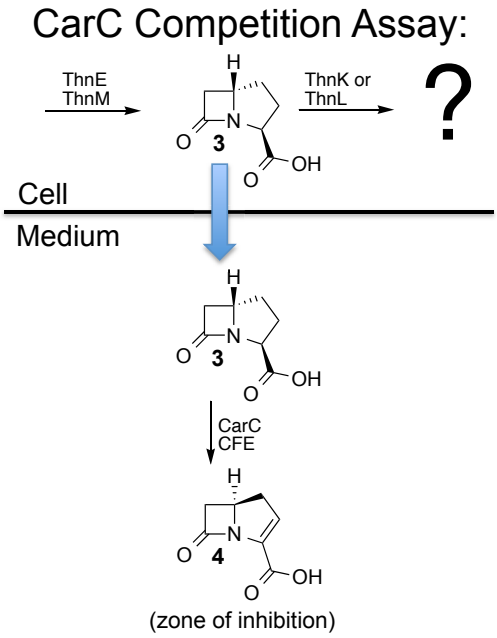

Figure 4.8: Schematic of CarC competition assay with EML or EMK strains.

When the CarC "competition" assay was performed, the medium from TK24-EML and M1154-EML strains typically gave comparable or slightly smaller zone sizes than the corresponding EM or EMK strains. Since ThnL is predicted to utilize cobalamin (10), we postulated that a possible deficiency of this cofactor could be limiting ThnL activity. The assay was repeated with two cultures for each strain (EM, EML, and EML in TK24 and M1154), one of which was supplemented with hydroxocobalamin (1 μM). While the zones corresponding to the EMK and EM strains showed no effect from the

added cobalamin, the zones from the EML strains were essentially non-existent (Figure 4.9). The absence of a zone strongly suggests that ThnL functions directly after ThnE/M in the biosynthetic pathway. The requirement of cobalamin for maximal effect supports the use of the cofactor by ThnL. Thus far, attempted isolation of an intermediate from the EML strains has proven unsuccessful, but highlights the utility of the highly sensitive CarC competition assay to glean clues about thienamycin biosynthesis.

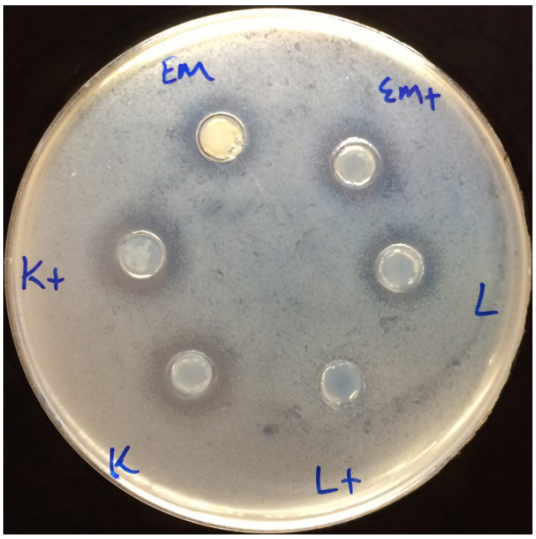

Figure 4.9: CarC competition assay with TK24-EM, EML, and EMK strains.

Strains with a (+) designation had 1 μM hydroxocobalamin supplemented in the growth medium. The EML+ strain medium did not produce a zone, suggesting the (3*S*,5*S*)-carbapenam was utilized by ThnL.

Conclusions

Thienamycin was first isolated over 35 years ago (24), yet difficult genetic manipulation in the producing strain and experimental limitations stemming from *in vitro* protein stability have thwarted elucidation of the biosynthetic pathway. In this work, we present an experimentally diverse approach to this problem including synthesis of

complex potential intermediates, anaerobic *in vitro* reactions, heterologous expression in *Streptomyces*, and a competition bioassay designed to shed light on the murky center of complex carbapenem assembly. *In vitro* reactions with ThnK showed that a small C2-substituent (SNAC) was clearly not preferred. The low ThnK catalytic activity with compounds **44** and **45** suggests that a small thiol such as cysteine is not likely added directly to the bicyclic structure. Until now, a pantetheinyl group represents the largest carbapenam(em) C2 side chain that has been tested *in vitro* in potential substrates for biosynthetic enzymes (5, 8). After synthesizing and analyzing phosphopantetheine and CoA derivatives, we observed that these are better substrates for ThnK, indicating that larger side chains are preferred biosynthetically. While the (2*S*)-CoA carbapenam **48** gave the highest levels of turnover, other extended side chain compounds (**46**, **47**, **49**) also gave good turnover, suggesting some promiscuity by the enzyme. This flexibility suggests a possible metabolic grid that allows for ThnR to remove the nucleotide-monophosphate either before or after alkylation by ThnK. We note that with the C2-thioethers, ThnK accepts both possible stereoisomers at C2. While phosphopantetheine cannot be definitively excluded, we propose that CoA itself is attached to the bicyclic carbapenam core prior to the methylations by ThnK.

Additionally, heterologous expression of ThnE/ThnM and ThnL combined with a CarC partition assay suggested that the (3*S*,5*S*)-carbapenam **3** is the substrate for ThnL. The lack of accumulation of **3** was observed in two separate EML-expressing species and was cobalamin-dependent, in further support of ThnL activity. Of further note, the CarC assay also implied that **3** is not an *in vivo* substrate for ThnK, as has been previously seen *in vitro* (5). As there is one chemical substitution separating the CoA-substituted **48** from

3, only one enzyme may function between ThnE/ThnM and ThnK. The *in vivo* expression experiments place ThnL as the missing step in the pathway and the probable enzyme for the linkage of the C2-CoA moiety. Examples of atomic sulfur inserting RS enzymes are known including both biotin synthase and lipoyl synthase, which use a second [Fe-S] cluster as a sulfur source (14). As a variation, the proteins MiaB and RimO catalyze methylthiolations and also contain a second [Fe-S] cluster, although the cluster is not cannibalized for sulfur. Instead, these proteins employ exogenous sulfide bound to the second cluster (25). Alternatively, the use of a sulfur-containing cofactor (CoA) and potentially cobalamin as well would be a novel adaptation in the RS enzyme family. Overall, the evidence for the role of ThnL in thienamycin biosynthesis presented here will guide future efforts to demonstrate directly the substrate of C2-attachment and elucidate the mechanism of C5-epimerization and C2/C3-desaturation.

Materials and Methods

P5C Preparation.

P5C was synthesized using established methods (26).

Synthesis of the ThnK substrates.

See Chapter 2

Purification of ThnK.

See Chapter 3, including FPLC purification

ThnK *in vitro* Reactions.

ThnK (2.9 μM) was mixed with 100 mM HEPES pH 7.5, 200 mM KCl, 1 mM SAM, 1 mM methyl viologen, 2 mM NADPH, and 1 mM substrate. Assays were conducted anaerobically at room temperature and were typically run for 2 h. LC-MS/MS detection of 5'-dA/SAH and LC-HRMS detection of carbapenams were conducted essentially as previously described (5).

Construction of the thnE/thnM Plasmid for Conjugation to *Streptomyces*.

The *thnE* gene was amplified by PCR from *thnE* in the pBluescriptII SK+ vector (27) using the following primers:

5'-GGCATATGGGCGCGGCCGCCGGCGAGCGGAGAACC-3'

5'-GGCTCGAGGCTCCGCCCGATGACGCGGCGCATCCGCAC-3'

The PCR product was ligated into pBluescript and verified to be correct by automated sequencing. The *thnE gene* was excised using NdeI/XhoI and ligated to the same restriction sites in pET29b, creating pET29b/*thnE.* This plasmid was then digested with BlpI, blunt-ended with Klenow DNA polymerase, and then digested with NdeI. The vector pUWL201PW (19) was digested with HindIII, treated with Klenow, and digested with NdeI. Ligating the NdeI-blunt *thnE* into the digested pUWL201PW gave the vector pUWL201PW/*thnE*.

thnM in pET29b (27) was digested with DraIII (*thnM* has a single BlpI site), treated with Klenow, and digested with NdeI. The NdeI-blunt *thnM* was ligated into the same digested pUWL201PW vector used for *thnE,* giving pUWL201PW/*thnM.*

pUWL201PW/*thnM* was digested with XbaI, treated with Klenow, and digested with PstI. This gave a RBS-*thnM*-C-His_6 insert. pUWL201PW/*thnE* was digested with EcoRI, treated with Klenow, and digested with PstI. The RBS-*thnM*-C-His_6 construct was ligated into the digested pUWL201PW/*thnE* to give pUWL201/*ermEp-EM* (Figure 4.10A), which was sequence-verified. The pUWL201/*ermEp-EM* was digested with PstI-HF followed by treatment with Klenow. The purified DNA was partially digested with KpnI (there is a single KpnI site in *thnM*). The 3.5-kb *ermEp*-RBS-*thnE*-C-His_6-RBS-*thnM*-C-His_6 fragment was ligated in pMS82 (20), which had been digested with HindIII/Klenow and KpnI. The pMS82/*ermEp-EM* plasmid (Figure 4.10B) was

electroporated into *E. coli* ET12567 (pUZ8002) cells and conjugated into spores of *S. coelicolor* M1154 and *S. lividans* TK24 for integration at the ϕBT1 site, creating the M1154-EM and TK24-EM strains.

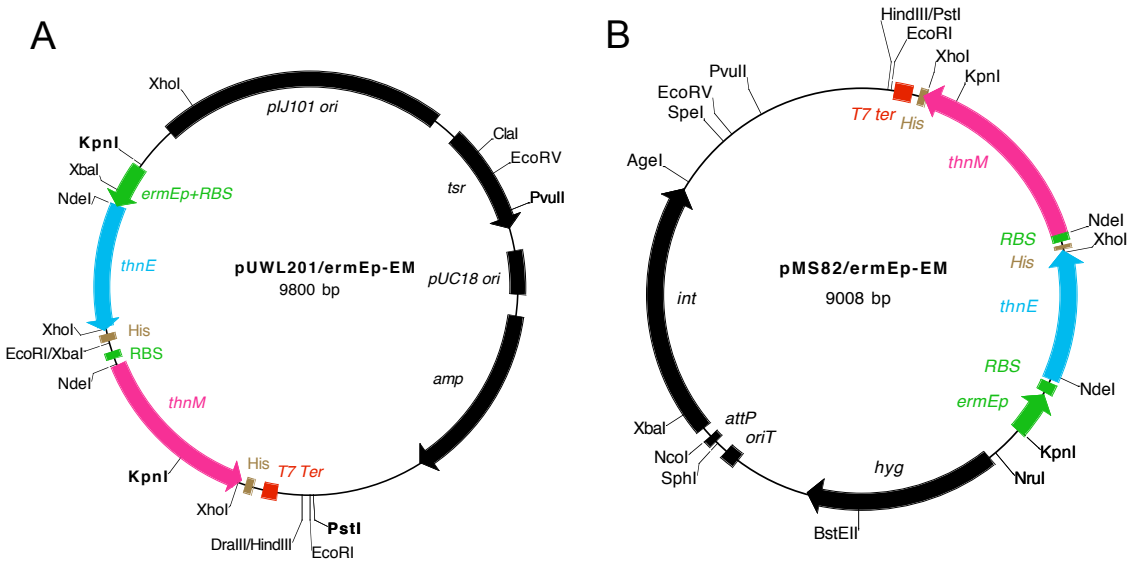

Figure 4.10: Plasmid Maps for pUWL201/*ermEp-EM* (A) and pMS82/*ermEp-EM* (B)

Construction of the thnK and thnL Plasmids for Conjugation to *Streptomyces*.

The *thnK* gene in the pET29b vector was previously described (5). The *thnL* gene was PCR amplified from *S. cattleya* (NRRL8057) genomic DNA using the following primers:

5'-CAAGACATATGAGGGTCTTGCTGGTGTGGCCTCGTAACGAG-3'

5'-TATCTCGAGTCCGGTGCCGGCGACCGTCTC-3'

The *thnL* PCR product was digested using NdeI and XhoI and ligated into pET29b (Novagen) using the same restriction sites to obtain the *C*-terminal-His_6 construct of *thnL*. The plasmid was sequence-verified. The *C*-term-His_6 genes (*thnK* and *thnL*) were digested (BlpI for *thnK*; DraIII for *thnL*), blunted with Klenow, and digested with NdeI. These fragments were inserted into pUWL201PW at HindIII/Klenow-NdeI sites. The

ermEp-C-term-His_6 genes were digested (partial KpnI for *thnK*; KpnI for *thnL*), purified after gel electrophoresis if necessary (for partial digests), digested again (PstI for *thnK*; EcoRI for *thnL*), and then blunted with Klenow. The inserts were ligated into the EcoRV site of pSET152 (23). The pSET152 plasmids for each gene were sequenced. The plasmids were electroporated into the *E. coli* strain ET12567 (pUZ8002) for conjugation to the *Streptomyces* EM strains at the ϕC31 site.

Conjugation to *Streptomyces*.

Spores were isolated from the desired *Streptomyces* strains (17, 18). The integrative plasmid (pSET152 or pMS82) containing the desired construct was electroporated into the *E. coli* strain ET12567 (pUZ8002). The *E. coli* culture (50 mL, LB medium) was grown to OD_{600} = 0.4. The cells were pelleted by centrifugation (4000 × *g*), washed twice (40 mL LB medium), and resuspended in 2 mL of LB medium. The *Streptomyces* spores (50 μL) were added to 0.5 mL of 2xYT media and kept at 50 °C for 10 minutes. The spores were mixed with 0.5 mL of the *E. coli* donor strain resuspension. The mixture was centrifuged and the cell pellet resuspended in 300 μL of LB medium. A sample of the resuspension (100 μL) was plated on MS + $MgCl_2$ agar medium. The cells were grown for 16-20 hours at 28 °C. Nalidixic acid, hygromycin B (pMS82), and apramycin (pSET152) were added to the top of the plates in sterile water and colonies were allowed to develop over 3-5 days.

Southern Blot Hybridization.

The plasmid pUWL201/*ermEp-EM* was digested with KpnI, NdeI, and XhoI to create DNA probes. The DNA bands corresponding to *thnE* and *thnM* were isolated (there is a single KpnI site in *thnM*, resulting in the probe being slightly smaller than the full gene). The gDNA from *S. lividans*-EM and *S. coelicolor*-EM strains was isolated. The particular EM strains for the Southern blot also contained *carC* at the ϕC31 site, the same location where either *thnL* or *thnK* was eventually inserted. The gDNA was digested with NdeI and XhoI and run on an agarose gel (1%) along with appropriate positive and negative controls. The DNA was transferred to a nylon membrane using the Whatman Turboblotter Rapid Downward Transfer System. The membrane was wrapped in a nylon cloth and placed in a sealed glass tube with prehybridization buffer (5× SSC, 5× Denhardt's, 50% formamide, 1% SDS, 100 μg/mL denatured salmon sperm DNA). The tube was rotated for 3 hours at 68 °C. The ^{32}P-labeled probe was prepared by mixing 5 μL New England Biolabs buffer 2, 25 μL primer mix, 2 μL dATP, 2 μL dTTP, 2 μL dGTP, 28 μL denatured probe DNA, 5 μL [α-P^{32}]dCTP, and 1 μL Klenow DNA polymerase. The reaction was run for 60 min at 37 °C. The probes were purified and denatured (90 °C for ~10 min, then on ice) and added to the glass tube with the nylon membrane and left overnight rotating at 68 °C. The membrane was washed using two buffers: A) 2 x SSC, 0.1 % SDS, rt 10 min and B) 0.2 x SSC, 1 % SDS, 68 °C 20 min. Two washes were done with buffer A and one wash with buffer B, monitoring ^{32}P levels with a Geiger counter. The membranes were placed in a sealed box with unexposed film overnight at -80 °C. The film was developed the next day.

Growth of *Streptomyces* Cultures.

R_2YE+ medium (per L): 103 g sucrose, 2 g tryptone, 4 g peptone, 4 g yeast extract, 10 g glucose, 1 g casamino acids, 0.25 g K_2SO_4, 10.12 g $MgCl_2 \cdot 6H_2O$, 100 mLTris-HCl (0.25M, pH 7.2), 80 mL $CaCl_2 \cdot 2H_2O$ (3.68%), 5 mL 1N NaOH, 10 mL KH_2PO_4 (0.5%), 2 mL trace soln, 2 mL element soln. (pH 6.5)

R5A+ medium (per L): 0.25 g K_2SO_4, 10.12 g $MgCl_2 \cdot 6H_2O$, 10 g glucose, 0.1 g casamino acids, 5 g yeast extract, 21 g MOPS, 0.2 mL trace soln, 2 ml element soln. (pH 6.8)

Trace soln (per L): 40 mg $ZnCl_2$, 200 mg $FeCl_3 \cdot 6H_2O$, 10 mg $CuCl_2 \cdot 2H_2O$, 10 mg $MnCl_2 \cdot 4H_2O$, 10 mg $Na_2B_4O_7 \cdot 10H_2O$, 10 mg $(NH_4)_6Mo_7O_{24} \cdot 4H_2O$

Element soln (1 L, 500x): 3 g $CoCl_2 \cdot 6H_2O$, 1.5 g $(NH_4)_2Fe(SO_4)_2 \cdot 6H_2O$, 1.5 g $ZnSO_4 \cdot 4H_2O$, 1.5 g $MnSO_4 \cdot 7H_2O$.

Seed cultures (50 mL R_2YE+ with glass beads) were inoculated from cell stocks and allowed to grow for 3-4 days at 28 °C shaking at 250 rpm. These cultures typically include 20 μg/mL hygromycin B, 8 μg/mL nalidixic acid, and 20 μg/mL apramycin (if the strains include *thnL* or *thnK*). These cultures were used to inoculate production cultures (1-1.5 ml into 20-30 mL R5A+). Cobalamin (1 μM) is added to the medium when desired. (3*S*,5*S*)-carbapenam production was monitored by the CarC CFE assay.

CarC Expression and Cell-Free Extract Isolation.

The *carC* gene in pET24a (3) was transformed into *E. coli* Rosetta 2(DE3) for expression. The cells were grown at 37 °C in LB medium supplemented with 35 mg/L ferrous ammonium sulfate hexahydrate and protein expression was induced with IPTG when the optical density reached 0.6. The cultures grew overnight at 19 °C and were then pelleted by centrifugation (4,000 × *g*). The cell paste was frozen for later use. Lysis Buffer (10% glycerol, 50 mM NaH_2PO_4, 300 mM NaCl, 10 mM imidazole, pH 8.0) was added to cell paste (~ 3 mL buffer for 1 g of cells) along with 1 mg/mL lysozyme and the

cells were resuspended. The mixture was sonicated on ice and then centrifuged at 10,000 × *g* for 30 min. The supernantant was used as the cell-free extract and was frozen at -80 °C for storage.

CarC CFE Assay.
(0.5-1 mL volume)
8 mM α-ketoglutarate
80 μM ammonium iron(II) sulfate hexahydrate
1-2 mM ascorbic acid
62-63% (by vol) cell-free medium from *Streptomyces* culture
25% (by vol) CarC CFE

After mixing, reactions are typically run for 1-1.5 h at 28 °C. 200 μL aliquots are plated on ESS.

References:

1. Coulthurst SJ, Barnard AML, & Salmond GPC (2005) Regulation and biosynthesis of carbapenem antibiotics in bacteria. *Nat. Rev. Microbiol.* 3(4):295-306.

2. Bodner MJ*, et al.* (2011) Definition of the common and divergent steps in carbapenem β-lactam antibiotic biosynthesis. *ChemBioChem* 12(14):2159-2165.

3. Li R, Stapon A, Blanchfield JT, & Townsend CA (2000) Three unusual reactions mediate carbapenem and carbapenam biosynthesis. *J. Am. Chem. Soc.* 122(1483):9296-9297.

4. Bodner MJ, Phelan RM, Freeman MF, Li R, & Townsend CA (2010) Non-heme iron oxygenases generate natural structural diversity in carbapenem antibiotics. *J. Am. Chem. Soc.* 132(1):12-13.

5. Marous DR*, et al.* (2015) Consecutive radical *S*-adenosylmethionine methylations form the ethyl side chain in thienamycin biosynthesis. *Proc. Natl. Acad. Sci. USA* 112(33):10354-10358.

6. Williamson J (1986) The biosynthesis of thienamycin and related carbapenems *Crit. Rev. Biotechn.* 4(1):111-131.

7. Okabe M*, et al.* (1982) Studies on the OA-6129 group of antibiotics, new carbapenem compounds. I. Taxonomy, isolation and physical properties. *J. Antibiot. (Tokyo)* 35(10):1255-1263.

8. Freeman MF, Moshos KA, Bodner MJ, Li R, & Townsend CA (2008) Four enzymes define the incorporation of coenzyme A in thienamycin biosynthesis. *Proc. Natl. Acad. Sci. USA* 105(32):11128-11133.

9. Núñez LE, Méndez C, Braña AF, Blanco G, & Salas JA (2003) The biosynthetic gene cluster for the beta-lactam carbapenem thienamycin in *Streptomyces cattleya*. *Chem. Biol.* 10(4):301-311.

10. Zhang Q, van der Donk WA, & Liu W (2012) Radical-mediated enzymatic methylation: a tale of two SAMS. *Acc. Chem. Res.* 45(4):555-564.

11. Ueda Y, Damas CE, & Vinet V (1983) Nuclear analogs of β-lactam antibiotics. XIX. Syntheses of racemic and enantiomeric *p*-nitrobenzyl carbapen-2-em-3-carboxylates. *Can. J. Chem.* 61:2257-2263.

12. Bateson JH, Roberts PM, Smale TC, & Southgate R (1980) Synthesis of 7-oxo-3-sulphinyl-1-azabicyclo [3.2. 0] hept-2-ene-2-carboxylates: olivanic acid analogues. *J. Chem. Soc., Chem. Commun.*:185-186.

13. Worthington AS & Burkart MD (2006) One-pot chemo-enzymatic synthesis of reporter-modified proteins. *Org. Biomol. Chem.* 4(1):44-46.

14. Broderick JB, Duffus BR, Duschene KS, & Shepard EM (2014) Radical *S*-adenosylmethionine enzymes. *Chem. Rev.* 114(8):4229-4317.

15. Bauerle MR, Schwalm EL, & Booker SJ (2015) Mechanistic diversity of radical *S*-adenosylmethionine (SAM)-dependent methylation. *J. Biol. Chem.* 290(7):3995-4002.

16. Rodríguez M*, et al.* (2011) Mutational analysis of the thienamycin biosynthetic gene cluster from *Streptomyces cattleya*. *Antimicrob. Agents Chemother.* 55(4):1638-1649.

17. Hopwood DA, Kieser T, Wright HM, & Bibb MJ (1983) Plasmids, recombination and chromosome mapping in *Streptomyces lividans* 66. *J. Gen. Microbiol.* 129:2257-2269.

18. Gomez-Escribano JP & Bibb MJ (2011) Engineering *Streptomyces coelicolor* for heterologous expression of secondary metabolite gene clusters. *Microb. Biotechnol.* 4(2):207-215.

19. Doumith M*, et al.* (2000) Analysis of genes involved in 6-deoxyhexose biosynthesis and transfer in *Saccharopolyspora erythraea*. *Mol. Gen. Genet.* 264:477-485.

20. Gregory MA, Till R, & Smith M (2003) Integration site for *Streptomyces* phage φBT1 and development of site-specific integrating vectors. *J. bacteriol.* 185(17):5320-5323.

21. Aoki H*, et al.* (1976) Nocardicin A, a new monocyclic beta-lactam antibiotic I. Discovery, isolation, and characterization. *J. Antibiot. (Tokyo)* 29:492-500.

22. Stapon A, Li R, & Townsend CA (2003) Carbapenem biosynthesis: confirmation of stereochemical assignments and the role of CarC in the ring stereoinversion process from L-proline. *J. Am. Chem. Soc.* 125(28):8486-8493.

23. Bierman M*, et al.* (1992) Plasmid cloning vectors for the conjugal transfer of DNA from *Escherichia* coli to *Streptomyces* spp. *Gene* 116(1):43-49.

24. Kahan JS*, et al.* (1979) Thienamycin, a new β-lactam antibiotic. I. Discovery, taxonomy, isolation and physical properties. *J. Antibiot. (Tokyo)* 32(1):1-12.

25. Forouhar F*, et al.* (2013) Two Fe-S clusters catalyze sulfur insertion by radical-SAM methylthiotransferases. *Nat. Chem. Biol.* 9(5):333-338.

26. Gerratana B, Arnett SO, Stapon A, & Townsend CA (2004) Carboxymethylproline synthase from *Pectobacterium carotorova*: a multifaceted member of the crotonase superfamily. *Biochemistry* 43(50):15936-15945.

27. Bodner MJ*, et al.* (2011) Definition of the common and divergent steps in carbapenem β‐lactam antibiotic biosynthesis. *ChemBioChem* 12:2159-2165.

Chapter 5

Thienamycin RS Enzymes: Current State and Future Directions

Introduction

When faced with the challenge of discerning the functions of the thienamycin RS enzymes, we initially favored traditional biosynthetic approaches. Gene knockout strains were not achievable in *S. cattleya*, but Dr. Rongfeng Li was able to generate such strains in a related carbapenem producer, *S. argenteolus* (1). Early efforts with the gene knockouts in this strain included cross-feeding experiments (K, L, P), chemical complementation with potential synthetic intermediates (K, L, P), and attempted isolation of pathway intermediates (L). Unfortunately, all of these strategies proved ineffective, motivating a move to *in vitro* experimentation. In addition to the *in vitro* work already discussed (Chapters 3 and 4), further groundwork has been laid in the areas of the ThnK mechanism and structure, the activity of ThnK homologs, and the chemistry performed by ThnL and ThnP. Now recent progress is discussed in these areas, highlighting possibilities for future experimentation, and concludes with a proposal for thienamycin biosynthesis.

Results and Discussion: ThnK Mechanism and Structure

The enzymatic activity of ThnK as well as an analysis of its variable specificities for the C2-thioether were addressed in Chapters 3 and 4, respectively. It was established that ThnK requires an Fe-S cluster and is dependent on cobalamin (Cbl). Mechanistically, ThnK likely follows the current proposal for Class B methylases (Figure 1.11), whereby a

methylcobalamin (Me-Cbl) intermediate is thought to transfer a methyl group to the substrate (2). The accumulation of SAH and 5'-dA in a 1:1 ratio (Figure 3.1) and the overall retention of absolute configuration of the terminal methyl in the C6-side chain (3) support this mechanism. Isolation of a Me-Cbl intermediate from the enzymatic reaction would provide additional evidence of the method of methylation. Furthermore, electron paramagnetic resonance (EPR) could be used in an attempt to detect a radical intermediate, while Mössbauer spectroscopy may confirm the presence of the [4Fe-4S] cluster. Kinetic experiments might yield additional mechanistic insight as well. We have completed an initial time course for ThnK, measuring 5'dA accumulation when the enzyme is incubated with the *trans* CoA-carbapenam **48** (Figure 5.1). Enzymatic turnover is likely complex, involving for a single catalytic cycle the binding of two molecules of SAM (one for the 5'dA radical, one as the methyl donor) and the substrate, the formation of the 5'-dA radical, hydrogen atom abstraction, and methyl transfer to the Cbl and then to the substrate.

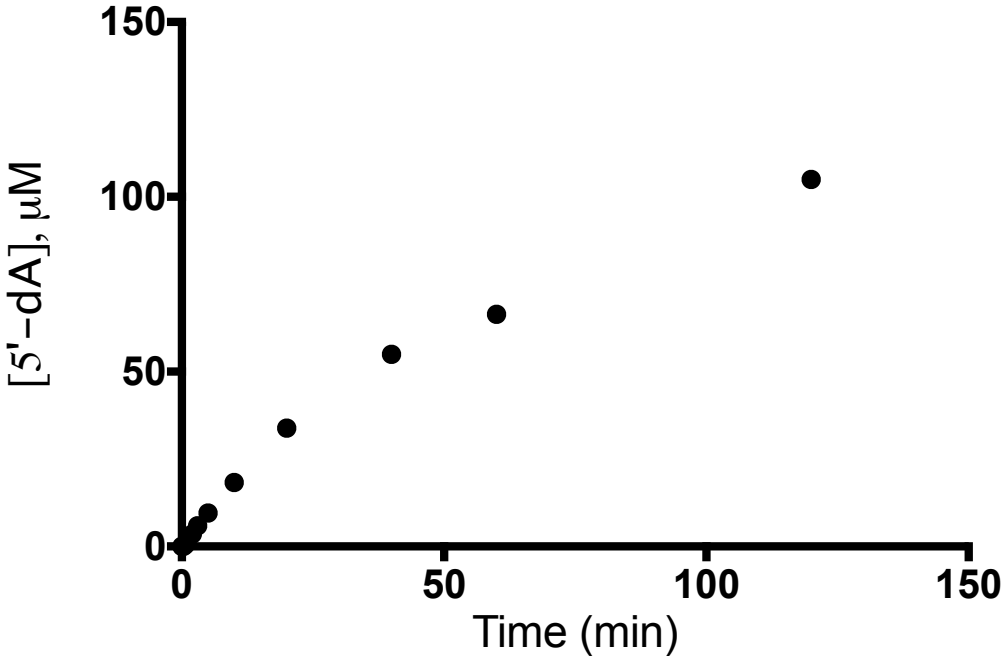

Figure 5.1: 5'-dA accumulation with ThnK.

ThnK, by comparison, is more soluble than some of its Class B family members (4, 5), so we have begun a structural collaboration with Dr. Amie Boal at the Pennsylvania State University. Currently, no structure is available of any Class B protein, and a crystal structure of ThnK would offer valuable information about the coordination of binding and chemical events. Hydrogen atom abstraction and methyl donation from Cbl may occur from opposite faces of the substrate and define the stereochemistry of the methylation.

Results and Discussion: ThnK Homologs

While thienamycin contains a C6-hydroxyethyl side chain, not all complex carbapenems contain two carbons on their C6-extensions. There are multiple examples such as PS-6 from *S. cremeus* (6) and the asparenomycins from *S. tokunonensis* (7) where the alkyl appendage contains three carbons (Figure 5.2). The double methylation by ThnK (8) suggests that a homolog could be responsible for adding all three carbons in these related species. An analysis of the ThnK homologs from *S. cremeus* (CreK) and *S. tokunonensis* (TokK) may yield insight into the control mechanism for the number of carbons that are added, which would aid future engineering efforts. Furthermore, CreK and TokK, if soluble, provide additional chances for obtaining an x-ray crystal structure of a Class B enzyme.

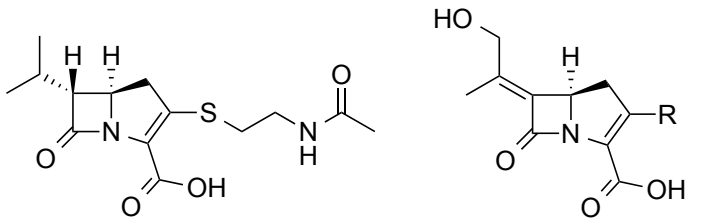

PS-6 (*S. cremeus*)

Asparenomycin A-C (*S. tokunonensis*)

Figure 5.2: Chemical structures of PS-6 and Asparenomycin A-C.

Work was begun on CreK and TokK in collaboration with Erica Sinner (JHU, CBI program). Initially, both genes were cloned into pET29b (*C*-His_6 construct) and transformed into *E. coli* Rosetta 2(DE3) also containing the plasmid pDB1282 (9), which over-expresses an Fe-S cluster operon. Expression tests in LB medium supplemented with Cbl (14 mg/L) showed a moderate level of soluble protein for TokK, but lower amounts for CreK. The *creK* gene was then moved to pET28b to generate His_6-tags at both ends of the protein. This construct was then placed into Rosetta2 + pDB1282, as done previously, and was also put into *E. coli* BL21 + pDB1282, along with the plasmid pG-KJE8 (10) that allows for co-expression of chaperones to assist protein folding. Additionally, the original pET29b/*creK* plasmid was put into BL21 + pDB1282 + pG-KJE8. CreK solubility was still problematic, but the BL21 pET29b/*creK* + pDB1282 + pG-KJE8 strain appears to give soluble CreK by SDS-PAGE, though not in high purity.

Activity assays were started with ThnK to assess whether RS activity could be obtained from an aerobic protein purification. The Rosetta 2 pET29b/*thnK* + pDB1282 strain was grown in ethanolamine-M9, as previously described (8). The purification was performed under an argon atmosphere and with sparged buffers whenever possible to reduce exposure to oxygen. Assay reactions included methyl viologen, NADPH, SAM, Me-Cbl, and the *cis* pantetheinyl-carbapenam **11**. Anaerobic ThnK reactions do not require Me-Cbl, but it was hoped that this addition would improve activity under slightly aerobic conditions. When the assay samples were filtered for analysis, it was noted that the red color associated with the Me-Cbl was predominately with the protein fraction, possibly indicative of cofactor binding with ThnK. By LC-HRMS (negative mode), the methylated product of **11** could be observed and was absent from the no-substrate control

reaction (Figure 5.3). We noted that the enzyme was more active if the buffer-exchange step was omitted after immobilized metal ion affinity chromatography. Using the enzyme as soon as possible may prevent additional oxidative damage. The presence of the methylated product was encouraging as it was the first demonstration of "aerobic" activity from ThnK, opening the door for additional RS activity screening under low oxygen tension.

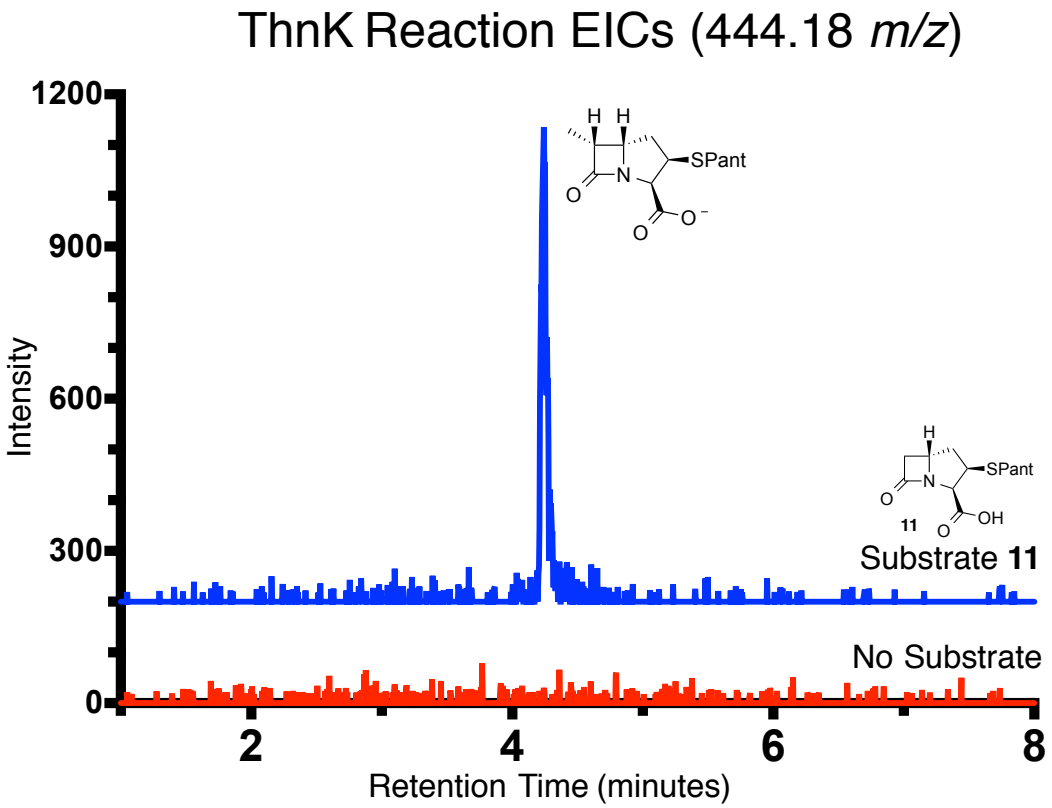

Figure 5.3: Extracted-ion chromatograms (EICS) showing "aerobic" methylation by ThnK. (Detection in negative mode)

Having observed methyl transfer activity with ThnK as a positive control, we next assayed TokK, which was expressed, purified, and assayed as described above for ThnK. Reactions were again conducted with Me-Cbl, which appeared to bind to the protein as was seen with ThnK. TokK produced a compound that matched the methylated product

of ThnK by mass and retention time (Figure 5.4), suggesting a comparable enzymatic activity. With both ThnK and TokK, multiple methylations were not detectable, though we attribute this to a decrease in activity due to the presence of oxygen. It is still anticipated that TokK is capable of catalyzing three methylations when analyzed in a more strictly anaerobic context. Overall, the encouraging activity observed with TokK paves the way for future experiments with this and other ThnK orthologs.

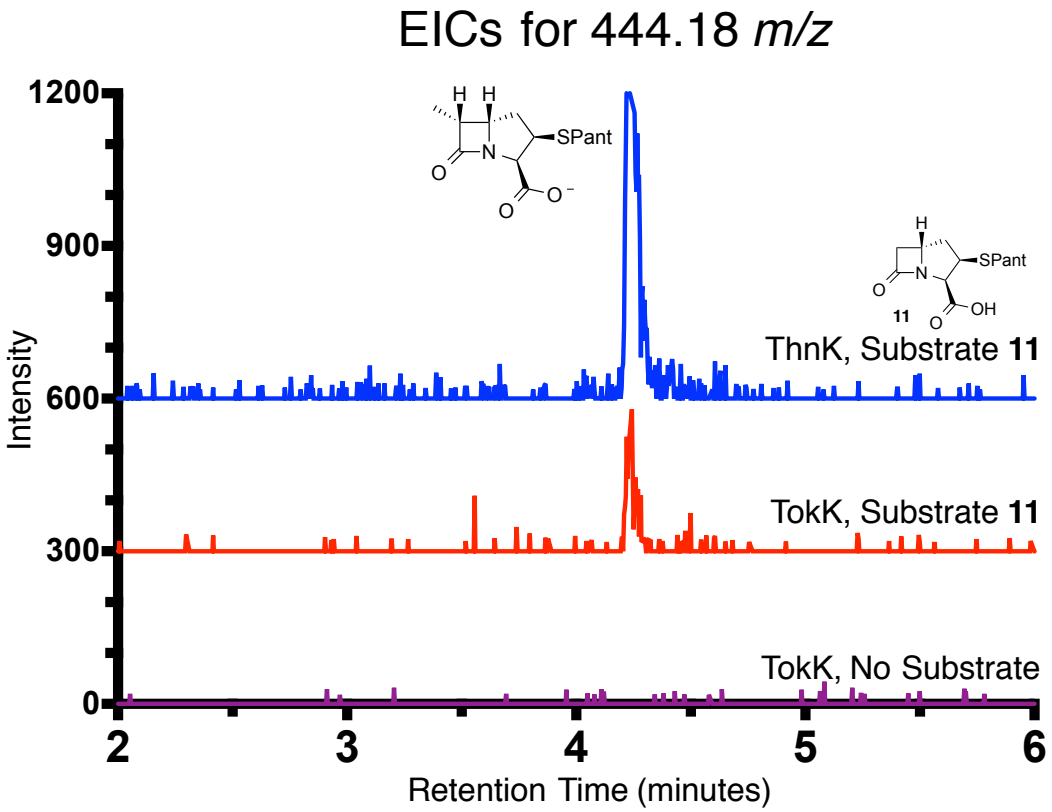

Figure 5.4: Extracted-ion chromatograms (EICS) showing "aerobic" methylation by TokK. (Detection in negative mode)

Results and Discussion: ThnL and ThnP

Demonstrating *in vitro* activity for ThnL and ThnP continues to be of central interest, especially because their catalytic activities are likely unprecedented among Cbl-dependent RS enzymes. While the wild type *thnK* gene as a *C*-terminal-His_6 construct in

E. coli was sufficient to obtain soluble protein, this strategy was not successful for ThnL and ThnP. Both the *thnL* and *thnP* genes were codon-optimized for expression in *E. coli*, ligated to the pET29b vector, and transformed into the BL21 strain along with plasmids providing the Fe-S cluster operon and molecular chaperones (pDB1282 and pG-KJE8, respectively). With this new expression strategy, soluble ThnL and ThnP could be obtained (Figure 5.5), albeit with some impurities.

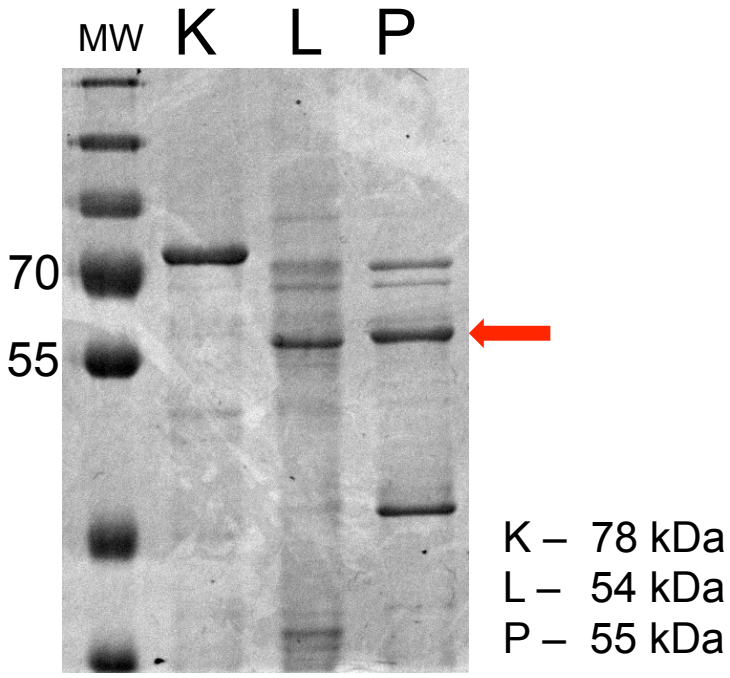

Figure 5.5: SDS-PAGE gel showing soluble ThnK, L, and P.

ThnK and ThnL were grown in M9 medium + Cbl and were purified anaerobically, while ThnP was grown in LB medium + Cbl and was purified aerobically. The red arrow indicates the band corresponding to ThnP, which is slightly larger than ThnL.

With soluble protein, we expressed, purified, and anaerobically assayed ThnL and ThnP as described for ThnK (Chapter 3). The CarC competition assay outlined in Chapter 4 suggested that ThnL acted directly after ThnE/M and used the (3*S*,5*S*)-carbapenam **3** as

its substrate. Thus, the ThnL assay included **3** as well as coenzyme A (CoA). The reaction with **3**, however, produced comparable levels of SAH and 5'-dA to the no substrate control (Figure 5.6); so if we are observing activity, it is very slight. Importantly, if ThnL is not a methylase, it may not produce significant amounts of SAH. Additional expression and/or assay conditions will need to be undertaken with ThnL, including testing other possible thiols, such as phosphopantetheine.

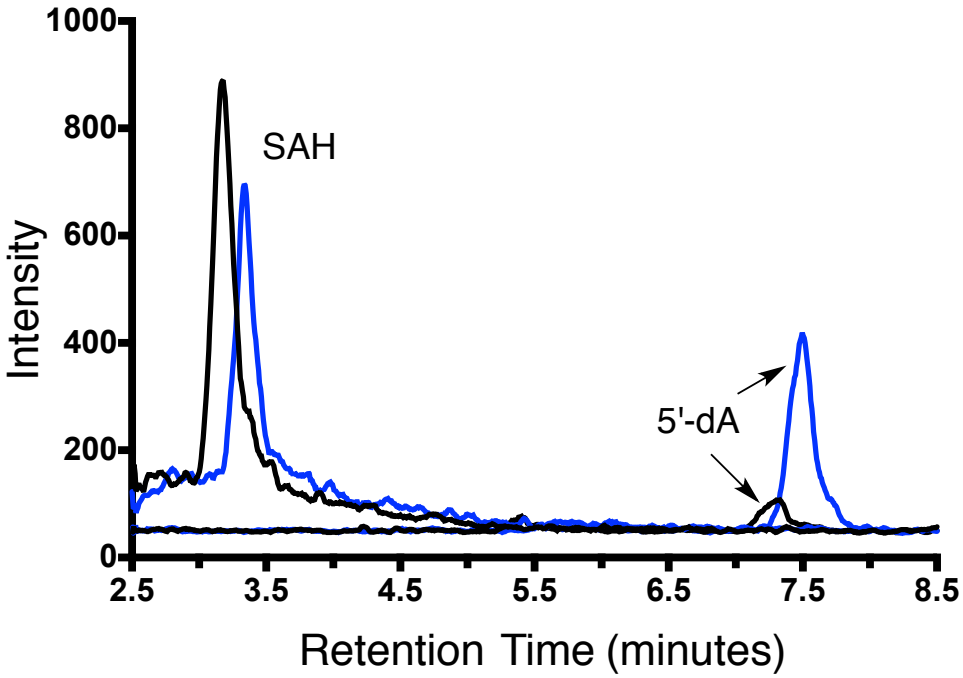

Figure 5.6: LC-MS/MS detection of enzymatic SAM-derived coproducts SAH (385.4 → 136 m/z) and 5′-dA (252.1 → 136 m/z) with ThnL.

The extracted-ion chromatograms (EICs) for the transitions of 5′-dA and SAH are shown for the reaction with compound **3** (blue) and the no substrate control (black).

In parallel with the experiment above, we elected to try refolding insoluble ThnL from inclusion bodies, a strategy that worked well for GenK (4). The same *thnL*$_{opt}$ strain described above was grown in LB medium, but without induction of the Fe-S operon or chaperones. The inclusion bodies were isolated and solubilized as outlined for GenK (4),

but our refolding buffer also contained 50 μM hydroxocobalamin (HO-Cbl). The procedure appeared to successfully resolubilize ThnL, and we note the red color from the HO-Cbl persisted with the protein fraction after concentration as evidence of proper refolding. This resolubilized ThnL was frozen and taken to PSU for anaerobic reconstitution of the Fe-S cluster. While performing the reconstitution, however, the protein appeared to precipitate out of solution and activity could not be observed. Yet, the overall refolding approach still remains a viable option and is worth further optimization.

ThnP was also assayed with the (3*S*,5*S*)-carbapenam **3** and CoA in a similar manner to ThnL, although we do not believe **3** to be the substrate for ThnP. This reaction produced background levels of SAH and 5'-dA (Figure 5.7), suggesting that either the protein is not active or **3** is not the correct substrate.

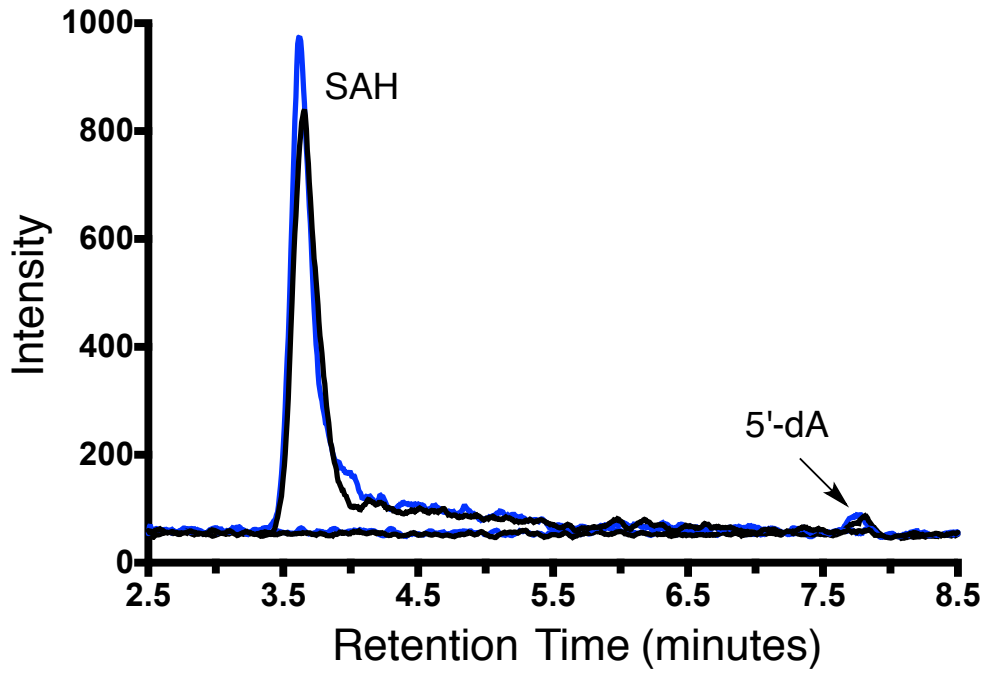

Figure 5.7: LC-MS/MS detection of enzymatic SAM-derived coproducts SAH (385.4 → 136 m/z) and 5′-dA (252.1 → 136 m/z) with ThnP.

The extracted-ion chromatograms (EICs) for the transitions of 5′-dA and SAH are shown for the reaction with compound **3** (blue) and the no substrate control (black).

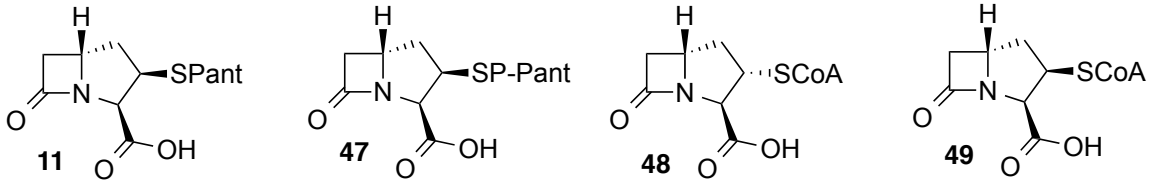

Figure 5.8: ThnK substrates tested with ThnP.

We have tried additional ThnP assays with substrates for ThnK, including compounds **11**, **47**, **48**, and **49** (Figure 5.8) as well. These reactions produce low, but above background levels of 5'dA, perhaps signifying enzymatic activity. LC-HRMS analysis showed evidence of methylase activity, although the turnover was much less than that observed for ThnK (Figure 5.9). Perhaps, even if ThnP is not primarily a methylase, it still retains some low activity for transferring methyl groups.

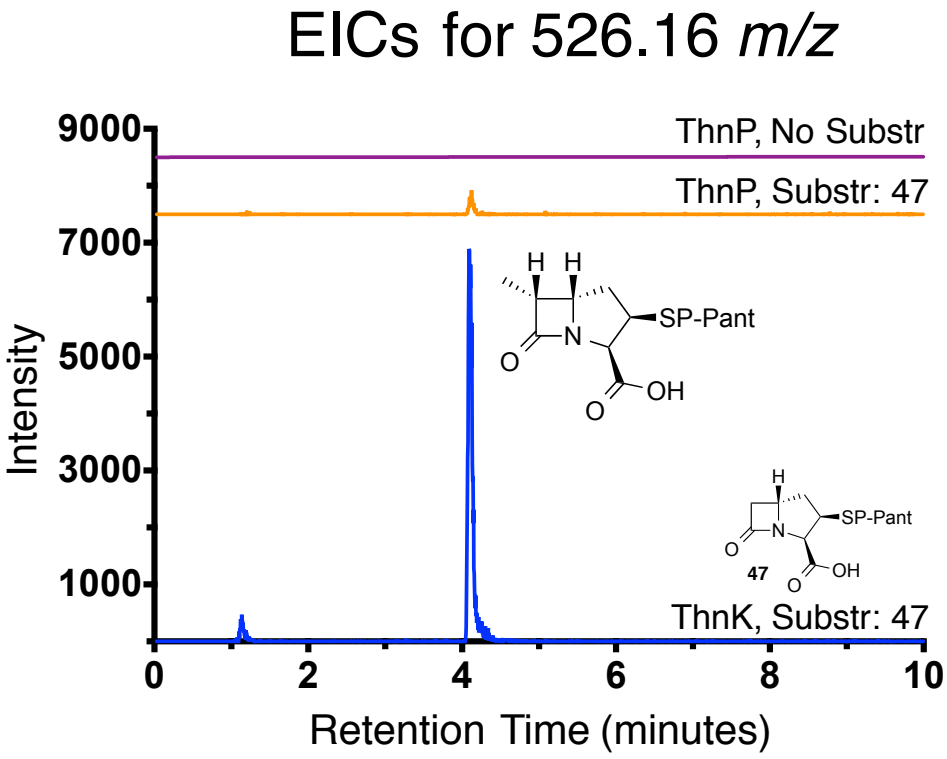

Figure 5.9: Extracted-ion chromatograms (EICS) showing low levels of methylation by ThnP.

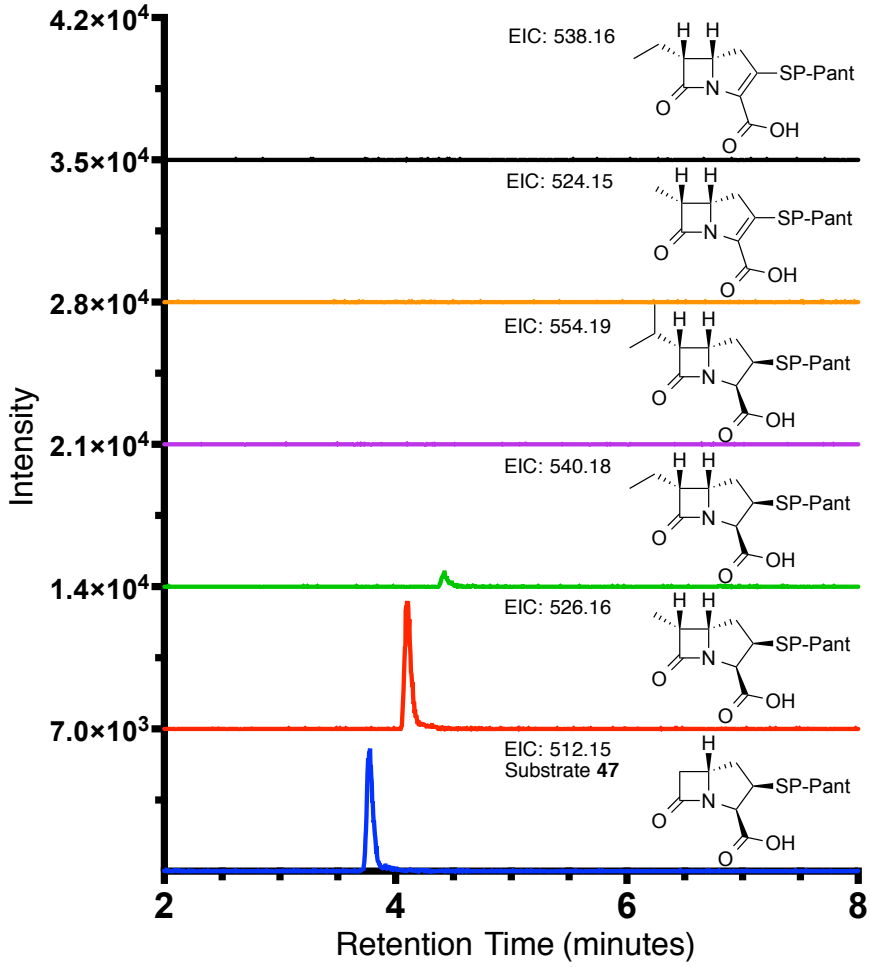

Figure 5.10: Extracted-ion chromatograms (EICS) to detect carbapenam(em) products from ThnK-ThnP coupled assays.

More ThnP assays were conducted with compounds **11**, **47**, **48**, and **49** and included ThnK in the reaction mixture. The levels of SAH and 5'-dA are not as diagnostic for these coupled assays since ThnK activity may obscure any additional effect from ThnP. The reactions were analyzed by LC-HRMS for carbapenam(em) products and the methylated and ethylated carbapenams were detected, attributable to ThnK activity (Figure 5.10). However, compounds corresponding to an additional alkylation or desaturation (possible transformations by ThnP) were not observed. Admittedly, if ThnP

was performing the C5-epimeriztion, it would be difficult to discern by retention time and there would be no mass difference from the substrate. Additional ThnP assays with a synthetic standard of the ThnK product may be required for determining the activity of ThnP.

Summary and Conclusions

From the CarC competition assay (Chapter 4), the product of ThnE/ThnM **3** is the substrate for ThnL, which we propose to install the C2-thioether (Figure 5.11). Substrate screening with ThnK (Chapter 4) revealed that CoA is the preferred C2 side chain for sequential ThnK methylations (Chapter 3) and is the likely candidate for the thiol added by ThnL. Thus far, thiol attachment by ThnL has not been demonstrated *in vitro*. The activity observed with ThnK also suggested that C5-epimerization occurs after C6-alkylation (Chapter 3). The C2/3-desaturation is believed to occur after alkylation as well, but has yet to be definitively shown. One approach to address the timing of the double-bond insertion would be to synthesize a C2/3-desaturated analog of **48** and compare the activity of ThnK with the analog and **48**. While ThnP displays low apparent methylase activity, we hypothesize that ThnP performs the epimerization and/or the desaturation. Regarding the C2 side chain truncation, ThnR likely acts sometime after C6-alkylation. Furthermore, the double-bond is expected to be in place before ThnH removes the terminal phosphate from phosphopantetheine (11). ThnQ and ThnT, perhaps in that order, are then able to complete the pathway. Additional understanding of the radical SAM enzymes will undoubtedly unlock the remaining mysteries of thienamycin biosynthesis.

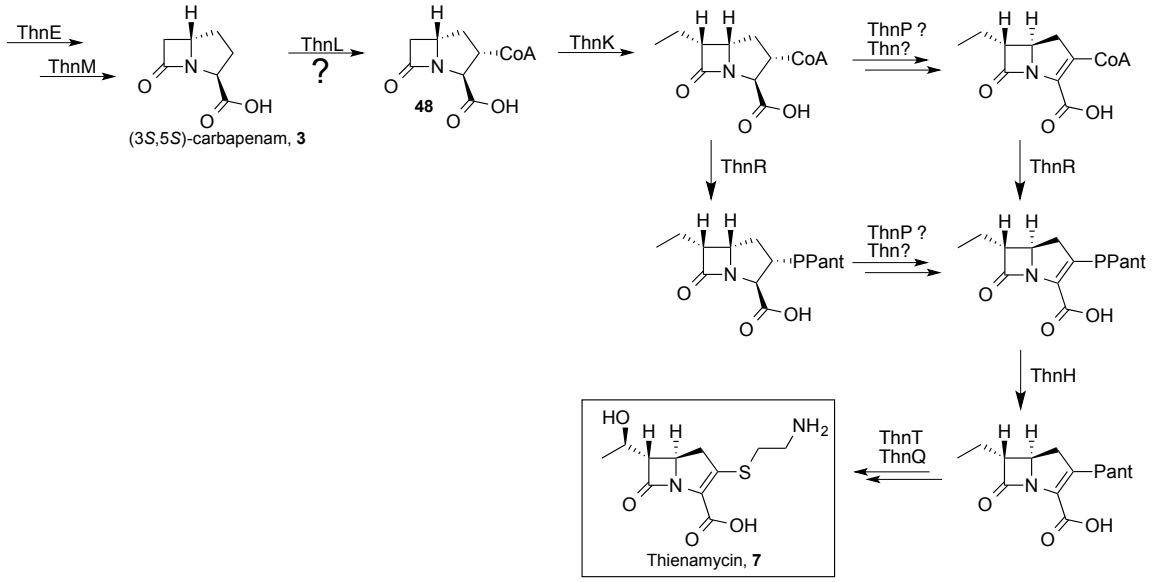

Figure 5.11: Outline of proposed thienamycin biosynthesis.

Materials and Methods

Substrates Preparation.

Substrates were synthesized as delineated in Chapter 2.

Mass Spectroscopy.

LC-MS/MS analysis for SAH and 5'dA was conducted as previously outlined (8), utilizing Method 1.

UPLC-HRMS analysis for carbapenams(ems) used prior methods (8), but was done in negative mode for detection from "aerobic" protein purification assays. Negative mode was found to give a superior signal to noise ratio.

ThnK Time Course.

ThnK (5.7 μM, FPLC purified, see Chapter 3) was mixed with 100 mM HEPES pH 7.5, 200 mM KCl, 0.5 mM SAM, 1 mM methyl viologen, 2 mM NADPH, and 2 mM substrate. Assays were conducted anaerobically at room temperature.

Cloning of TokK and CreK.

The gene clusters containing *tokK* (*S. tokunonensis*) and *creK* (*S. cremeus*) were placed into cosmids by Dr. Rongfeng Li. The two *thnK* homologs were PCR amplified from the respective cosmids using the following primers:

creK:
5'-GGGCATATGTCCACCGAATCCTCCCGCCGCCGC-3'
5'-GGGCTCGAGCAGCTGCTCGCTGAACGCGGGTTCCGC-3'

tokK:
5'-GGGCATATGTCCGCCGAACTCGCCAGCCGCGGC-3'
5'-GGGCTCGAGCCACTGTTCGCTGACCACCGGCTCCGC-3'

The PCR products were digested with NdeI and XhoI and ligated into pET29b, which had been digested with the same restriction enzymes. The two plasmids, pET29b/*creK* and pET29b/*tokK*, were verified to be correct by DNA sequencing and were electroporated into *E. coli* Rosetta 2(DE3) with the plasmid pDB1282 (9). Additionally, *creK* was ligated into pET28b using the NdeI and XhoI restriction sites and the resulting plasmid was transformed into Rosetta 2(DE3) + pDB1282 as well. Both pET29b/*creK* and pET28b/*creK* were also electroporated in *E. coli* BL21 + pDB1282 along with the chaperone plasmid pG-KJE8 (10).

Expression, Purification, and Aerobic Assays of ThnK and TokK.

ThnK and TokK were expressed in ethanolamine-M9 medium as has been described (8). Frozen cell paste was resuspended in lysis buffer (10% glycerol, 300 mM NaCl, 50 mM sodium phosphate pH 8.0, 10 mM BME, 5 mM imidazole) along with lysozyme (1 mg/mL final volume). Cells were lysed by sonication and insoluble material was removed by centrifugation (25,000 × g for 30 min at 4 °C). Soluble ThnK/TokK was

bound to TALON Co^{II} resin (Clontech) and purified by immobilized metal affinity chromatography (IMAC). The resin was washed with 5 mM and 10 mM imidazole in lysis buffer. 250 mM imidazole in the lysis buffer was used to elute the protein. The enzyme was concentrated using Amicon centrifugal filter devices (Millipore) with a 10 kDa molecular weight limit. The additional step of buffer-exchange of the protein was found to be detrimental to activity. All buffers were sparged with argon prior to use and the purification was done under a head of argon. Assays included: protein (in buffer from IMAC), 100 mM potassium phosphate pH 7.5, 200 mM KCl, 1 mM SAM, 1 mM methyl viologen, 2 mM NADPH, 1 mM Me-Cbl, and 1 mM substrate. Assays were run for at least 1.5 h prior to LC-MS analysis.

Cloning, Expression, Purification, and Assays of ThnL and ThnP.

The genes *thnL* and *thnP* were codon-optimized and synthesized by the commercial vendors DNA2.0 (Menlo Park, CA) and GenScript (Piscataway, NJ), respectively. The $thnP_{opt}$ gene was designed with flanking NdeI and XhoI restriction sites, which were used to ligate the gene into pET29b, creating pET29b/$thnP_{opt}$. Dr. Andrew Buller used a similar approach to create pET29b/$thnL_{opt}$. The terminal *C*-His_6 constructs for the two genes were transformed into *E. coli* BL21 + pDB1282 + pG-KJE8. Expression and purification of ThnL and ThnP were conducted as described for ThnK (8); however, the lysis buffer contained 2-2.5 mM imidazole and washes were done with this lysis buffer and lysis buffer with 5 mM imidazole. The ThnL assays with the (3*S*,5*S*)-carbapenam **3** (1 mM) included: 50 mM HEPES pH 7.5, 200 mM KCl, 1 mM SAM, 1 mM methyl viologen, 4 mM NADPH, 0.5 mM Me-Cbl, 0.5 mM HO-Cbl, 1 mM CoA,

and 1 mM cysteine and were run for approximately 2 h. The ThnP assays with **3** were carried out in a similar manner, but lacked cysteine and contained 2 mM CoA. Reactions with ThnP (79 μM) and compounds **11**, **47**, **48**, or **49** (2 mM) contained 100 mM HEPES pH 7.5, 200 mM KCl, 1 mM SAM, 1 mM methyl viologen, and 2 mM NADPH and were allowed to react for 6 h. The ThnK-ThnP coupled assays had the same components with the addition of ThnK (2.9 μM).

Refolding ThnL from Inclusion Bodies.

Refolding of ThnL was performed as delineated for GenK (4), but the ThnL refolding buffer included 50 μM HO-Cbl. Anaerobic reconstitution of the Fe-S cluster was attempted at PSU using standard laboratory protocols.

References:

1. Li R, Lloyd EP, Moshos KA, & Townsend CA (2014) Identification and characterization of the carbapenem MM 4550 and its gene cluster in *Streptomyces argenteolus* ATCC 11009. *ChemBioChem* 15(2):320-331.

2. Zhang Q, van der Donk WA, & Liu W (2012) Radical-mediated enzymatic methylation: a tale of two SAMS. *Acc. Chem. Res.* 45(4):555-564.

3. Houck DR, Kobayashi K, Williamson JM, & Floss HG (1986) Stereochemistry of methylation in thienamycin biosynthesis: example of a methyl transfer from methionine with retention of configuration. *J. Am. Chem. Soc.* 108:5365-5366.

4. Kim HJ*, et al.* (2013) GenK-catalyzed C-6' methylation in the biosynthesis of gentamicin: isolation and characterization of a cobalamin-dependent radical SAM enzyme. *J. Am. Chem. Soc.* 135(22):8093-8096.

5. Werner WJ*, et al.* (2011) In vitro phosphinate methylation by PhpK from *Kitasatospora phosalacinea*. *Biochemistry* 50(42):8986-8988.

6. Shibamoto N*, et al.* (1980) PS-6 and PS-7, new β-lactam antibiotics. Isolation, physicochemical properties and structures. *J. Antibiot. (Tokyo)* 33:1128-1137.

7. Tsuji N*, et al.* (1982) Asparenomycins A, B and C, new carbapenem antibiotics. III. Structures. *J. Antibiot. (Tokyo)* 35:24-31.

8. Marous DR*, et al.* (2015) Consecutive radical *S*-adenosylmethionine methylations form the ethyl side chain in thienamycin biosynthesis. *Proc. Natl. Acad. Sci. USA* 112(33):10354-10358.

9. Lanz ND*, et al.* (2012) RlmN and AtsB as models for the overproduction and characterization of radical SAM proteins. *Method. Enzymol.* 516:125-152.

10. Nishihara K, Kanemori M, Yanagi H, & Yura T (2000) Overexpression of trigger factor prevents aggregation of recombinant proteins in *Escherichia coli*. *Appl. Environ. Microbiol.* 66(3):884-889.

11. Moshos KA (2011) Design and synthesis of substrates and standards used to elucidate activities of enzymes in carbapenem gene clusters. Ph.D. Thesis (The Johns Hopkins University, Baltimore, MD).

Daniel R. Marous

Department of Pharmacology and Molecular Sciences
Townsend Research Group
Johns Hopkins School of Medicine
Baltimore, MD 21205
Email: dmarous2@jhmi.edu
Born: Columbus, OH 6-15-86

EDUCATION

Johns Hopkins University, Baltimore, MD — November 2015
Ph.D. Pharmacology and Molecular Sciences
Dissertation: "Radical SAM Enzymes in Thienamycin Biosynthesis"

Wittenberg University, Springfield, OH — May 2009
B.A., Biochemistry/Molecular Biology and Mathematics
Summa Cum Laude, University Honors
Cumulative GPA: 4.00/4.00

RESEARCH EXPERIENCE

Johns Hopkins University — 2009-Present
Graduate Research Advisor: Craig A. Townsend, Dept. of Chemistry

- Three radical SAM/B_{12}-dependent enzymes (ThnK, ThnL, ThnP) necessary for thienamycin biosynthesis have been expressed and purified/reconstituted anaerobically.
- Library of potential carbapenam substrates was synthesized. Activity-screen identified substrates for ThnK, which suggest the enzyme's placement in the pathway. The activity of ThnK was determined: stereospecific sequential methylations to form the ethyl side chain in thienamycin.
- Heterologous expression of the RS proteins in *Streptomyces* coupled with designed bioassay implies that ThnL installs a thioether side-chain, acting between known steps and ThnK.

North Carolina State University — 2008
Advisor: Mansoor A. Haider, REU in Modeling and Industrial Applied Mathematics

- A differential equation mathematical model was developed for cartilage regeneration.

Wittenberg University — 2007
Research Advisor: Jay A. Yoder, Dept. of Biology

- Squalene and phenolic compounds were assessed as potential attractants for the dog tick.

HONORS AND AWARDS

- Scheinberg Travel Award, Dept. of Pharmacology and Molecular Sciences (JHU) 2015
- Invited Instructor for JHU Summer Programs (JHU) 2014
- Phi Beta Kappa inductee (WU) 2009
- Faculty Award for Outstanding Achievement in Biochemistry/Mole. Bio. (WU) 2009
- Richard A. Little Fund Award (achievement in mathematics) (WU) 2009
- ACS Division of Analytical Chemistry Award (WU) 2008
- The Paul Hessler Award (outstanding achievement in mathematics) (WU) 2008
- Outstanding Performance in General Chemistry Award (WU) 2006
- Mathematics 202 Award (for best performance in the calculus sequence) (WU) 2006

PUBLICATIONS AND PRESENTATIONS

- Marous, D.R., Lloyd, E.P., Buller, A.R., Moshos, K.A., Grove, T.L., Blaszczyk, A.J., Booker, S.J., and Townsend, C.A. "Consecutive radical S-adenosylmethionine methylations form the ethyl side chain in thienamycin biosynthesis" *Proceedings of the National Academy of Sciences USA* 2015, *112* (33), 10354-10358.
- Haider, M.A., Olander, J.E., Arnold R.F., Marous, D.R., McLamb, A.J., Thompson, K.C., Woodruff, W.R., and Haugh, J.M. "A phenomenological mixture model for biosynthesis and linking of cartilage extracellular matrix in scaffolds seeded with chondrocytes." *Biomechanics and Modeling in Mechanobiology* 2011, *10*, 915-924.
- Yoder, J.A, Ark, J.T., and Marous, D.R. "Use of squalene and phenolic pheromone derivatives on nonfed stages of the brown dog *tick Rhipicephalus sanguineus* (latreille) (acari: ixodidae), with observations for attraction potential." *International Journal of Acarology* 2008, *34*, 191-195.
- Marous, D.R. *et al.* "Consecutive radical SAM methylations form the ethyl side chain in thienamycin biosynthesis" Poster, Gordon Research Conference: Enzymes, Coenzymes, and Metabolic Pathways, Waterville Valley, NH (July 2015)
- Marous, D.R. "Mathematical Modeling of Cartilage Regeneration via Hydrogel" MAA Ohio Section, Student Research Presentation, Bowling Green, OH (April 2009)
- Marous, D.R, Arnold, R.R., Thompson, K.C., Woodruff, W.R., McLamb, A.J. and Haider, M.A. "Mathematical Modeling of Cartilage Regeneration via Hydrogel" MAA-CUPM Undergraduate Poster Session, Washington, DC. (January 2009)

TEACHING AND LEADERSHIP EXPERIENCE

Johns Hopkins University

- *Graduate Rotation-Student Research Mentor* 2014-2015
  Students were trained in molecular biology techniques including cloning, bacterial conjugation, heterologous expression, and enzyme assays as well as chemical synthesis.
- *Summer Programs Faculty* 2014
  Invited to teach self-designed course (*Mini-Term I: Magic Bullets: How Drugs Really Work*, AS.030.303.71) for undergraduates and advanced high school students. Expanded previously designed course to incorporate additional "in-the-news" readings, discussions, and quizzes. Course was offered for letter grade.
- *Preparing Future Faculty Teaching Academy* (Completed 2014):
  I. Intersession Instructor (Teaching Mentor: Chris Falzone, Dept. of Chemistry) 2014
  Conceived, designed, and implemented course *Magic Bullets: How Drugs Really Work* (AS.030.303.12) for winter intersession for undergraduates. Designed and utilized materials, lectures, activities, and assessments for class of approximately 20 students.
  II. JHU Summer Teaching Institute Participant 2014
  Institute provided interactive training on being an effective educator for undergraduates.
  III. Selected as "Focus Group" Participant for *Introduction to Effective Instruction* 2012
  Course introduced primary components of effective instruction and allowed students to develop instructional skills. (Taught by David Andrews, Dean of the School of Edu.)
- *Guest Lecturer, Mechanisms in Bioorganic Chemistry* 2012-13
  Advisor: Caren L. Freel Meyers, Dept. of Pharmacology and Molecular Sciences
  Organized and delivered lesson on enzymatic deprotonation of carbon and provided assessment for graduate students for two sections.
- *Judge for STEM Fair,* Pleasant Plains Elementary School (two years) 2014-2015

REFERENCES

Prof. Craig A. Townsend
Dept. of Chemistry
Johns Hopkins University
Remsen Hall 252
3400 N. Charles St.
Baltimore, MD 21218
Tel: (410) 516-7444
ctownsend@jhu.edu

Prof. Caren L. Freel Meyers
Dept. of Pharmacology & M.S.
Johns Hopkins School of Medicine
Wood Basic Science Building 307-A
725 N. Wolfe St.
Baltimore, MD 21205
Tel: (410) 502-4807
cmeyers@jhmi.edu

Prof. Philip A. Cole
Dept. of Pharmacology & M.S.
Johns Hopkins School of Medicine
Hunterian 316
725 N. Wolfe St.
Baltimore, MD 21205
Tel: (410) 614-8849
pcole@jhmi.edu